NAVAL POSTGRADUATE SCHOOL
Monterey, California

THESIS

CLASSIFICATION OF SUMMERTIME WEST COAST FOG AND STRATUS EVENTS AND THE DEVELOPMENT OF FOG AND STRATUS FORECAST TECHNIQUES

by

Greg S. Ireton
September 2001

Thesis Advisor:	Wendell A. Nuss
Second Reader:	Douglas K. Miller

Approved for public release; distribution is unlimited

Report Documentation Page

Report Date	Report Type	Dates Covered (from... to)
30 Sep 2001	N/A	-

Title and Subtitle	Contract Number
Classification of Summertime West Coast Fog and Stratus Events and the Development of Fog and Stratus Forecast Techniques	
	Grant Number
	Program Element Number

Author(s)	Project Number
Greg S. Ireton	
	Task Number
	Work Unit Number

Performing Organization Name(s) and Address(es)	Performing Organization Report Number
Research Office Naval Postgraduate School Monterey, Ca 93943-5138	

Sponsoring/Monitoring Agency Name(s) and Address(es)	Sponsor/Monitor's Acronym(s)
	Sponsor/Monitor's Report Number(s)

Distribution/Availability Statement
Approved for public release, distribution unlimited

Supplementary Notes

Abstract

Subject Terms

Report Classification	Classification of this page
unclassified	unclassified

Classification of Abstract	Limitation of Abstract
unclassified	UU

Number of Pages
149

1. AGENCY USE ONLY *(Leave blank)*	2. REPORT DATE September 2001	3. REPORT TYPE AND DATES COVERED Master's Thesis	
4. TITLE AND SUBTITLE: Title (Mix case letters) Classification of Summertime West Coast Fog and Stratus Events and the Development of Fog and Stratus Forecast Techniques			**5. FUNDING NUMBERS**
6. AUTHOR(S) Greg S. Ireton			
7. PERFORMING ORGANIZATION NAME(S) AND ADDRESS(ES) Naval Postgraduate School Monterey, CA 93943-5000			**8. PERFORMING ORGANIZATION REPORT NUMBER**
9. SPONSORING / MONITORING AGENCY NAME(S) AND ADDRESS(ES) N/A			**10. SPONSORING / MONITORING AGENCY REPORT NUMBER**

11. SUPPLEMENTARY NOTES The views expressed in this thesis are those of the author and do not reflect the official policy or position of the Department of Defense or the U.S. Government.

12a. DISTRIBUTION / AVAILABILITY STATEMENT Approved for public release; distribution is unlimited	12b. DISTRIBUTION CODE A

ABSTRACT

The fog and stratus that frequently plagues the West Coast in the summer months is responsible for a variety of impacts on everyday life, the greatest impact on aviation. Many flight delays and cancellations that are experienced around the Pacific Rim are attributed to the development and evolution of the fog and stratus on the U.S. West Coast.

This thesis studies the evolution of the fog and stratus events during the summer of 2000 through the use of geostationary, GOES-10, visual satellite imagery to develop a classification scheme. The synoptic-scale weather patterns as well as the mesoscale coastal regime were then associated with a type of stratus evolution. The Navy's mesoscale model, coupled ocean/atmosphere mesoscale prediction system (COAMPS), provided detailed simulation of 11 events to highlight the boundary layer evolution and its relationship to fog and stratus evolution. The fog and stratus classification scheme produced several consistent synoptic and mesoscale signals associated with stratus evolution. These relationships provide some forecasting techniques that should aid forecasters with predicting the evolution of fog and status events.

14. SUBJECT TERMS Fog, Stratus, Marine Stratiform Cloudiness (MSC), Coastal Regime, Synoptic-scale, Mesoscale, Satellite, COAMPS, GEMPAK, Vis5D, Model(s), Forecasts, Trajectory(ies), Q-vector(s), Marine Boundary Layer, Thermal Wind, and Aviation.		15. NUMBER OF PAGES 131
		16. PRICE CODE

17. SECURITY CLASSIFICATION OF REPORT Unclassified	18. SECURITY CLASSIFICATION OF THIS PAGE Unclassified	19. SECURITY CLASSIFICATION OF ABSTRACT Unclassified	20. LIMITATION OF ABSTRACT UL

CLASSIFICATION OF SUMMERTIME WEST COAST FOG AND STRATUS EVENTS AND THE DEVELOPMENT OF FOG AND STRATUS FORECAST TECHNIQUES

Greg S. Ireton
Lieutentent, United States Navy
B.S., University of North Carolina-Asheville, 1997

Submitted in partial fulfillment of the
requirements for the degree of

MASTER OF SCIENCE IN METEOROLOGY AND PHYSICAL OCEANOGRAPHY

from the

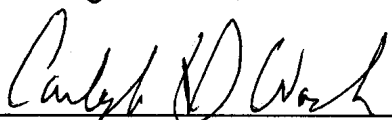## NAVAL POSTGRADUATE SCHOOL
September 2001

Author: _____
Greg S. Ireton

Approved by: _____
Wendell Nuss, Thesis Advisor

_____
Douglas Miller, Second Reader,

_____
Carlyle Wash, Chairman
Department of Meteorology

THIS PAGE INTENTIONALLY LEFT BLANK

ABSTRACT

The fog and stratus that frequently plagues the West Coast in the summer months is responsible for a variety of impacts on everyday life, the greatest being on aviation. Many flight delays and cancellations that are experienced around the Pacific Rim are attributed to the development and evolution of the fog and stratus on the U.S. West Coast.

This thesis studies at the evolution of the fog and stratus events during the summer of 2000 through the use of geostationary, GOES-10, visual satellite imagery to develop a classification scheme. The synoptic-scale weather patterns as well as the mesoscale coastal regime were then associated with a type of stratus evolution. The Navy's mesoscale model, coupled ocean/atmosphere mesoscale prediction system (COAMPS), provided detailed simulation of 11 events to highlight the boundary layer evolution and its relationship to fog and stratus evolution. The fog and stratus classification scheme produced several consistent synoptic and mesoscale signals associated with stratus evolution. These relationships provide some forecasting techniques that should aid forecasters with predicting the evolution of fog and status events.

THIS PAGE INTENTIONALLY LEFT BLANK

TABLE OF CONTENTS

LIST OF FIGURES

xi

LIST OF TABLES

THIS PAGE INTENTIONALLY LEFT BLANK

EXECUTIVE SUMMARY

The fog and stratus that frequently plagues the West Coast in the summer months is responsible for a variety of impacts on everyday life, the greatest being on aviation. Many flight delays and cancellations that are experienced around the Pacific Rim are attributed to the development and evolution of the fog and stratus on the U.S. West Coast.

This thesis studies at the evolution of the fog and stratus events during the summer of 2000 through the use of geostationary, GOES-10, visual satellite imagery to develop a classification scheme. The synoptic-scale weather patterns as well as the mesoscale coastal regime were then associated with a type of stratus evolution. The Navy's mesoscale model, coupled ocean/atmosphere mesoscale prediction system (COAMPS), provided detailed simulation of 11 events to highlight the boundary layer evolution and its relationship to fog and stratus evolution. The fog and stratus classification scheme produced several consistent synoptic and mesoscale signals associated with stratus evolution. These relationships provide some forecasting techniques that should aid forecasters with predicting the evolution of fog and status events.

THIS PAGE INTENTIONALLY LEFT BLANK

ACKNOWLEDGMENTS

THIS PAGE INTENTIONALLY LEFT BLANK

I.   INTRODUCTION

A.   PURPOSE/OBJECTIVE

1.   Background

Marine stratiform cloudiness (MSC) (stratus, stratocumulus, and fog) is a widespread, primarily summertime, event over the eastern subtropical oceans where cold ocean currents predominate. The United States West Coast it is one of the foggiest areas in the country. Ballard et al. (1991) stated that, "forecasting the formation, evolution, and the dispersal of fog is one of the most difficult problems facing local forecasters in many parts of the world." In particular, the MSC events along the West Coast of the United States during the summer are often responsible for numerous flight delays and cancellations at major airports from Seattle, Washington to San Francisco, and Los Angeles, California. These events are so costly to airlines and airports that several research projects (California Coastal Studies program at Scripps Institute of Oceanography in San Diego, the University of Washington Department of Atmospheric Sciences, and the Marine Research Division at the Navy Research Laboratory in Monterey, California) have taken an active interest in studying the problem. However, the most focused of research programs resides with the Federal Aviation Administration's (FAA) Aviation Weather Research Program (AWRP) ceiling and visibility studies, which solely focus on the problem of MSC events. If MSC events can be accurately forecast including formation, evolution, and dissipation; airlines could use this information for flight scheduling that currently affects the entire Pacific Rim. Airlines could thus save millions of dollars due to delays, not to mention an increase in customer satisfaction/understanding. Naturally, imparred MSC forecasting would be very valuable for DoD operations and military aviation safety. To this end, the purpose and objective of this thesis is to develop a coastal cloud classification algorithm that is related to the synoptic-scale meteorological conditions that can be used as a coastal forecasting aid.

This objective will be investigated through the use of relatively new technology, namely the use of a mesoscale model the Navy's Coupled Ocean/Atmosphere Mesoscale

Prediction System (COAMPS) and through the use of a software visualization program developed at the University of Wisconsin called Vis5D. Both of these tools are discussed in more detail in Appendix B, along with the General Meteorology Package (GEMPAK) Analysis and Rendering Program (GARP), which is also used.

Vis5D will allow for a five-dimensional look at the coastal features and processes that produce MSC events. By viewing the atmosphere using this method, atmospheric processes can be confirmed; discarded, or developed that will improve forecasting techniques and accuracy.

2.   Limited Discussion (Summary) of Previous Work

Based on climatology from the National Climatic Data Center (NCDC) in Asheville, North Carolina the entire area between Seattle and Los Angles experiences fog greater than 60 days per year when surface visibilities are one quarter mile or less, largely during the summer. The exception to this region, oddly enough, is the San Francisco Bay region where the occurrence of fog is less than 60 days, but more than 40 days, using the same visibility criteria. Additionally, the bight region of California (Point Conception to Baja) also experiences fog less than 60 days, but more than 40 days per year.

MSC events in the bight region are often a result of the formation of a Catalina Eddy, which is briefly described as an interruption of the predominately northerly flow along the coast with southerly flow, elevated marine layers, and an increase in low-level cloudiness. It is limited to a narrow zone of approximately 100km from the coastal mountains and results in cooler temperatures and improved air quality for coastal residences. Mass and Albright (1989) describe the dynamics of the Catalina Eddy while others (Davis et al 2000, Thompson et al 1996, Ulrickson et al 1995, and Ueyoshi and Roads 1993) investigate the dynamics through computer simulations and case studies. All are insightful and informative.

The Catalina Eddy, while not observed during the 11 case studies that are presented in this thesis, is an important meteorological event that takes place in the bight region of California. The feature is addressed in the following paragraphs to remind the forecasters of its importance to the development of fog and stratus.

The Cataline Eddy is initiated by the change from the climatological northwesterly to northerly winds and the impact of that northerly flow with the topography in the region. As a result of synoptic-scale pressure falls along the central California coast and/or lee troughing southeast of Point Conception, south-north along shore pressure gradient is established in the coastal region, which interacts with the adjacent mountain barrier to cause the establishment of a southerly flow with a Rossby radius of about 100km within the coastal mountains. This southerly flow results in considerable cyclonic vorticity in the coastal regions.

Additionally, the eddy is strongly influenced by the diurnal cycle. The northwesterly flow aloft, around 500m above mean sea level, impinges on the mountains north of the bight region. The flow is enhanced during the late afternoon, mainly in response to the land-sea temperature contrast. The strengthening flow overlaps temporally with a minimum in low-level stratification due to surface heating. The result is air that is characterized by a relatively high Froude number, which transverses over the coastal mountains and strongly depresses the marine layer over the bight region. The depression in the marine layer causes a warm anomaly and cyclonic circulation. Later at night, the incident northwesterlies weaken and the flow becomes more stable, which results in flow that goes around the coastal mountains rather than over them.

During the early stages of a Catalina Eddy there may be little or no stratus in the bight region even though a circulation is present. As the southerlies and the associated marine layer deepen, coastal stratus and fog develops and thickens. Many studies have shown that in many cases, but not all, eddies form during the night as the moisture-laden southerly flow with (stratus and fog) surges westward south of Point Conception and then is advected south by the strong northerly flow at and to the west of Point Conception.

The West Coast fog is a marine fog. It is associated with the cool waters of the Pacific Ocean and the California Current in particular. This phenomenon is a year-round occurrence, but MSC events are not always present. The ever-changing coastal atmosphere and microclimates controls it. The examinations of interannual variability of MSC events have been the subject of recent studies by Norris 1998, Norris et al 1998,

Norris and Leovy 1994, and Klein and Hartmann 1993. Norris (1997) has examined the seasonal variability of MSC over the North Pacific Ocean. He showed that variability is largest in two regions, the central and western Pacific Ocean. He contended that MSC events play an important role in the atmosphere-ocean coupling during the summertime when latent and sensible heat flues are not as dominant and the coupling between atmospheric circulation and sea surface temperature (SST) is not as strong as in winter. The seasonal variability observed over the Eastern Pacific Ocean is weaker but shows the maximum frequency of MSC events to occur in summer and that they are collocated with the region of strong SST gradient, i.e. the California Current.

While this thesis will attempt to address the entire west coast, numerous studies on MSC events have focused on specific regions along the U.S. West Coast, particularly in California (Haack et al. 2001, Dorman et al. 2000, Dorman and Winant 2000, Dorman et al. 1999, Burk and Thompson 1996, Jannuzzi 1994, Felsch and Whitlatch 1993, Bridger et al. 1993, and Winant et al. 1988). Although it is likely that terrain influences at least the evolution of MSC events; only one recent study addresses this issue, (Golding 1999) and is limited by the fact that its primary focus is on Perth, Australia. However, the concepts are sufficiently general to be applied to the U.S. West Coast.

Others have addressed such issues as wind reversals (sometimes referred to as coastally trapped disturbances, Kelvin waves and gravity currents) (Bond et al. 1996 and Mass and Bond 1996). Such events for the most part occur during the summer and are broken down into two categories; coastally trapped wind reversals, in which the southerly flow is highly ageostrophic and restricted to the coastal zone, and synoptic wind reversals, which are associated with land falling fronts or troughs. Coastal MSC events often accompany wind reversals, but by no means all of them.

While much research has looked at parts of the MSC problem, the relationship to larger-scale patterns has not been systematically explored. Only one article, Leipper 1995, was found that discussed forecast techniques relevant to the MSC problem. Leipper developed a system called Leipper inversion base statistics (LIBS) that emphasized the air-sea relationships. His objective was limited to visibility forecasting only, and therefore, did not address the entire MSC event.

Leipper's system is based on commonly observed sequences of day-to-day changes in the height of the inversion base and was a result of many years of analysis, experiment, and practice related to fog research on the West Coast beginning in the 1940's. LIBS utilizes a single variable, the early morning value of the height of the inversion base, as the index of synoptic scale day-to-day weather affecting local visibility. After determining the height of the inversion base, he compiled data whereby he showed the relationship between height of the inversion base with resulting observed visibility and duration. He further broke down both inversion height and visibilities into ranges. While helpful, it is very limited in scope. Many times, forecasters look for that single key to unlock the mysteries of an event, but rarely find it. This is a great example. The atmosphere is very dynamic and always demonstrating to mere mortal forecasters that following a single fluid is not always enough. We must chase them all.

There is no doubt that most, if not all, National Weather Service stations and private forecasting companies have "thumb rules" to help forecast the MSC problem, but fail on many occasions for one reason or another. For example, the San Francisco weather office utilizes a technique whereby the pressure gradient force is measured from San Francisco to Eureka (along shore) as well as a cross-shore pressure gradient force (SFO to SAC) to determine the intensity of the on-shore flow. This relationship is used to determine the extent of stratus expected.

3.   Objectives

This thesis addresses large-scale patterns in four regions along the West Coast with interesting and positive results. Those regions are approximated as follows: Seattle region covers Washington to Southern Oregon; Eureka region covers Southern Oregon to Cape Mendocino; Monterey region covers Cape Mendocino to Point Conception; and Los Angeles region covers Point Conception to Baja. This study examines the unique relationship between the synoptic pattern and MSC events for each of the four regions and then looks for similarities between the regions that can be used by coastal forecasters.

While not the focus of this project, the potential influences of El Nino, La Nina, or La Nada may limit the general applicability of these results. Numerous studies have shown that MSC events exhibits interannual variability that is associated with the

climatological changes given by El Nino and La Nina events. These events will cause an increase or decrease in MSC events and is not addressed in this thesis. The data used for this thesis (addressed in subpart B below) were obtained during a La Nada event, the transition between El Nino and La Nina events.

B. DATA USED AND PERIOD OF STUDY

The period examined in this thesis is from 1 June to 31 August 2000. The focus was on the summertime regime, and the daylight hours when visible satellite imagery was available. There was no assumption that this particular period was "typical" for the entire region of study. Over 12000 GOES-10 visual satellite pictures, broken down into four regions along the U.S. West Coast at 30 minutes intervals, were examined to characterize the evolution of the MSC events. Detailed discussion of satellite imagery and how it was manipulated is provided in Chapter II.

In addition to the satellite imagery, observations, and model generated analyses and forecasts were obtained locally through the Naval Postgraduate School's archived data of FNMOC's NOGAPS fields for the period of study. These data fields were used to classify the synoptic patterns. For a limited set of 11 representative MSC events, more extensive fields for 00Z were used to run COAMPS to examine additional aspects of MSC events. From these cases, data was obtained from the Master Environmental Library (MEL) at the Naval Research Library in Monterey, California to initialize COAMPS.

II. METHODOLOGY

A. CLASSIFICATION OF STRATUS EVOLUTION

The first step to characterize MSC evolution was to examine all visual GOES-10 satellite imagery from 1 June to 31 August 2000. The imagery consisted of; a western region that included the western United States and the coastal area of the Eastern Pacific Ocean (not shown), as well as four regional, one kilometer resolution pictures titled Seattle, Washington, Eureka, Monterey, and Los Angeles, California that correspond to the National Weather Service (NWS) forecast office that they support. Figures 1 through 4 are examples of the regional satellite pictures studied. These pictures were archived at 30-minute increments with some limited exceptions, i.e. picture was too dark, missing pictures, and the occurrence of corrupt files for one reason or another. The satellite imagery was compiled on three CD-R's; each one containing one month's worth of data, approximately 650MB for each month. The data set was relatively complete with the following breakdown. There were 3877 pictures for the month of June of which 176 were unusable or corrupt, and there were no pictures available for the 11th of June. July and August contained 4380 images each. July had 380 unusable or corrupt pictures with the 2nd-4th of July experiencing the phenomena of "ground hog day" where the satellite images were identical, but correctly labeled in 30-minute increments. August had 390 unusable or corrupt files. The nature of the unusable or corrupt files was sporadic and therefore, did not hinder the classification of MSC evolution for nearly all days in the three-month period.
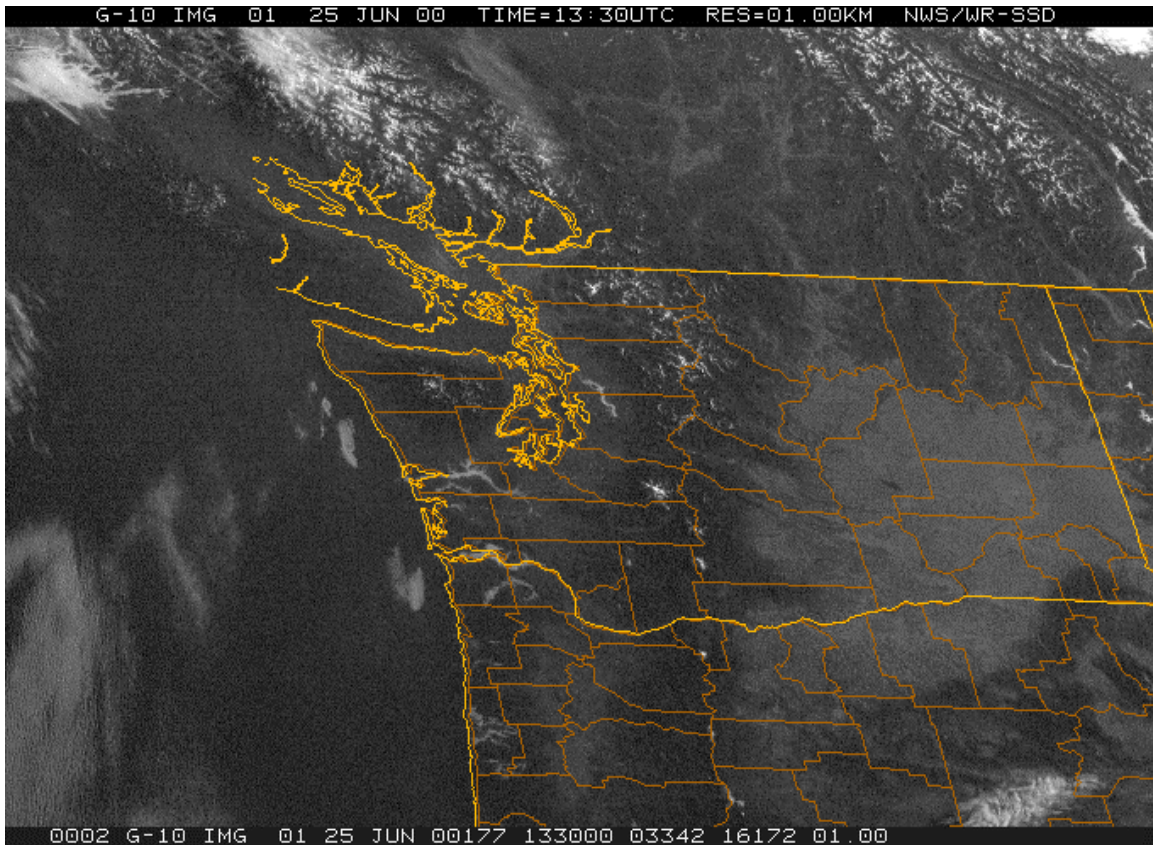
Figure 1. Seattle, Washington GOES-10 regional imagery.

To facilitate the classification of fog and stratus tendencies, each month's satellite imagery was transferred to a laptop computer, where it could be animated for easier initial evaluation of the imagery. Thumbnails of images were created using an evaluation copy of a program called Graphic Workshop Professional, version 2.0a by Alchemy Mindworks Inc. 1998 (patch 18). This particular software package allowed for the display of numerous images at once and could further evaluate a series of images through the use of the slideshow feature set at one-second delay between images. This allowed for a near continuous loop of images and hence easy classification of fog and/or stratus tendencies for each of the four required sections.
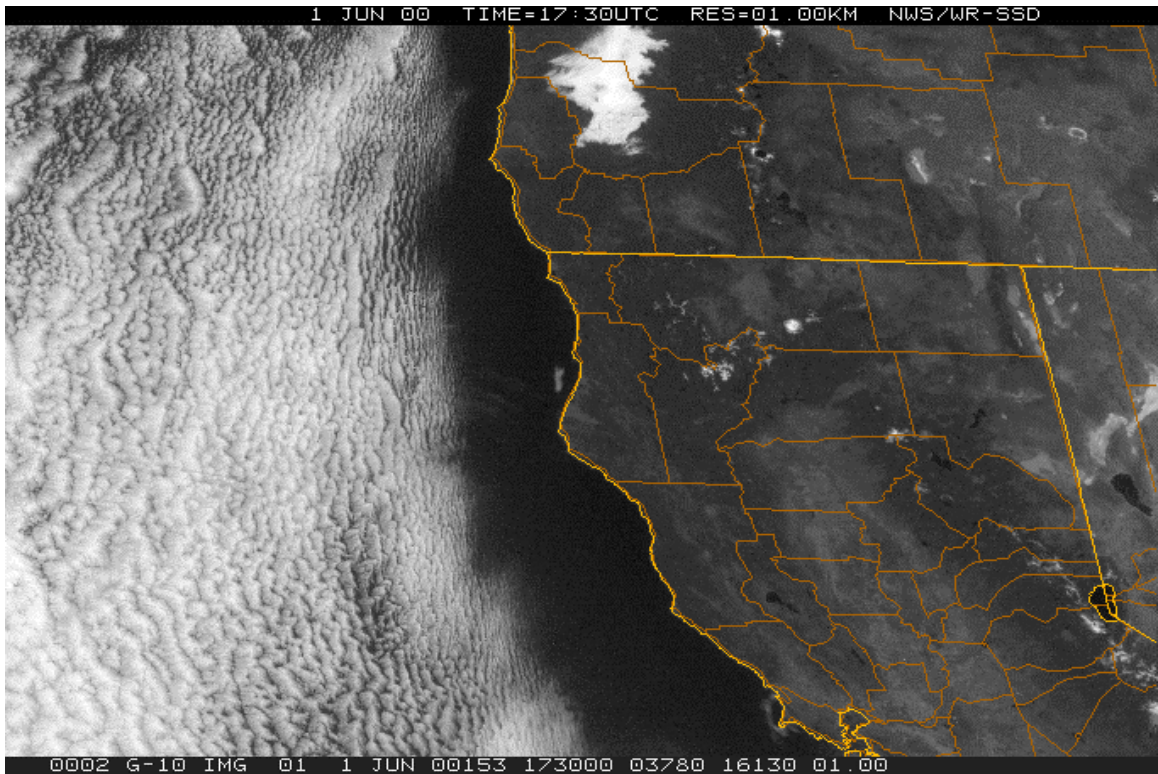
Figure 2. Eureka, California GOES-10 regional imagery.
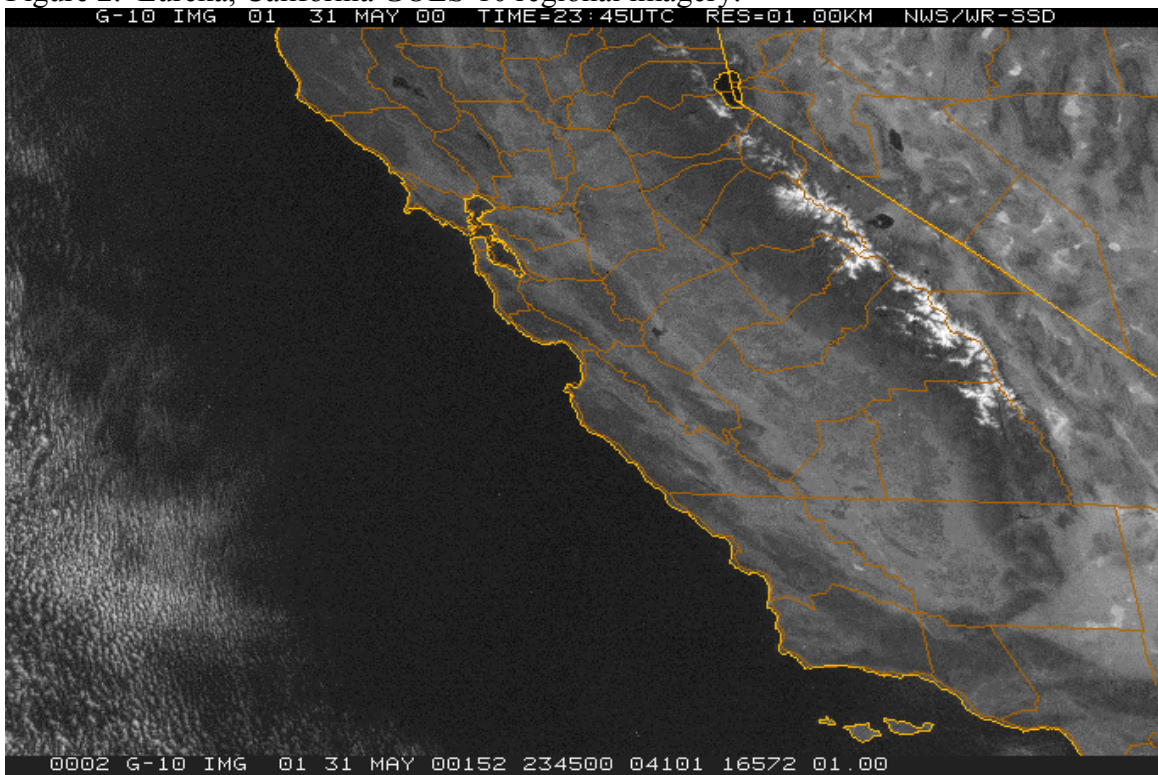
Figure 3. Monterey, California GOES-10 regional imagery.
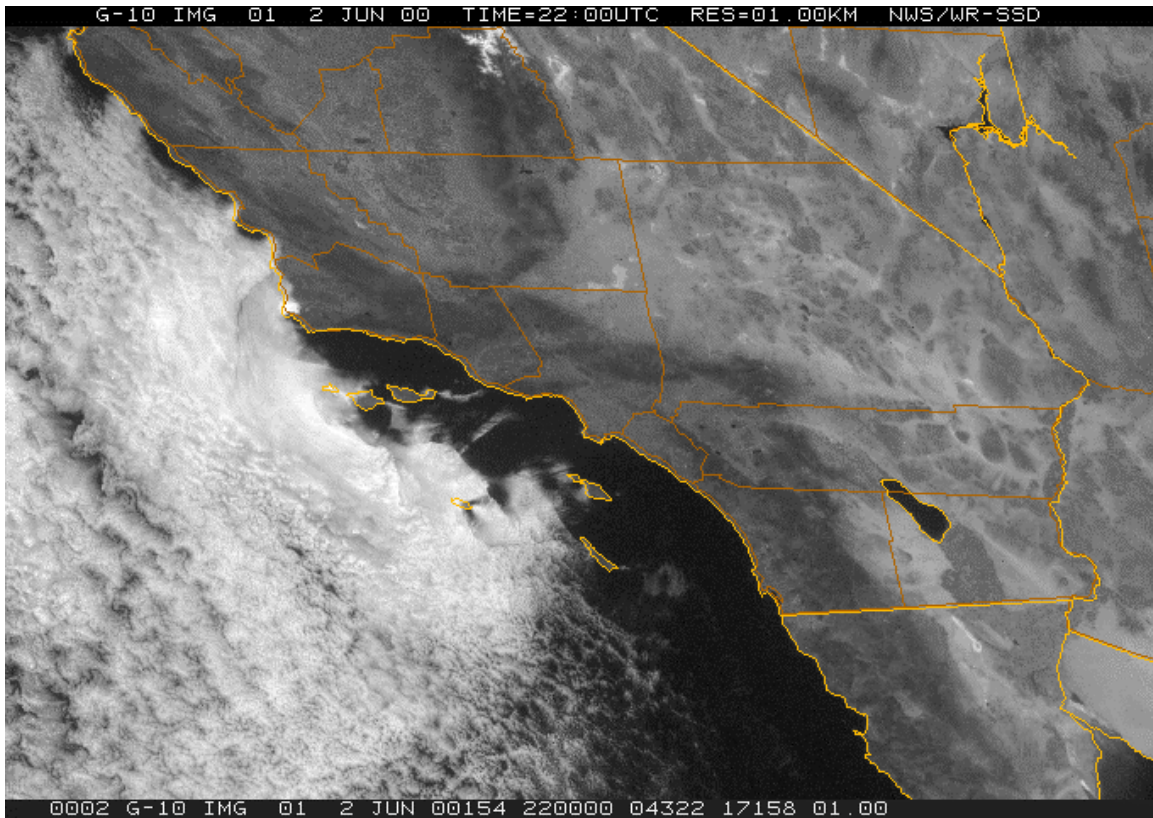
Figure 4. Los Angeles, California GOES-10 regional imagery.

After the initial evaluation of imagery, it was decided to characterize the large number of images into the daily, daytime (visual satellite images) evolutions only. In particular, only the fog and stratus that occurred within approximately 3km of the coast and its daily evolution was considered.   The following categories were developed to initially separate the MSC events that occurred within 3km of the coastline and are based on the tendency of the MSC event during the daylight portion of the day.

- MSC category 1. Fog and stratus dissipating or decreasing in coverage.
- MSC category 2. Fog and stratus developing or increasing in coverage.
- MSC category 3. Fog and stratus associated with a front.
- MSC category 4. No change or decreasing coverage in fog and stratus then increasing coverage.
- MSC category 5. No change or increasing coverage of fog and stratus then decreasing coverage.
- MSC category 6. Little or no change in coverage in fog and stratus.

10

- MSC category 7. Fog and stratus not present.

Examples of each category with the exception of MSC category 7 are given in limited sequences in Figures 5 through 10 on the following pages to give a clearer indication of the tendency of the MSC event. The figures show a sequence of three images beginning in the early morning to midday, and finally late afternoon.
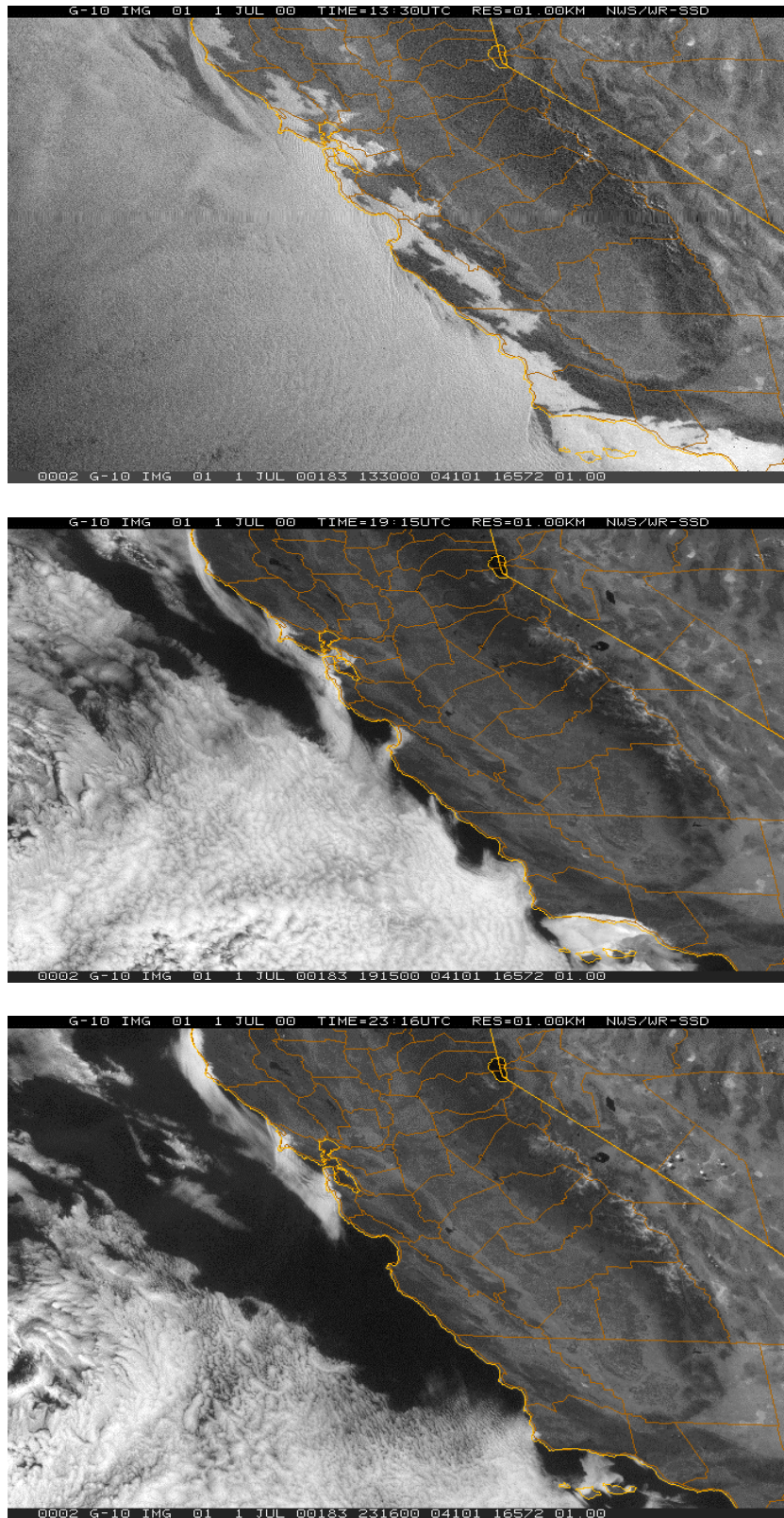
Figure 5. Example of MSC category 1. (Decreasing)
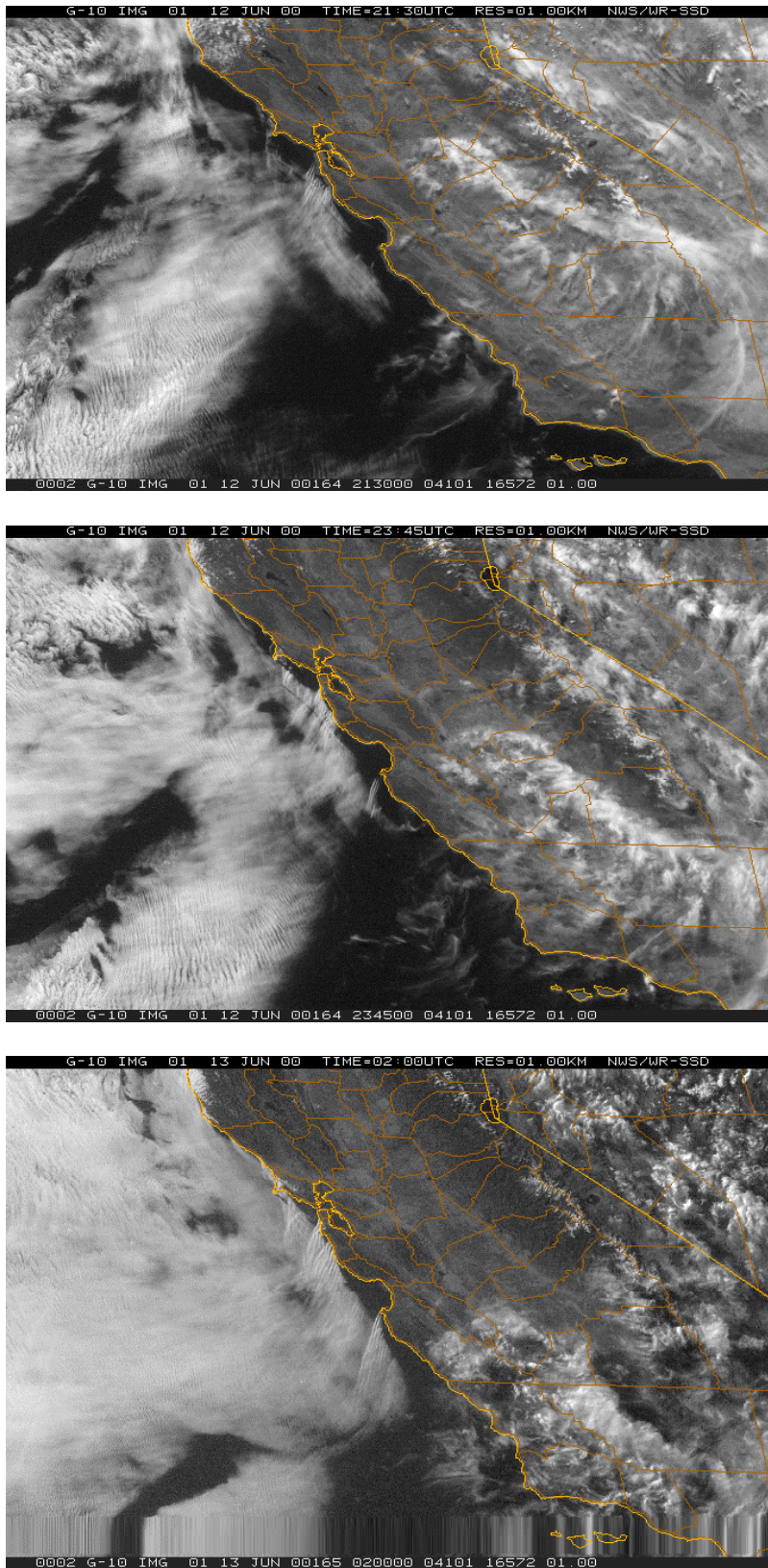
Figure 6. Example of MSC category 2. (Increasing)
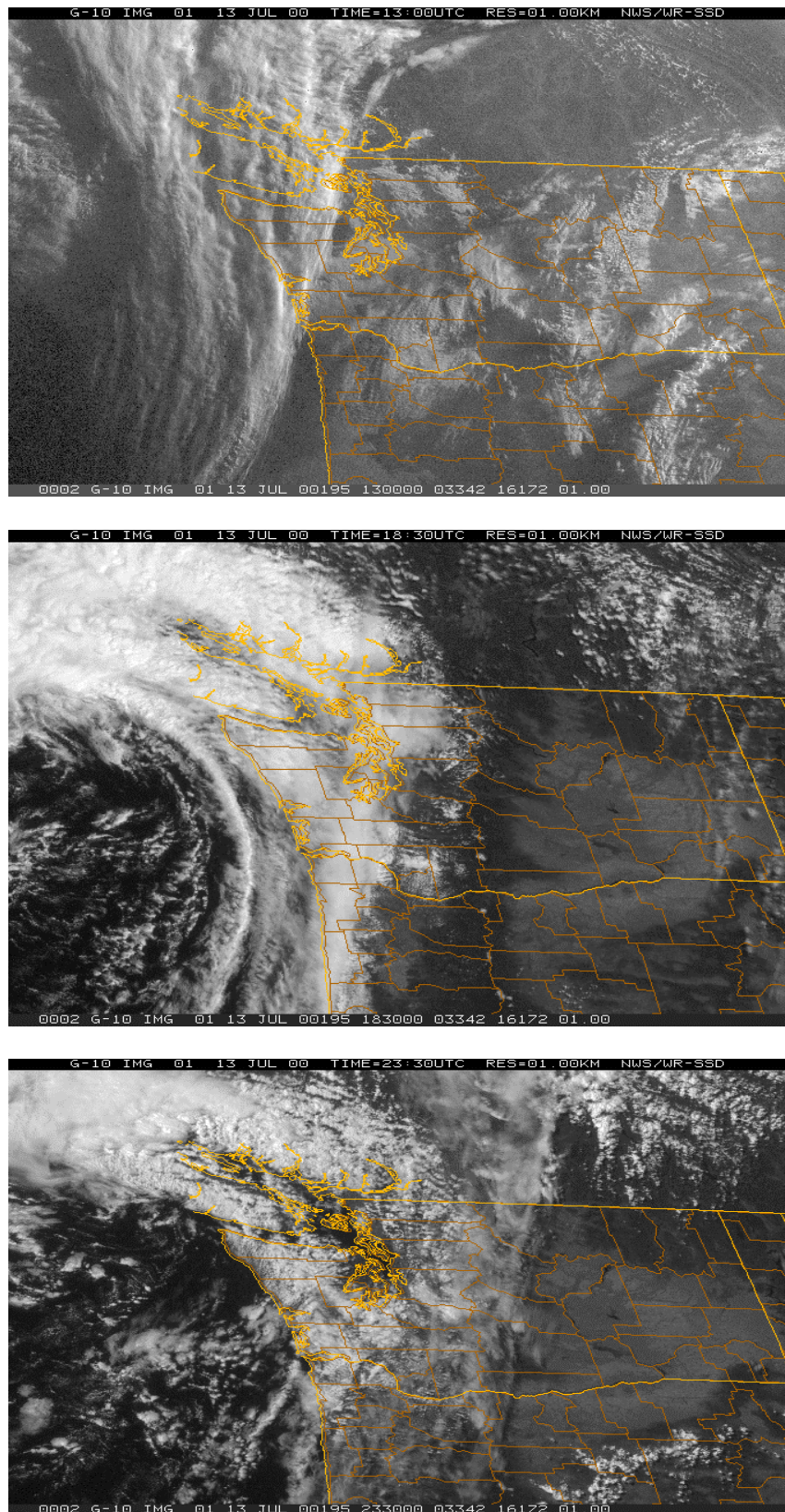
Figure 7. Example of MSC category 3. (Frontal)
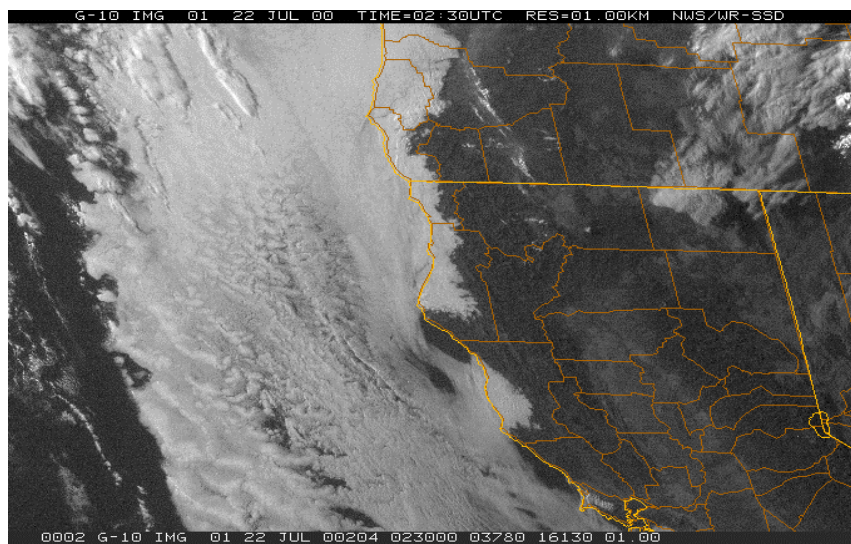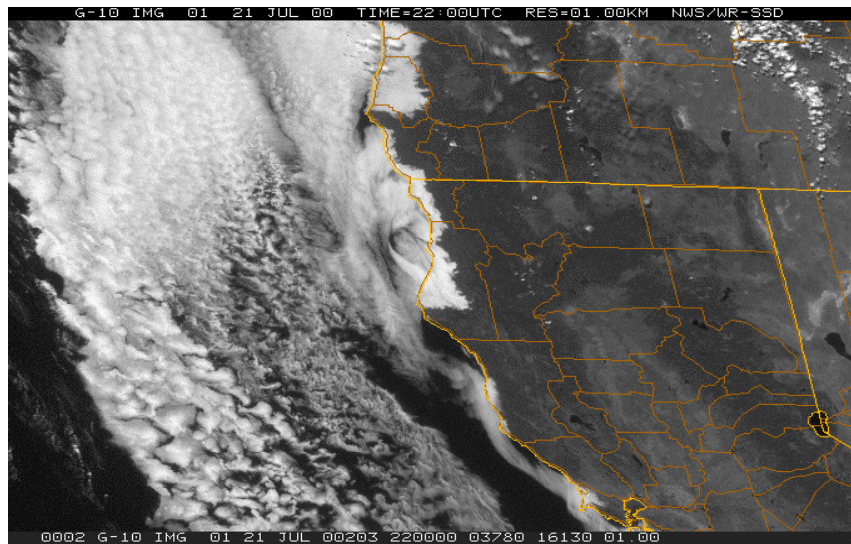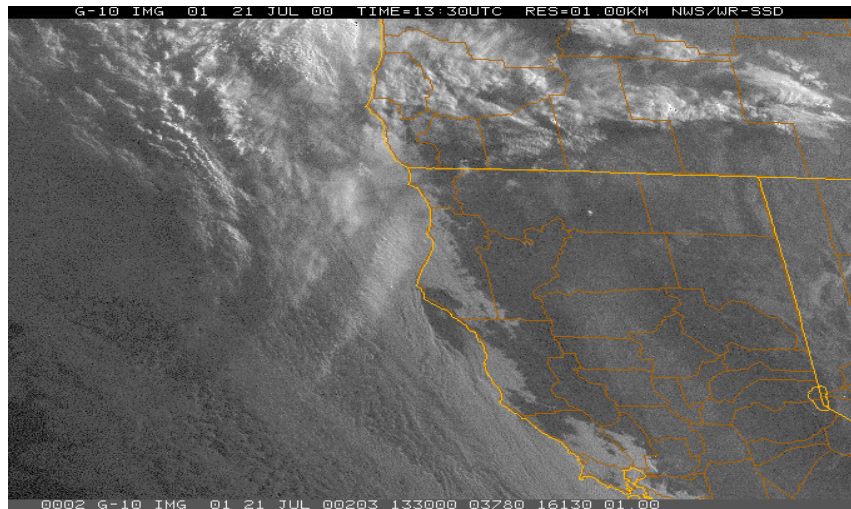
Figure 8. Example of MSC category 4. (Decrease then increase)

15
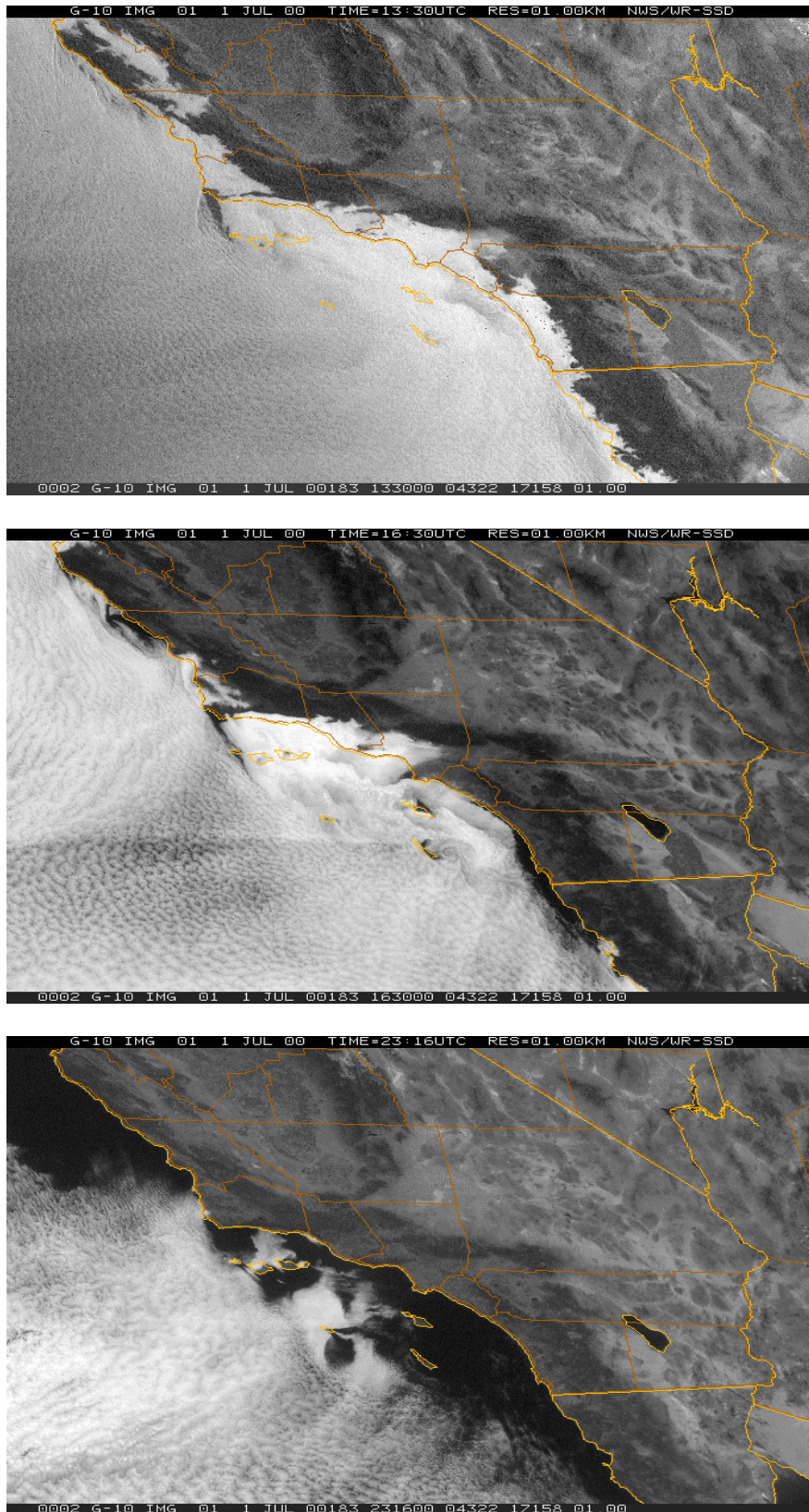
Figure 9. Example of MSC category 5. (No change then decrease)
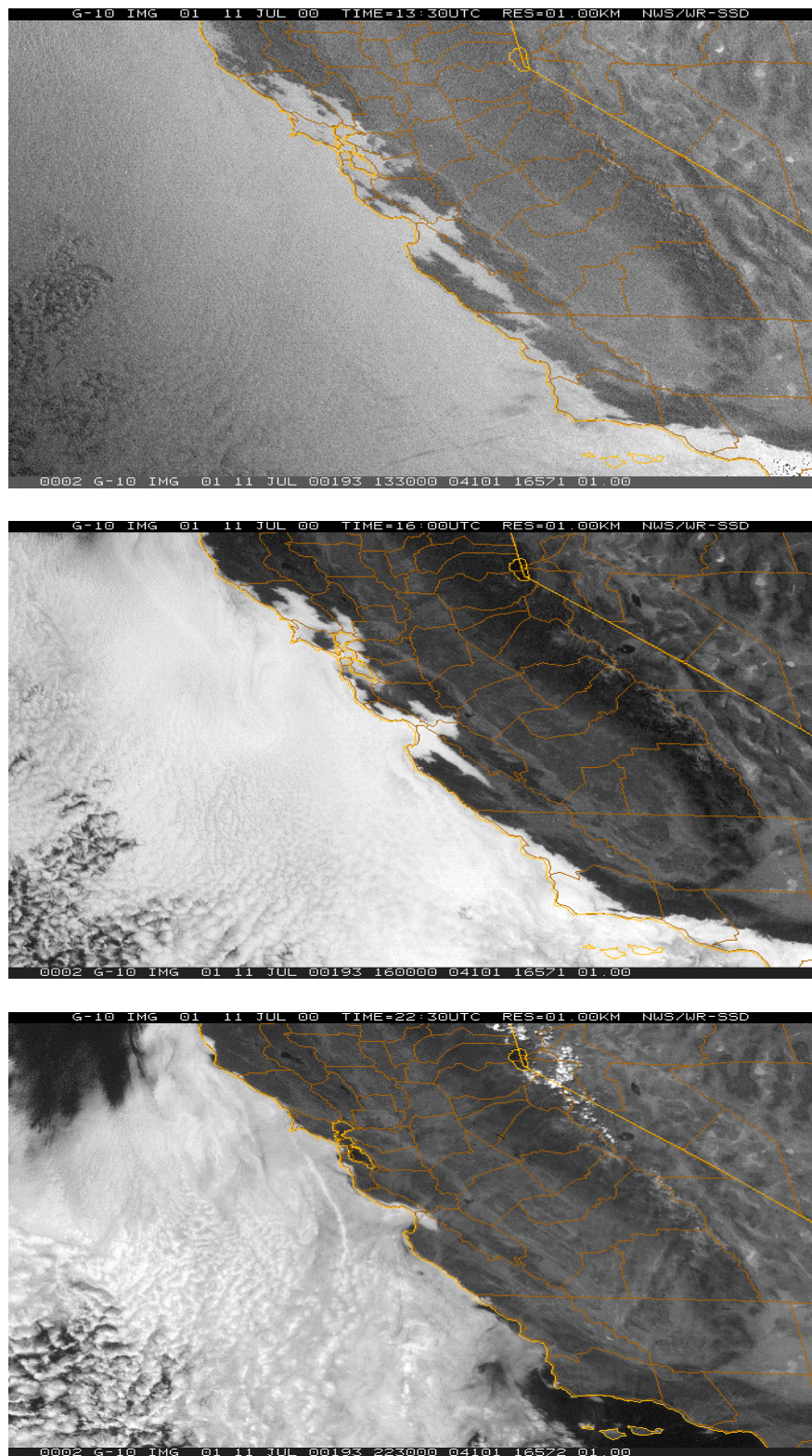
Figure 10. Example of MSC category 6. (Little change)

MSC category 1, Monterey region shown in Figure 5, is where the daily, daytime visual imagery of the evolution of the MSC event showed dissipating or decreasing coverage without any perturbations in the sequence. The satellite sequence showed clear evidence of dissipation or decrease in coverage in any of the particular regions described. This is not to imply cloudy to clear, but indicates a tendency towards less fog and stratus.

MSC category 2, Monterey region shown in Figure 6, is where the daily, daytime visual imagery of evolution of the MSC event showed forming or increasing coverage without any perturbations in the sequence. The satellite sequence showed clear evidence of formation or increase in coverage in any of the particular regions described. This is not to imply clear to cloudy, but to indicate a tendency towards more fog and stratus.

MSC category 3, Seattle region shown in Figure 7, is where an MSC event is associated with a frontal system regardless of tendency during the daytime. The dynamics of the evolution of any fog and stratus are clearly related to the front, albeit pre- or postfrontal.

MSC category 4, Eureka region shown in Figure 8, is where the MSC coverage is static or undergoing a decrease in coverage followed by an increase in coverage during the daytime visual imagery of evolution of the MSC event. This category differs from MSC category 1 by the perturbation in the beginning of the sequence there is static or decreasing coverage prior to the increasing tendency. The satellite sequence showed clear evidence of several hours of static or decrease in coverage followed by an increase in coverage in any of the particular regions described.

MSC category 5, Los Angles region shown in Figure 9, is where the MSC coverage is static or undergoing an increase in coverage followed by a decrease in coverage during the daylight hours. This category differs from MSC category 2 in that the beginning of the sequence there is static or increasing coverage prior to the decreasing tendency. The satellite sequence showed clear evidence of several hours of static or

increase in coverage followed by a decrease in coverage in any of the particular regions described.

MSC category 6, Monterey region shown in Figure 10, is where the MSC event exhibits little to no change in coverage throughout the day. Any change is one tenth or less in any given region. The satellite sequence showed clear evidence of little or no change in any of the particular regions described.

MSC category 7 is where there was no fog and stratus present within 3km of the coast during the day.

These category definitions describe the coastal conditions only and, therefore, do not reflect meteorological conditions further offshore or inland. As shown in many satellite images thus far, many times there are marine clouds that cover several thousand kilometers (offshore), but are not affecting the shoreline.

It is clear and deliberate that these categories are based on tendency throughout the day of the MSC events, and further broken down to the four individual regions described previously. This was done in anticipation of using a mesoscale model to search for mesoscale features that may be unique to each of the four regions, i.e. a Catalina Eddy in the bight region of California.

The majority of the MSC events were clearly identifiable using this technique; however, there were a small number of events that were borderline between categories. This was especially true when satellite imagery for a particular day was missing in part or in total. In these cases, 23 years of forecasting and satellite evaluating experience were used in making a subjective judgment call. While not perfect, it was a logical and confident step. While only seven percent of all satellite pictures experienced problems, the MSC tendencies were evaluated before and after the missing pictures, compared to the known synoptic situation as evaluated against other known synoptic situations, and finally compared to surface observations to make certain that fog and/or stratus was or was not reported.

Once categorized, several statistical analyses were performed to separate the individual categories for the individual regions by month, and to make a detailed

accounting of the dates of occurrence for each type of MSC event. These steps were vital in running composites of the synoptic situation. The examination of individual categories will be discussed in more detail in Chapter III, while the statistical accounting is discussed below.   Tables 1 through 3 illustrate the results of this statistical analysis of the MSC events, i.e. based on tendency of the MSC event, for each month during the summer of 2000.

Table 1 depicts three central categories into which the MSC events fall. Over 53 percent of the MCS events were category one, while only 19 percent were in category six and 14 percent were in category four. The remaining categories were inconsequential. The results clearly indicated that fog and stratus events had a strong tendency to dissipate

Category	1	2	3	4	5	6	7
Seattle	16	0	4	2	1	2	3
Eureka	14	0	3	3	1	8	0
Monterey	14	2	1	1	0	11	0
Los Angeles	17	0	0	10	0	2	0
Total cases:	61	2	8	16	2	22	3

Table 1. June MSC events statistical breakdown per category. Note the preponderance of category 1 cases (MSC dissipating or decreasing in coverage).

throughout the day in all regions studied. Consider categories one and four combined, both indicate dissipation in the fog and stratus events, the resulting percentage is now 68 percent.

Category	1	2	3	4	5	6	7
Seattle	15	4	1	4	0	6	0
Eureka	15	0	1	6	1	8	0
Monterey	21	2	0	1	0	8	0
Los Angeles	25	1	0	4	0	2	0
Total cases:	86	7	2	15	1	24	0

Table 2. July MSC events statistical breakdown per category.

During July, the statistical breakdown was far more dominated by MSC decreases than June. Table 2 shows a strong predominance towards fog and stratus dissipation with nearly 75 percent of the days experiencing category one or four events. The remaining category, six, occurred nearly 18 percent of the time.

When compared to June and August, July exhibited the greatest frequency of dissipation of fog and stratus events. July also exhibited the greater frequency of fog and stratus events that showed no or little change throughout the day. No region experienced a clear day during July, making the month the foggiest of the summer.

Category	1	2	3	4	5	6	7
Seattle	21	1	1	3	0	5	0
Eureka	18	0	0	2	1	8	0
Monterey	19	1	0	2	4	5	0
Los Angeles	15	0	0	9	1	4	2
Total cases:	63	2	1	16	6	22	2

Table 3. August MSC events statistical breakdown per category.

While August was nearly a clone of July, there were some indications that the MSC events began to lessen near the end of the month. Nearly 71 percent of the cases as shown in Table 3 show dissipation, nearly 20 percent of the time the fog and stratus exhibits no or little change. Two days, both of which were in the Los Angeles region, did not experience any fog and stratus as compared to July where these days were clear.

The summer cycle seems to indicate a maximum influence of frontal-associated fog and stratus in June; the beginning of summer, while cases of dissipation is the lowest. July brings fog and stratus events to all regions, with the dominant tendency being dissipation throughout the day. August is also a month where fog and stratus events occur nearly everyday. However, there were some indications of a slight break in the tenacity of the fog and stratus near the end of the month.

B. CHOOSING REPRESENTATIVE CASES

1. Extraction of Dates and Composites

In order to characterize the relationships between MSC categories and the evolution of the synoptic-scale circulations, the dates of each type of MSC event were identified. This was done simply through the use of Microsoft's Windows Find routine, since the files were named by date. During the previous step, the image files for the MSC events in each category had already been separated and it became a simple procedure to count each MSC event in each category and to make note of the dates of the MSC events for each month. Further discussion of the actual results using this classification will be given in Chapter III.

After compiling the dates for each MSC event and separating the MSC events into categories and regions, 135 files (each of the seven categories – where applicable – in each of the four regions by three months at 00Z and 12Z = 82 files and averaging the 00Z and 12Z left 53 files) listing the dates for each classification were created to use in constructing synoptic composites. Consequently, each file contained dates separated by category and region broken down by month, i.e. all category 1 MSC events for the Seattle region for the month of June. This process was initially done for all regions and all categories broken down separately at 00Z and 12Z for each month. This separation into

00Z and 12Z composites was to examine any diurnal signature. In addition, the 00Z and 12Z analysis were combined, thus averaging the diurnal effect to highlight the background synoptic-scale structure for each month.   This also allowed a comparison of the effect and strength of the diurnal change to the average.

In addition, the 00Z and 12Z files were combined for each month by region and category over the entire summer period of this study, i.e. all category one MSC events for Seattle, Eureka etc. These were created monthly for each region to examine the summer average without diurnal change. This was done for comparison purposes to the entire summer averages to determine the effect and strength of any summer variability, especially within the synoptic patterns.

Composites of the synoptic situation for all 135 different collections were done through a computer routine based in FORTRAN 77 code that averaged eleven atmospheric parameters by summing each field over all events and then dividing by the number of events. This was done from the surface to the 300mb level using the standard atmospheric levels. See Appendix A for a copy of the FORTRAN 77 code used. Additionally, after the composites were produced, the results were converted into a GEMPAK grid format in order to be viewed using GARP.

Once in GARP, overlaying the mean sea-level pressure with 10-meter winds and 2-meter temperature at 2 degree Fahrenheit increments was done to characterize the synoptic pattern over of a large portion of the Pacific Ocean and the western one third of the U.S. This step allowed for the comparison of the various composites to determine the synoptic similarities that might exist and the strength of any such similarities between the MSC event categories previously described.

2.   Representative Cases Chosen for COAMPS Simulations

To gain additional insight into the physical relationships that force the various MSC evolutions, 11 dates were chosen to simulate using COAMPS. Only the most prevalent categories were chosen for analysis in order to keep the analysis manageable. The 11 days were based on comparisons with composites to best match the day-to-day synoptic patterns as well as to match a particular category for all regions; i.e. the same MSC categorical event occurred on the same day for each of the four regions. This was a high priority in order to minimize computer simulation time. Further considerations were

also taken into account in decreasing level of prioritization. Dates were chosen in the middle of the month to best depict monthly variability throughout the period of study and dates were picked if three of the four regions had MSC events that occurred on the same day. The only exception to this was the dates selected to run simulations for category four MSC events. This event occurred throughout the period of study, but not necessarily on the same day for each region. Since this type of event manifested itself as a reoccurring event, five days were chosen to adequately study this type of MSC evolution more closely.

The above described priority factors resulted in the following COAMPS simulations: category one (three days), category four (four days), category six (three days), and category five (one day). The data fields at 00Z were used to initialize the model, which was allowed to run for 36 hours with output at three-hour increments. The 00Z initialization allowed any model perturbations to smooth out prior to the examination period between 12Z and 00Z for the next afternoon local time. The selected dates are listed in Table 4.

Month	June	July	August
Dates	1st, 8th, 28th	18th, 19th, 20th, 30th	4th, 7th, 16th, 18th

Table 4. Summary of date's chosen for COAMPS simulation runs.

C.   COAMPS SIMULATION RUNS

The model simulations were initialized with the data obtained from the Master Environmental Library (MEL) for 00Z on the day to be examined (afternoon of previous day local time). While a cold start was done for each day selected, the forecasts from 12Z to 00Z were used for this study to allow the model to adjust any imbalances in the initial structure.

The COAMPS model configuration used for these simulations was chosen to allow ample synoptic and larger-scale mesoscale resolutions. A detailed description of COAMPS is given in Appendix B. The grid resolution used for the COAMPS simulations were 63 km for the outer grid and 21km for the next nested grid. The model domain for

both grids is shown in figures 11 and 12. These grids adequately capture the large-scale evolution on the outer nest and mesoscale evolution on the inner nest. While higher resolution nests could have been included, the focus was on the relationship between MSC events and synoptic evolution. Consequently, no additional fine-scale nests were used.
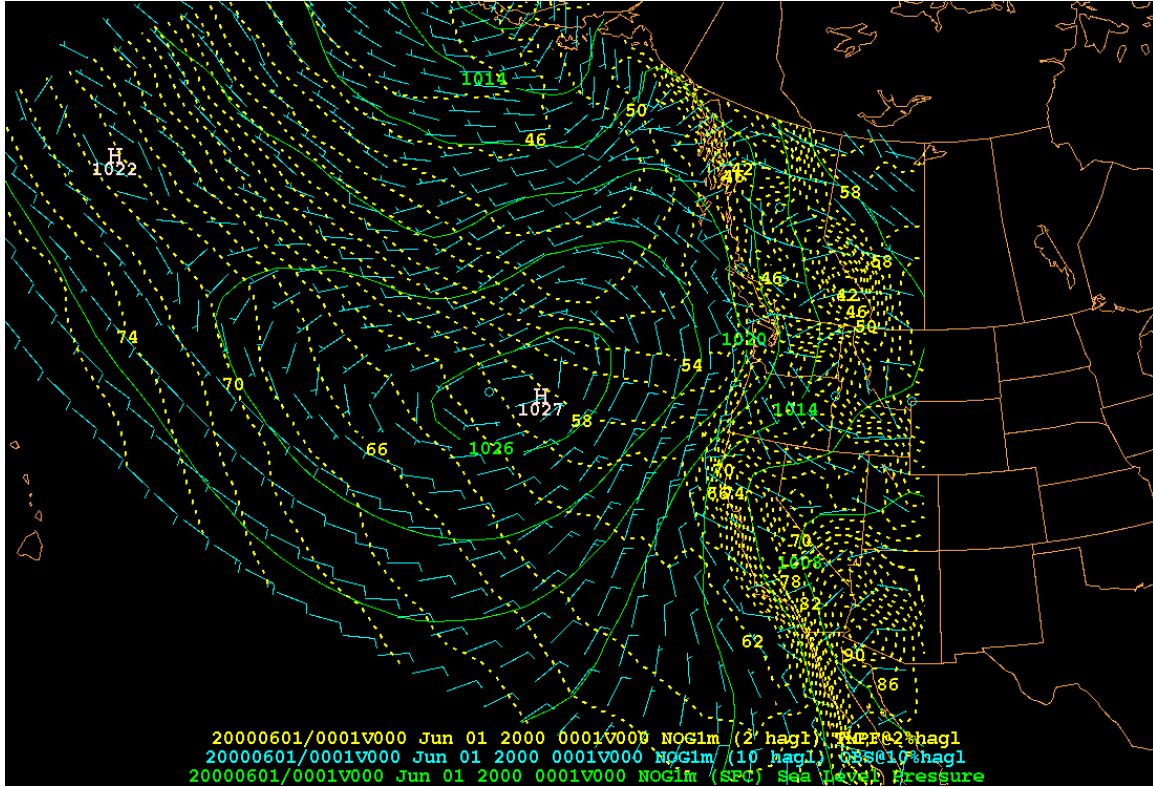
Figure 11. Example of aerial coverage of the outer COAMPS grid used (63km).
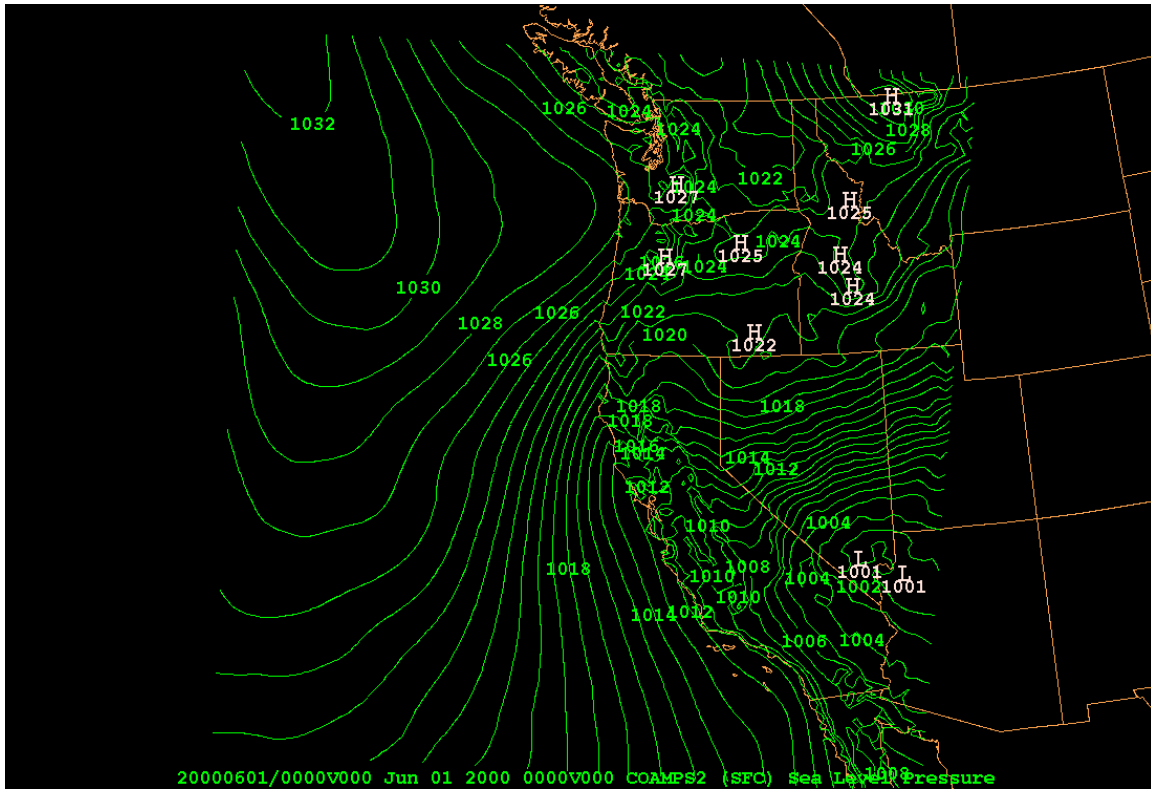
Figure 12. Example of aerial coverage of the middle COAMPS grid used (21km)

The 11 case studies selected were simulated using NOGAPS boundary conditions on the outer nest. Their results were evaluated for inconsistencies and compared to limited hand analyses for verification through the use of GARP. While it is widely accepted that computer simulations result in errors, there are consistent signals, especially in the synoptic pattern that can be utilized with a high degree of confidence. These particular simulations were no different. All simulations began with perturbations that even a rookie forecaster would have been able to pick out, but in all cases, the simulations smoothed out quickly and were reasonable, with the notable exception that the moisture variable was somewhat inconsistent when depicted in Vis5D. There was a consistent tendency to over develop the clouds where none exisited as seen on the various satellite images.

The forecast fields at both the 63 and 21km resolution were put into GRIB format for ingesting into GARP where several meteorological parameters were evaluated beginning with the synoptic patterns followed by an examination of the coastal regimes

26

through the use of cross-sectional analysis. The fields were studied at three-hour increments from 12Z to 00Z, the local daylight timeframe. A worksheet was developed to streamline the process of evaluation.

Upon conclusion of the GARP portion of the study, the fields were put into Vis5D to evaluate mainly the air-parcel trajectory from the synoptic-scale to the mesoscale coastal regime. While a host of other parameters could have been evaluated in Vis5D, the priority was trajectory analysis. This was done since other aspects of the analysis were covered using other techniques. Several examples of the output fields are presented in Chapter IV.

THIS PAGE INTENTIONALLY LEFT BLANK

III. SYNOPTIC PATTERNS ASSOCIATED WITH MSC EVOLUTIONS

To characterize the relationship between the various MSC events and the synoptic evolution, the composite analyses as well as individual synoptic charts were examined. Since the days that produced a given MSC category varied by region, each region was examined separately. The diurnal variation in the synoptic forcing was examined for the predominate MSC categories by combining 00Z and 12Z composites and analyses. In addition, individual months were examined separately in order to highlight any variation through the summer. This examination revealed some very consistent relationships between synoptic pattern and MSC evolution for each region, which are described in the following sections.

A.   SEATTLE REGION

During the month of June, only three days (25-27 June), did not experience a MSC event of some type. In other words, no fog and/or stratus/stratus cumulus clouds were present in the coastal regime. The synoptic pattern that was consistent in producing the non-MSC event, MSC category 7 – No MSC present, was the northward extension of the coastal inverted trough from the desert southwest. Figure 13 shows an example of synoptic pattern.   The remaining 27 days of June experience some type of MSC event, primarily MSC case 1 – MSC dissipating or decreasing throughout the day; 16 days. The synoptic pattern that was most closely associated with this event was the result of ridging into the Pacific Northwest. Typical cases associated with MSC
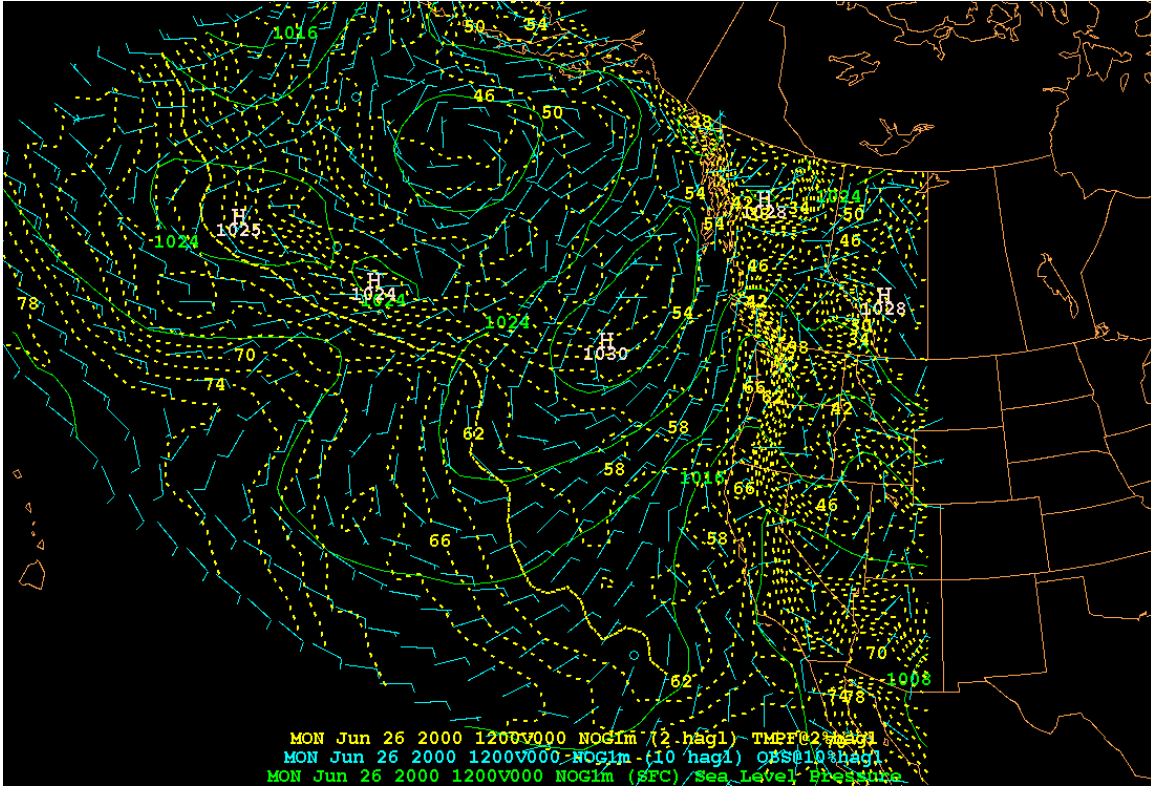
Figure 13. NOGAPS 26/12Z June 00 surface analysis. Note the coastal inverted trough along the entire west coast.

category one indicate an important relationship between the character of the surface ridging and the MSC evolution. Ridging from a cold-core high-pressure system, Figure 14, had the tendency to completely clear out the region rather quickly, prior to noon local. Whereas ridging that originated from the subtropical high-pressure system (shown later) had the tendency to show a slow decreasing amount of MSC coverage (category one or four) that for the most part never completely cleared the entire coastline. This type of MSC event was generally long term, i.e. lasted several days
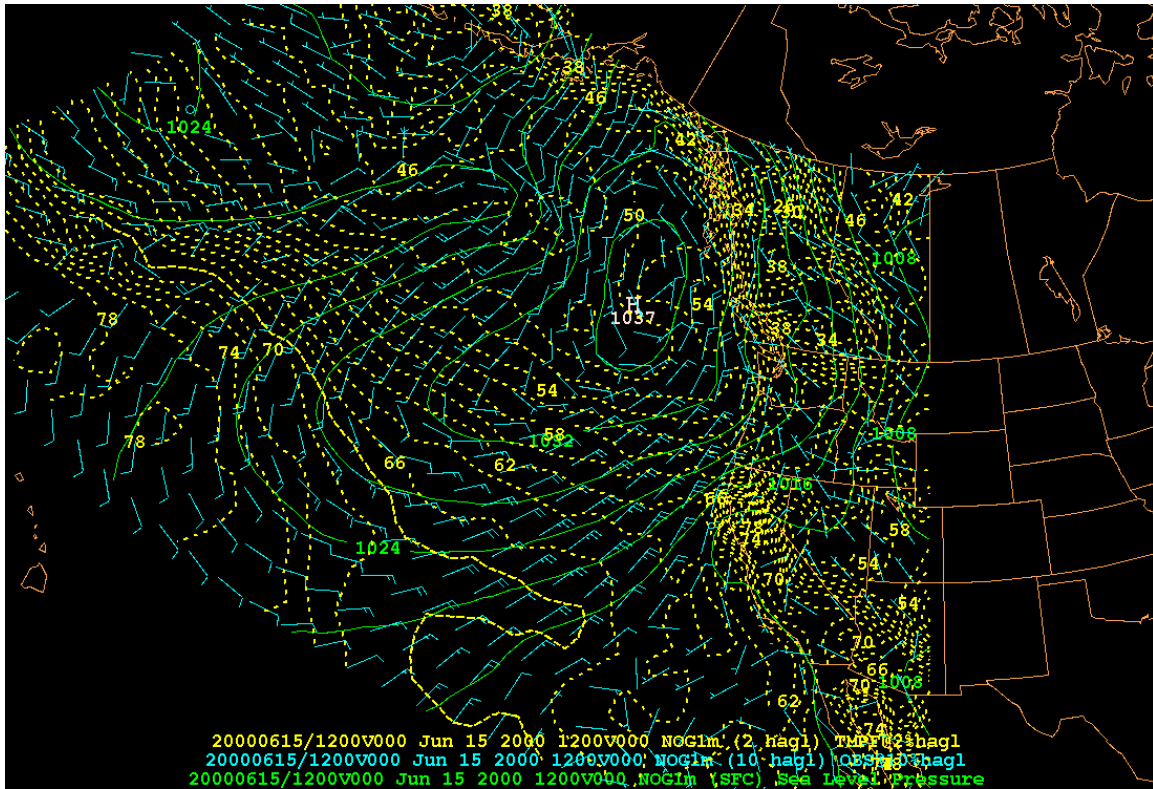
Figure 14. NOGAPS 15/00Z June 00 surface analysis. Note the ridging into the Pacific Northwest.

with some minor perturbations to the overall synoptic pattern. The MSC event reoccurred each day that subtropical ridging was present.

Table 1 described the statistical breakdown by MSC category for the month of June. As described previously, MSC category one was the predominate event for the Seattle region, with a small number of events occurring in the other categories. Figure 15 depicts a typical analysis that shows ridging into the Pacific Northwest that was commonly found to result in category one events.

31
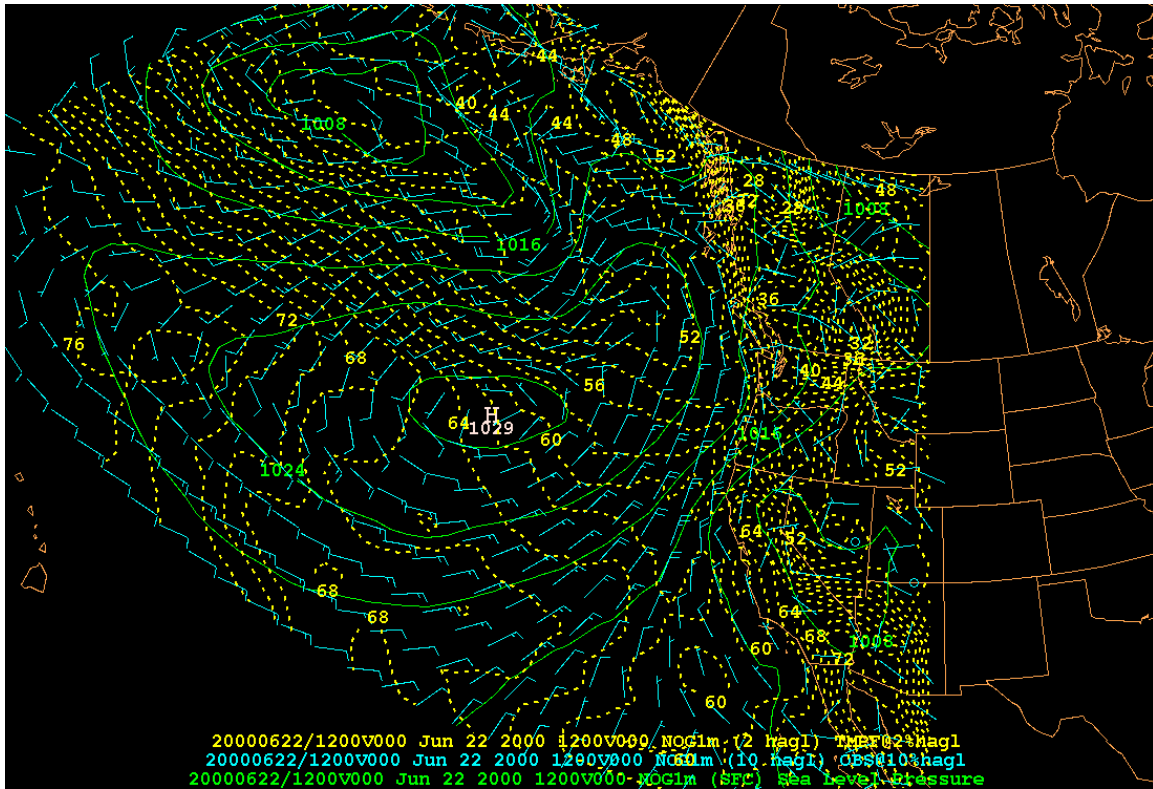
Figure 15. NOGAPS 22/12Z June 00 surface analysis. Note the subtropical ridging into the Pacific Northwest.

Although MSC category one dominated the July pattern, there were four days that the MSC pattern did not change during the course of the day, (i.e. MSC category 4, little or no change in MSC coverage). These days typically experienced strong ridging from the subtropical high, i.e. 1030mb or higher. A more eastward extension of the high is seen by the 1027mb center closer to the coast as shown in Figure 16. This eastward portion of the synoptic pattern is similar to that discussed for the Seattle region for the month of June. The central pressure of the subtropical high pressure was not a clear indication of a persistent fog and status event, whereas the near shore structure was more indicative. Other days during the month of July saw the subtropical high-pressure center exceed 1030mb with more prominent ridging in the Pacific Northwest, which resulted in numerous MSC category one events.
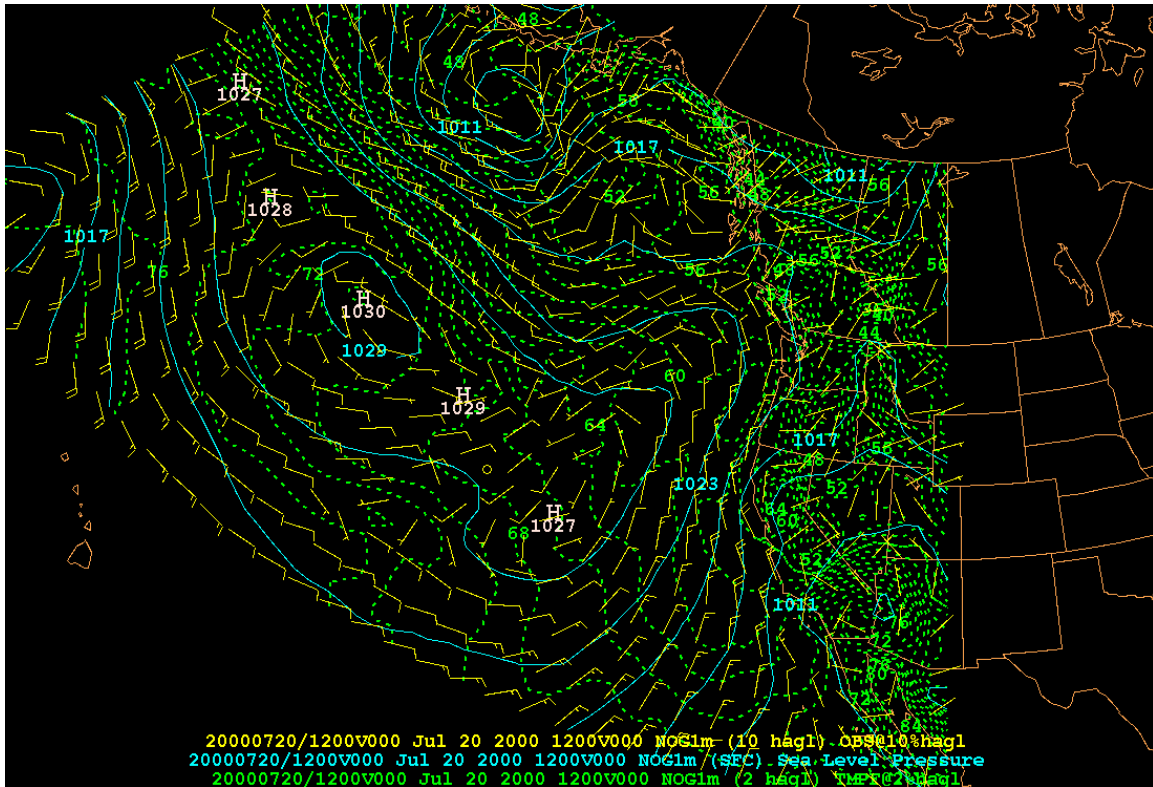
Figure 16. NOGAPS 20/12Z July 00 surface analysis. Note the strong subtropical high over the central Pacific Ocean and ridging into the Pacific Northwest.

Little change occurred for the Seattle region during the month of August. Again, a MSC event occurred in each day of the month with MSC category one being the overwhelmingly dominant case. While five days went with little or no change in MSC coverage, the synoptic situations that caused MSC category six were not any different than those that produced MSC category one except that the surface ridging did not diminish. Specifically, the anticyclonic curvature, which is the key, did not diminish. This is an import distinction that results in a MSC category one or four event from a category six event. During the month of August, the subtropical high-pressure center had moved further north to its climatological home and has strengthened. Its central pressure was consistently greater than 1030mb as illustrated in Figure 17. The ridgeline remained consistently extended into the Pacific Northwest. This resulted in numerous MSC events during the month.

Figure 17. NOGAPS 08/12Z August 00 surface analysis. Note the position, strength of subtropical high-pressure cell and continued ridging into the Pacific Northwest.

The composite near-surface synoptic scale structure for the 16 days of MSC category one is shown in Figures 18 and 19 are for the Seattle region at 12Z and 00Z respectively. The two composites show subtle diurnal changes that are associated with the diurnal decrease in stratus in MSC category one. Category six (no or little change on MSC coverage) and category seven (no fog and stratus) were the most prevalent other types during the month of June, with a few frontal events also.

Figure 18. Composite of NOGAPS June surface analysis at 12Z for MSC category one events in the Seattle region.

Comparing the 12Z and 00Z composites show a weakening of the surface ridge into the Pacific Northwest. This is a key synoptic signal that indicates dissipation of the fog and stratus event. The weakening of the surface ridging is due to daily inland warming, which results in lower surface pressure.
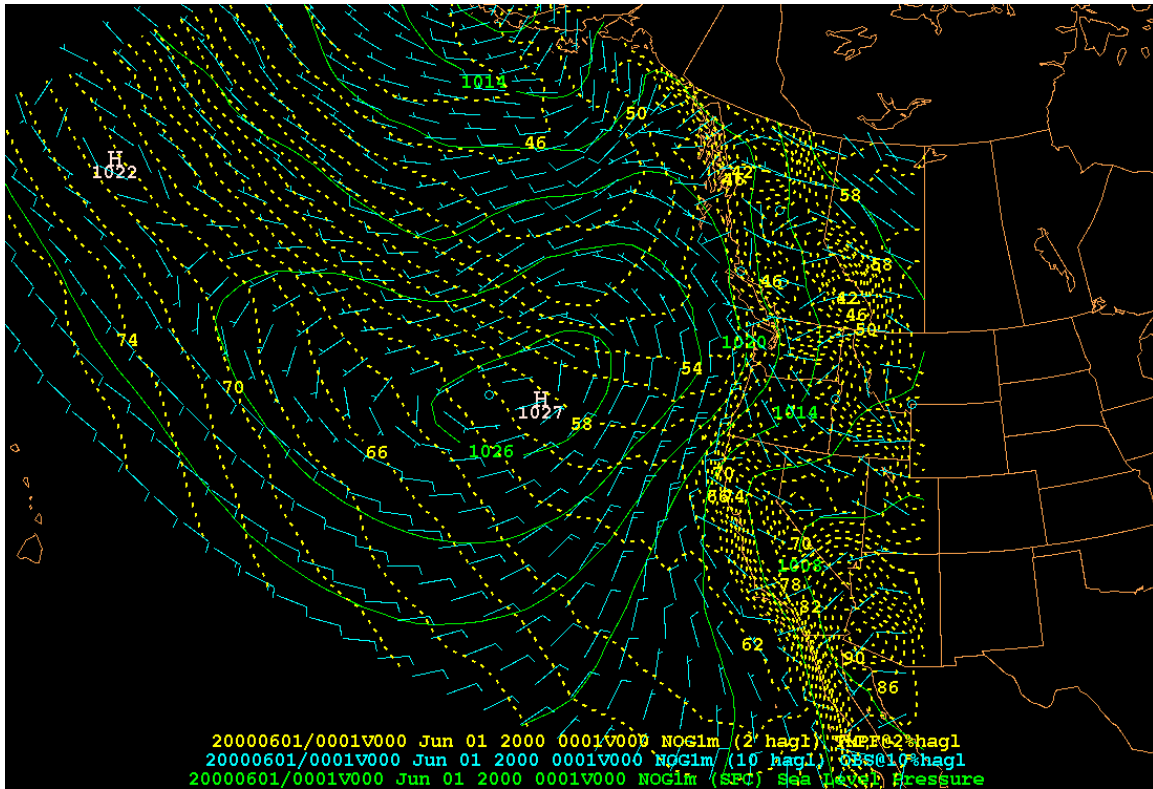
Figure 19. Composite of NOGAPS June surface analysis at 00Z for MSC category one in the Seattle region.

The morning or "cold" composite surface analysis, shown in Figure 18, where the MSC coverage is at its peak is characterized by the dominant subtropical high-pressure system that has a mean central pressure of 1026mb and produces a significant ridgeline into the Pacific Northwest. Coastal surface winds are light at approximately 10kts and slightly oriented onshore to parallel to the coast. The land-sea temperature contrast along the coastline is minimal, which is characteristic of low-level marine air over the inland areas and due to cold land surface's due to nighttime cooling if clouds are not present.

At the afternoon or "hot" composite surface analysis, shown in Figure 19, the subtropical high-pressure center is one milibar higher at 1027. The land-sea temperature contrast has increased slightly while the coastal surface winds have increased to 20kts in response to the increase in the pressure gradient force. The most telling signature is the decrease in anticyclonic turning of the sea-level isobars, which indicates a weakening of the surface ridging (not necessarily the surface pressure) into the Pacific Northwest. This

decrease in surface ridging is consistent with inland warming, which is due in part to decreased coastal stratus, i.e. more incoming short-wave radiation. Figure 20
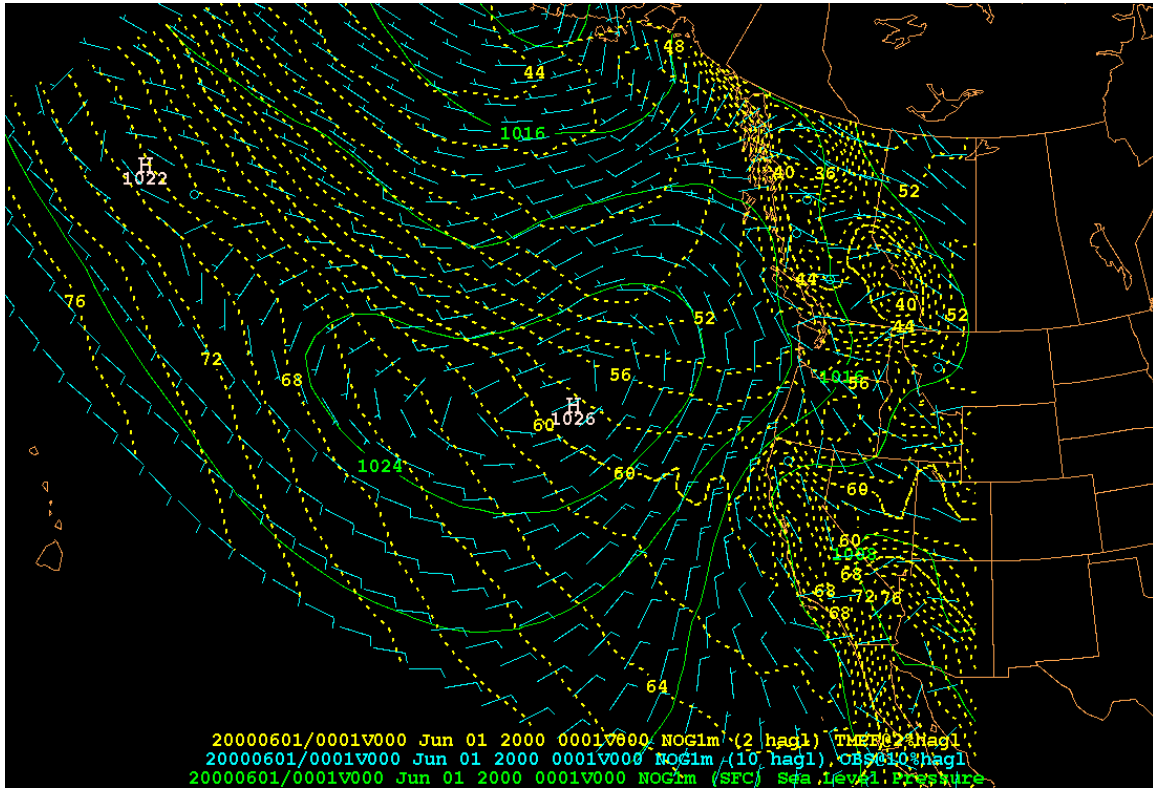
Figure 20. Composite of June MSC category one without diurnal variation for the Seattle region.

represents the composite of June MSC category one without the diurnal variation. Of interest is the lack of a baroclinic zone along the coast that is common in the more southern regions.

For a MSC category six event, no or little change, the composites (not shown) are similar to those for category one in Figures 18 and 19. However, the surface ridging into the Pacific Northwest does not abate during the day, but maintains its significant curvature throughout the day with little diurnal signature. This is consistent with a lack of inland warming and the persistence of MSC event inland.

In the somewhat rare cases where an MSC event does not occur, i.e. no fog and stratus present, this synoptic pattern is characterized by an inverted trough oriented along

the coast as illustrated in the composite shown in Figure 21. While the composite shows troughing, it fails to adequately show an offshore component to the winds, which were
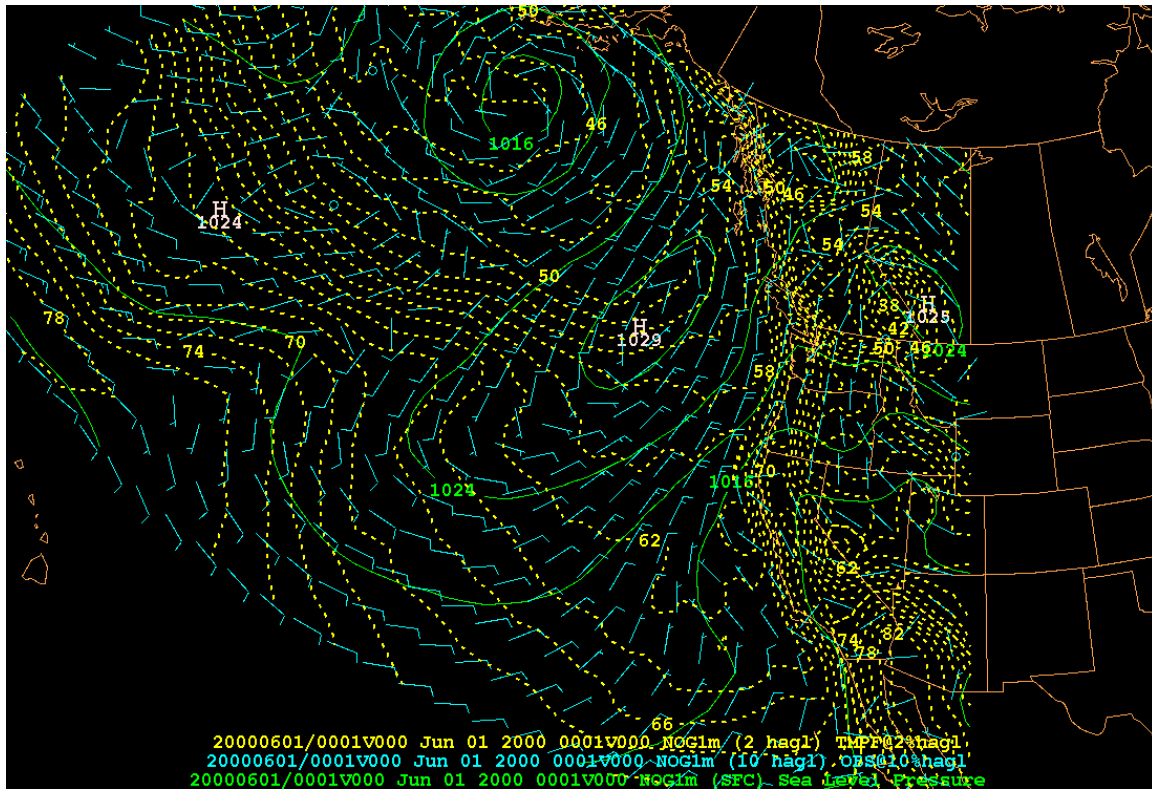
Figure 21. Composite of NOGAPS surface analysis for the month of June depicting a non fog/stratus event.

evident in many of the individual surface analyses such as shown in Figure 13. This offshore flow is a critical coastal process that prohibits fog and stratus formation and is best seen in the composites as coastal warming and troughing.

The July composites for MSC category one reveal little variation compared to the June pattern. The diurnal changes in the surface ridging over the Pacific Northwest remain the same as June. The biggest differences are in the position of the subtropical high and in the coastal winds. As shown in Figure 22, the surface coastal winds are now very light, less than 10 knots and are oriented more onshore. This is consistent with the more offshore location of the subtropical high, which tends to weaken the cross-coast pressure gradient. Even though the cross-coast pressure gradient is weaker, surface ridging into the Pacific Northwest is evident and its diurnal change continues to be the synoptic signature that indicates the evolution of category one fog and stratus events.
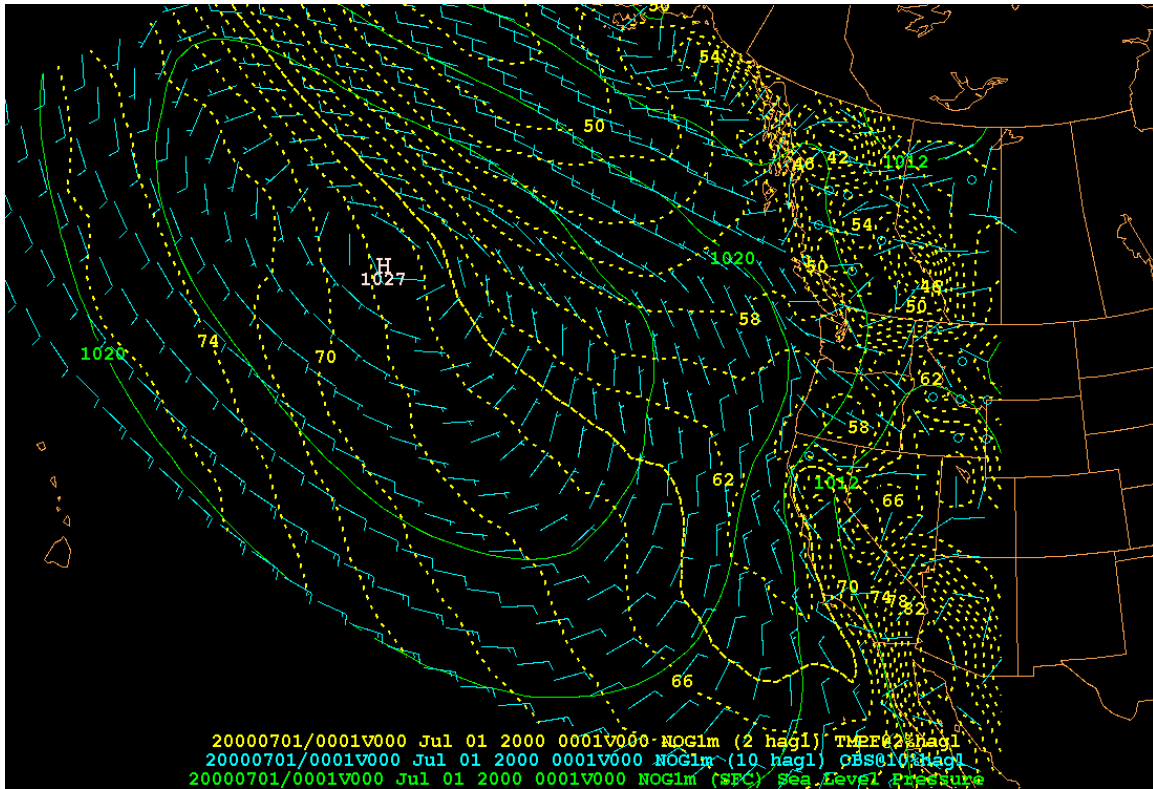
Figure 22. Composite of NOGAPS July surface analysis of MSC category one without diurnal effects.

Summer variability is exemplified most during the month of August. Table 3 shows that Seattle region experienced 21 occurrences of MSC category one events during August where the composite structure is quite different. Figure 23 shows the subtropical high much stronger and further north than in June or July. The ridging into the Pacific Northwest that characterized category one is less prevalent during August.

MSC category one patterns, shown in Figure 23 an example, shows the subtropical ridge now has a central pressure of 1031mb, which is a significant increase over June. Additionally,
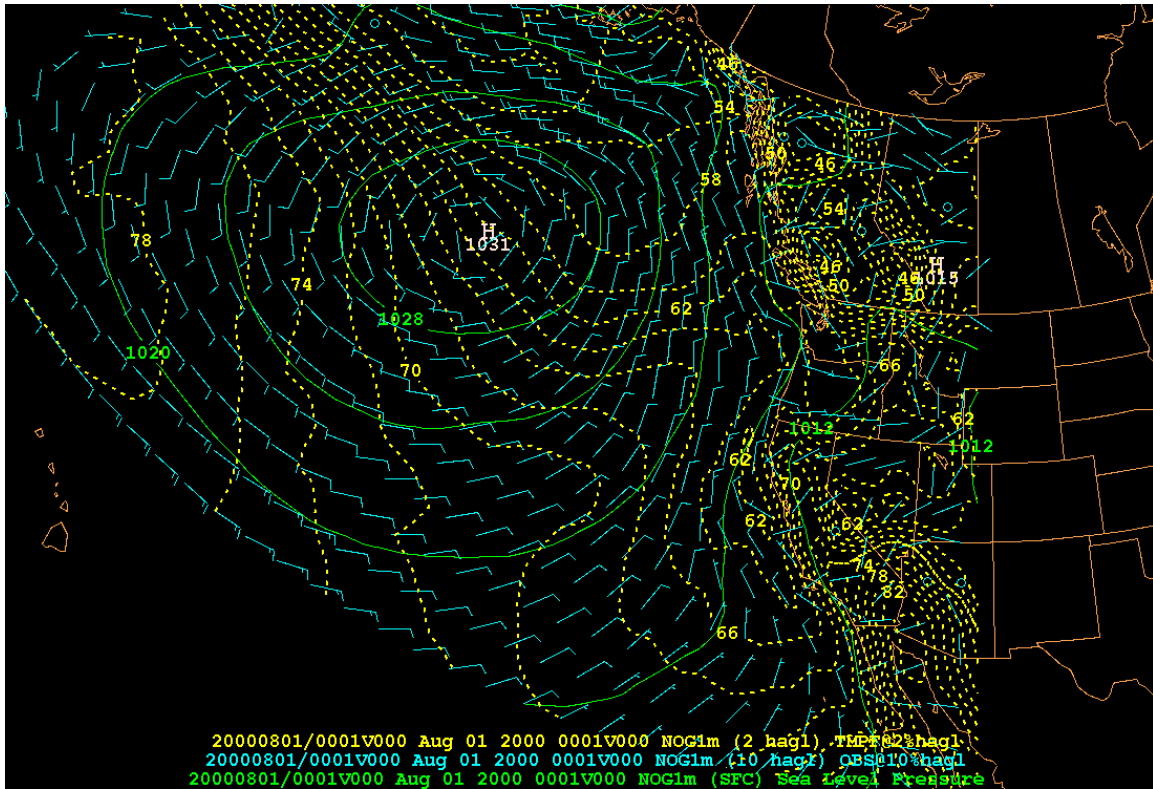
Figure 23. Composite of NOGAPS August surface analysis of MSC category one without diurnal change.

the ridgeline that was so prevalent earlier in the summer is now much less in anticylonic curvature. Earlier in the summer, this would be the telling signature of fog and stratus dissipation, but now in late summer it is not. The key synoptic relationship is the strength of the subtropical high-pressure cell, greater than 1030mb, to the degree of anticyclonic curvature into the Pacific Northwest that keeps the fog and stratus buttressed up against the coast and results in a category six event. This is due to increased subsidence and longer low-level trajectories that bring in cooler air.

Potentially, day-to-day variations in coastal sea surface temperatures during the month might account for differing MSC evolutions. Although only three buoys and a small handful of ships provided the coastal SST observations, they indicate that SST varied from 10-15 degrees Centigrade along the Pacific Northwest coast. Coastal buoys along the Washington coast varied only from 13 to 15 degrees C with 13-14 degrees C as the norm. The greatest variability appeared along the Oregon coast with SST's from 10-15 degrees C, although temperatures remained primarily in the 13-14 degree C range.

These SST's were comparable to or slightly warmer than the composite air temperatures seen in figures 18 and 19. However, the slight variability in SST's did not seem to impact the MSC events along the Pacific Northwest coast.

July SST observations along the coast continued to show the same variability as described for the month of June. However, there was a slight increase in coastal temperatures, especially toward the end of the month where SST's off both the coast of Washington and Oregon were consistently 16 degrees C. This is consistent with overall general summertime warming.

Sea surface temperatures continued the summer rise into August. Temperatures were very consistent at 15 to 16 degrees C with the exception of 18-degree water in the vicinity of the Washington and Oregon border near Cape Disappointment, i.e. the Columbia River outflow region. Even though SST changes through the summer, there was no clear correlation with any individual mesoscale MSC events and the SST in this region.

B.   EUREKA REGION

The Eureka region experienced an MSC event everyday during June. The events fell primarily into two categories; MSC category one and six (no or little change), with MSC category one once again being the predominant type of event.

The synoptic signal that resulted in the MSC category one is somewhat misleading and is quite different from that described for the Seattle region. Where ridging was the primary feature affecting the MSC events in the Pacific Northwest, it is more of a cyclonic to parallel flow that is occurring along the coast for the Eureka region. The cyclonic turning, as shown in the June MSC category one composites in Figures 24 and 25, results from an extended trough that originates in the high desert of Nevada and extends to just
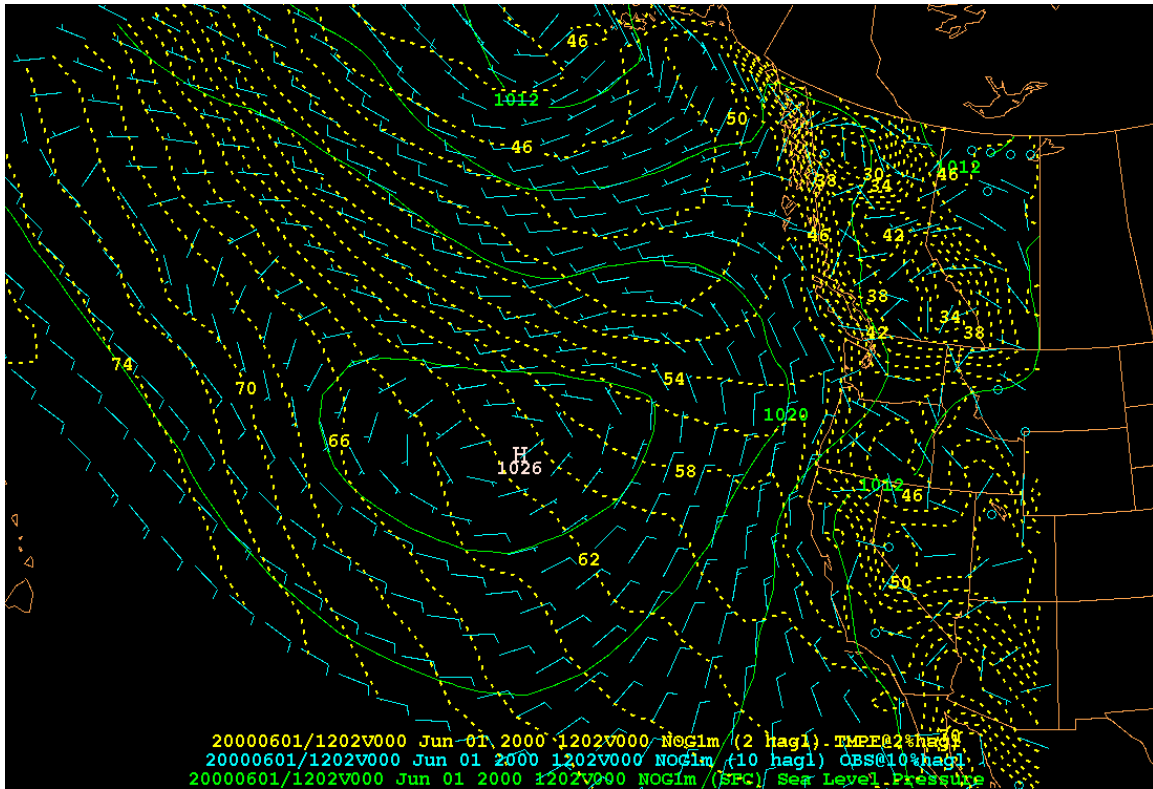
Figure 24. Composite of NOGAPS 12Z June 00 surface analysis. This is the morning composite analysis where the MSC category one is established most.

offshore of the Northern California region. The orientation of this trough is important for airflow considerations as it can produce either weak offshore flow or along-coast flow, which tend to result in different stratus evolutions.

Unlike the Seattle region, a comparison between the 12Z morning composite and the 00Z afternoon composite, shown in Figures 24 and 25, give no clear indication of the MSC evolution. Close examination of the diurnal variation reveals nothing useful. While there is clear evidence of a thermal ribbon along the coast, a baroclinic zone, which did not occur in the Seattle region, it seems to have no clear function as a predictor of MSC evolution for the Eureka region. The clear indications appear to be seen best in the flow
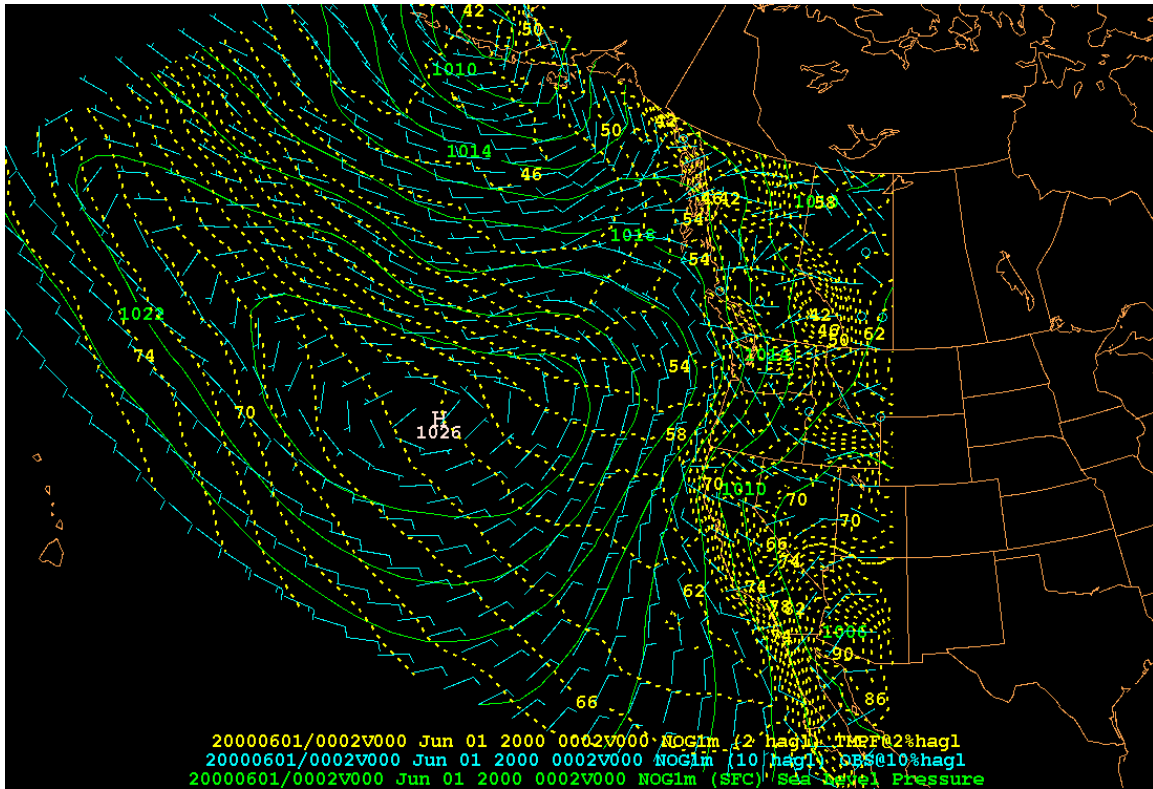
Figure 25. Composite of NOGAPS 00Z June 00 surface analysis. This is the afternoon composite where the MSC category one has abated.

patterns for this region. Although the flow patterns are implied from Figures 24 and 25, the composites tend to smooth out important details that seem to be key predictors.

The subtropical high-pressure system offshore is unchanged diurnally as is the coastal wind regime. However, the isobar pattern hints at the very core of the problem. In Figure 24, the trough appears to be having greater cyclonic curvature and a weaker pressure gradient in the near shore area while in Figure 25, the cyclonic curvature is less and the pressure gradient is increased. The 12Z pattern, shown in Figure 24, seems to suggest a tendency for weak offshore flow, which favors decreasing stratus in the afternoon.

The relationship between weak offshore flow and stratus dissipation is illustrated in Figure 26 that shows a typical synoptic pattern, which results in the dissipation of fog and stratus in the Eureka region. It is important to note that where the offshore flow no

longer exists; the fog and stratus will most likely persist. Comparison of Figures 26 and 27 show a loose correlation between where offshore flow is occurring and the lack of fog and stratus along the coast. The notable exception is the region from Eureka to the Oregon border where topography and vegetation (maintenance of moisture) has a clear influence on the small-scale structure.
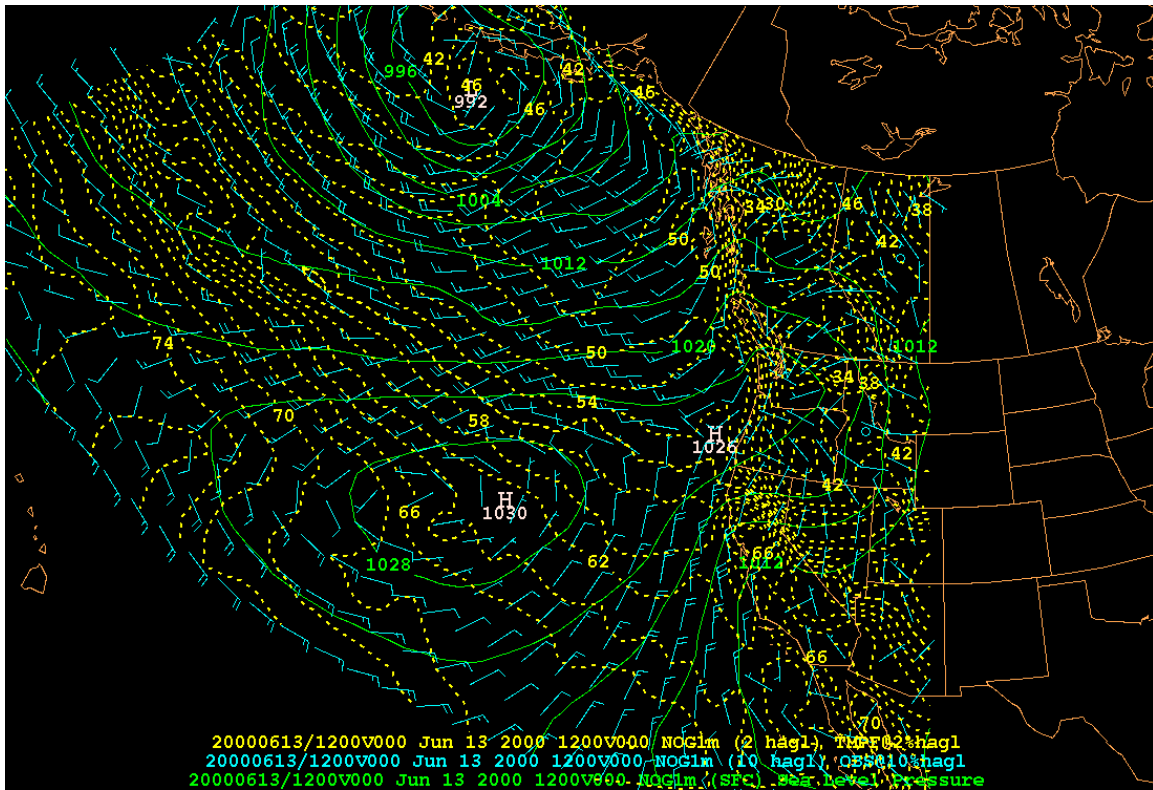
Figure 26. NOGAPS 13/12Z June 00 surface analysis. Note the deep inverted trough along the California coast (MSC category one).
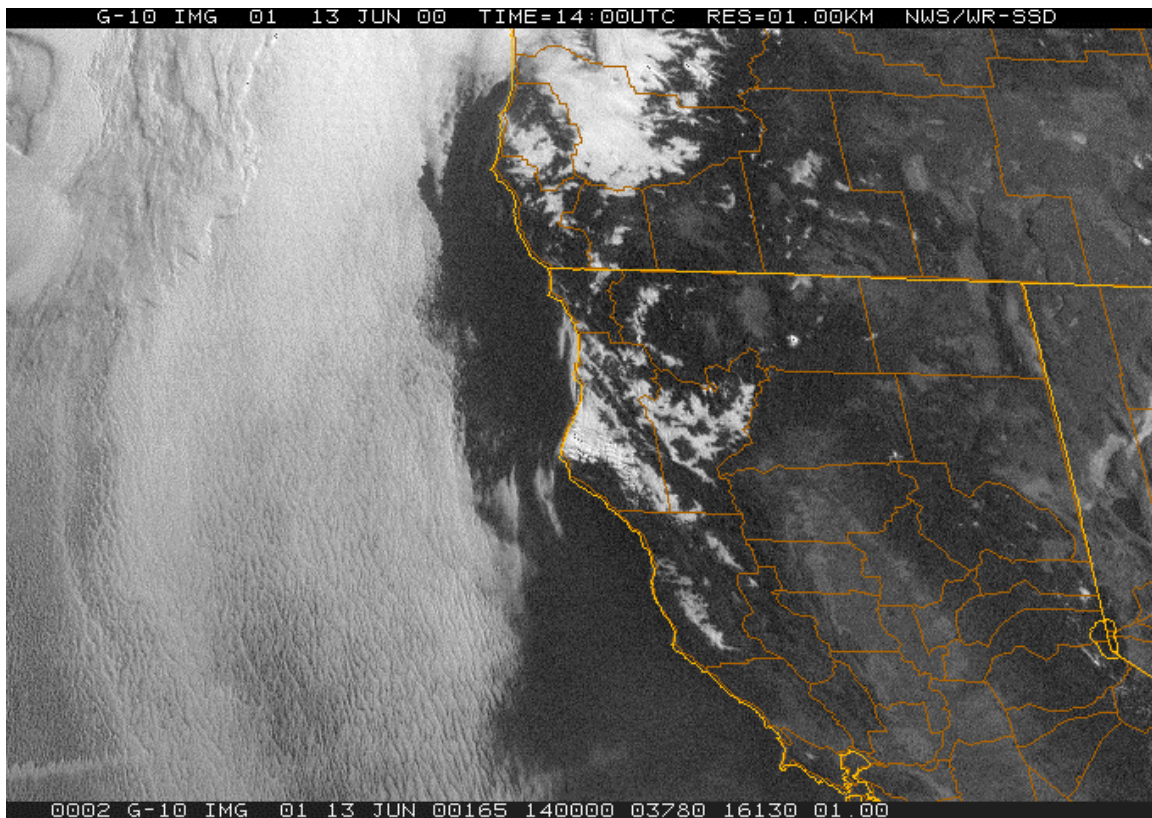
Figure 27. GOES-10 13/1425Z June 00 Satellite imagery.

The Eureka region also experiences a fair number of occurrences in June of MSC category six, little or no change. The relationship between MSC and the synoptic pattern in this case seemed to be more apparent than in category one. As Figure 28 shows, there appears to be three differences in the overall pattern compared to category one. First, the subtropical high-pressure system is located further north in the Pacific than normal, it is 3mb's higher in central pressure (1026 to 1029mb), and the most telling sign is the reorientation of the trough. The tough now is originating from the desert southwest, vice the Nevada desert. This changes the flow pattern from a cyclonic trough to one that is much weaker and less cyclonic. In addition, there is no easterly flow present, which allows the MSC event to continue with little to no change during the day.
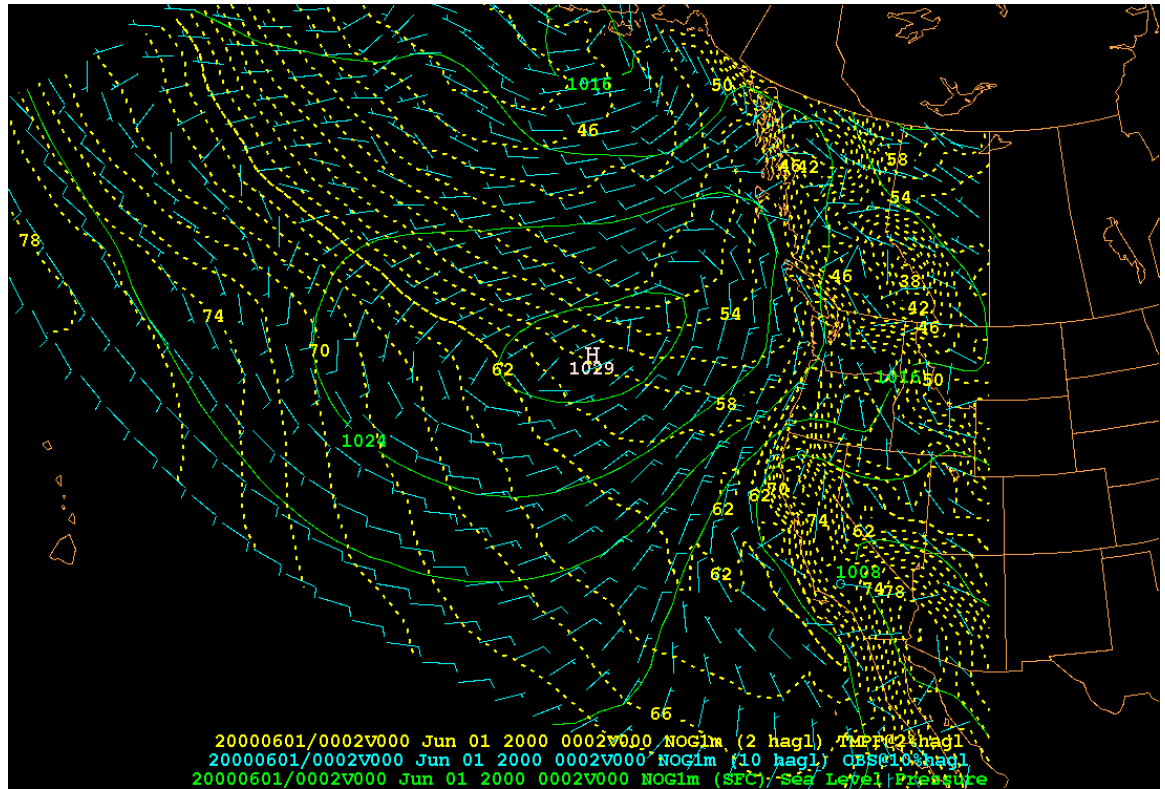
Figure 28. Composite of NOGAPS June 00 surface analysis. This shows the mean
synoptic pattern without diurnal change (MSC category six).
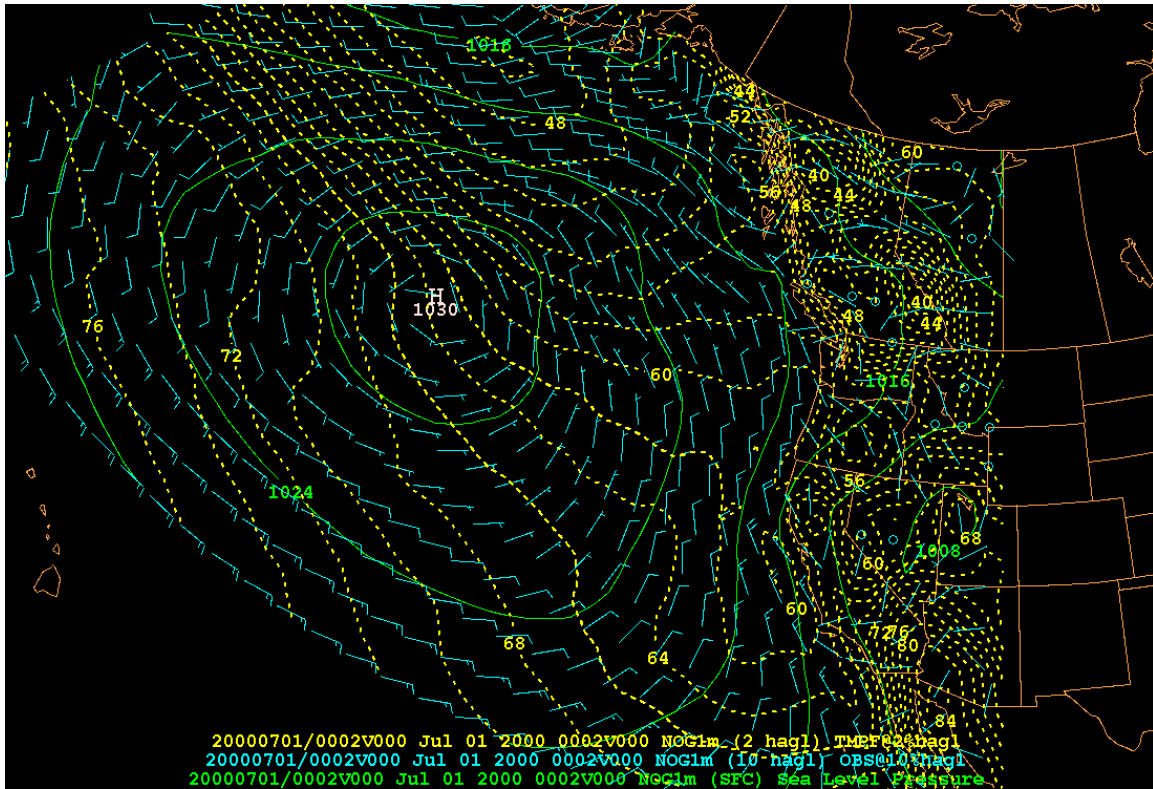
Figure 29. Composite of NOGAPS July surface analysis for MSC category six. Note coastal trough is no longer present.

An example of the synoptic situation that resulted in MSC category six for the Eureka region is not unlike the one that resulted in MSC category one. Figure 29 shows a remarkable likeness to that of Figure 26. However, the biggest difference appears to be the extension of the subtropical high into the Pacific Northwest. This surface extension into the Pacific Northwest results in a slight reorientation of the sea-level pattern over the Eureka region. This large-scale pattern manifests itself once again as an inverted trough, but more aligned now in an east to west fashion. This pattern no longer produces an offshore flow, but due to the continued cyclonic nature of the pattern, which suggests weak lifting is persistent in the boundary layer. It is hypothesized that a rather strong negative (downward) heat flux is occurring due to cold upwelling as a result of the 15-20kts of wind along the coast, which maintains the integrity of the boundary layer. Any incoming short-wave radiation apparently falls short in causing boundary layer decoupling that would normally lead to fog and stratus dissipation. Decoupling is a

process whereby two stratified layers, normally separated by an inversion, become mixed as a result of the inversion weakening significantly or breaking up.

The analysis field shown in Figure 30 indicates a high-pressure cell inland
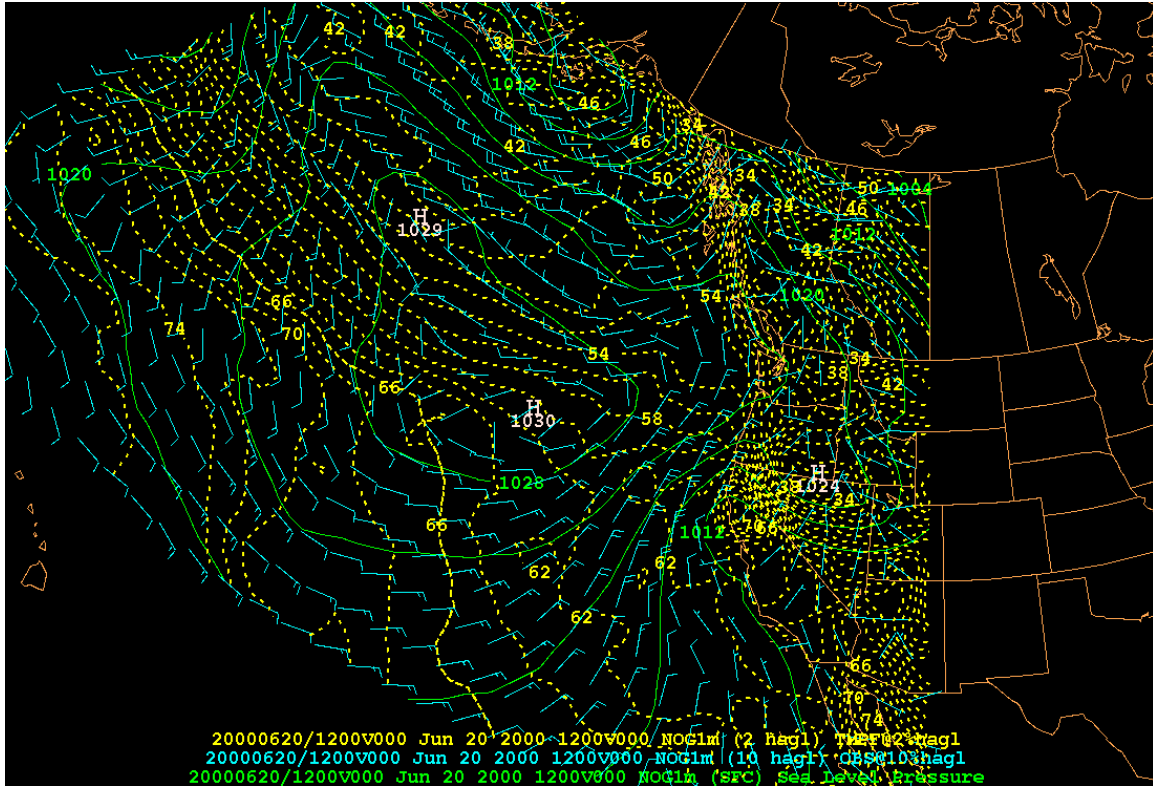
Figure 30. NOGAPS 20/12Z June 00 surface analysis. Note the 1024mb high-pressure cell over southern Oregon. (MSC category six)

over southeastern Oregon, which is consistent in producing MSC category six events for the Eureka region. This inland high-pressure center contributed to the persistence and perhaps a slight strengthening of the inverted trough extending over the coast. The presence of the inland high-pressure center is different in comparison to MSC category one events for the Eureka region.

Comparison of Figures 30 and 31 reveal a clear region along the coast. This is likely the effect of the coastal mountains upon the coastal region, which provide an effective barrier to land-falling storm systems. Larger-scale forcing is causing clearing further seaward. However, the trajectory of the air in this case would come from the east. If the flow were significant enough, i.e. a Froude number greater than one, the flow

would go over the mountains and dry adiabatically on the Pacific Coast side (this case, leeward). This effect would be stronger than any lift created as a result of the cyclonic turning in the inverted trough and hence dryness. Of note also in Figure 31, (20 June) is a small area of fog south of Cape Mendocino to Point Arena. This region closely correlates to the lack of an offshore flow in the base of the trough.
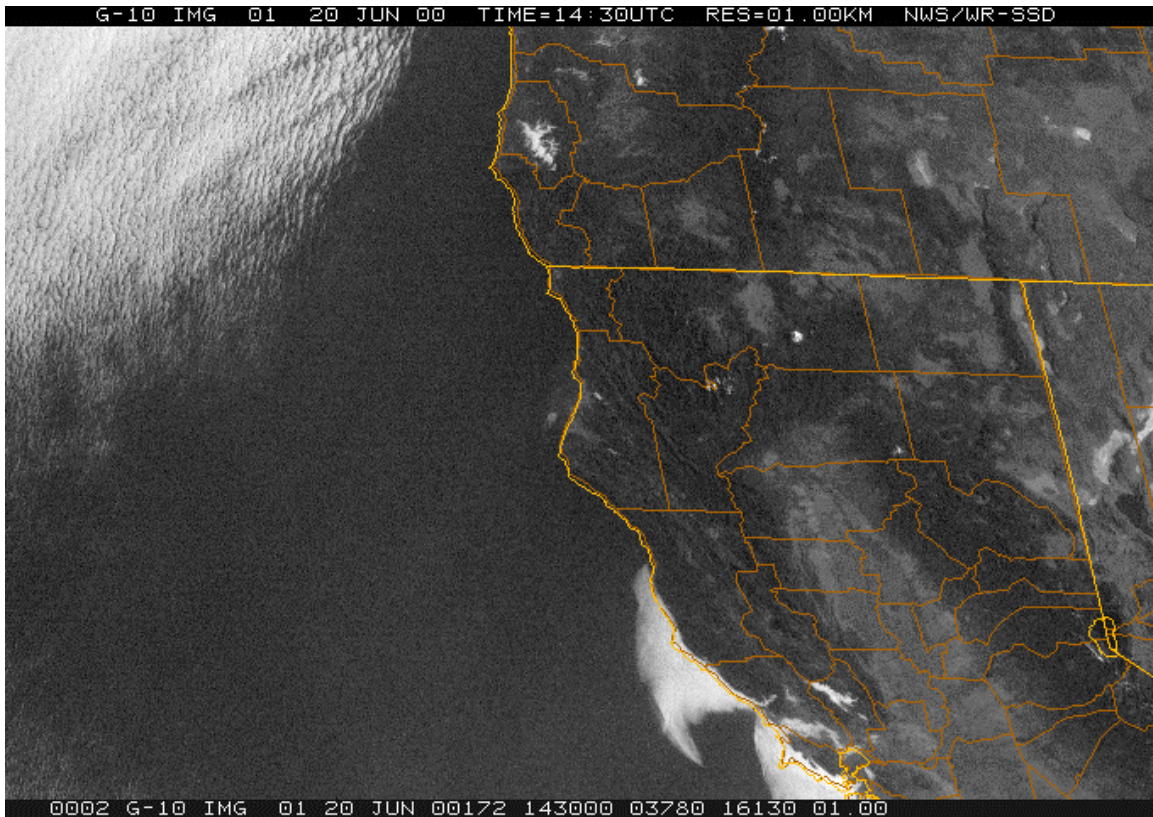
Figure 31. GOES-10 20/1430Z June 00 satellite imagery. Note that the only fog and stratus present appear at the base of the inverted trough.

The month of July simply emphasized what was seen for June for the Eureka region, little summer variability. The month was once again dominated by MSC events that occurred daily with the large majority of MSC events falling into category one, (decreasing or dissipation). However, the forecasting challenge during the month of July is changed significantly. While the same synoptic patterns as June continue to exist in July for MSC category one, which includes the same MSC evolution perturbations, the challenge now spreads to MSC category six. Figure 29 shows little change in the synoptic pattern as compared to the months of June and July that resulted in MSC

category one. Composite of MSC category six without the diurnal variation is shown for simplicity.

The key is the change of processes that cause persistence in MSC events. While subtle changes are occurring in the synoptic scale such as a 2mb increase in the central pressure of the subtropical high-pressure system, this is not the key. The key now lies in the trajectory of airflow along the coast. The cyclonic turning may or may not be evident, but if the flow has a very long near-shore trajectory, there is persistence in the MSC event.

The MSC events were closely associated with the same synoptic patterns as described for June. Of note, the subtropical high had move further north and had strengthened. The inverted trough remained the tell tale sign for the region and was the key synoptic-pattern indicator. It was noted that the pattern that resulted in dissipation was always the same. The pattern of dissipation was also very consistent. It first dissipated beginning in the north where an easterly flow developed during the day. An important comment at this time is to point out that while the synoptic pattern indicated an offshore flow at night, the pressure gradient was sufficiently weak that any flow would be too weak to cause significant change.   Nighttime air-sea temperature differences were minimal in the marine layer coastal regime. Only in the daylight hours did the larger-scale motions begin to invigorate sufficiently as to cause significant motion of the air.

The last area to experience clearing, if clearing were to occur, was the region from Eureka to the Oregon Border. This region depended on the base of the inverted trough; i.e. no easterly flow meant any clearing. Figures 32 and 33 are typical examples of fog and stratus in this region and the associated synoptic pattern that produced them. Additionally, topographic and to a lesser extent, coastal vegetation may play a role for the region.
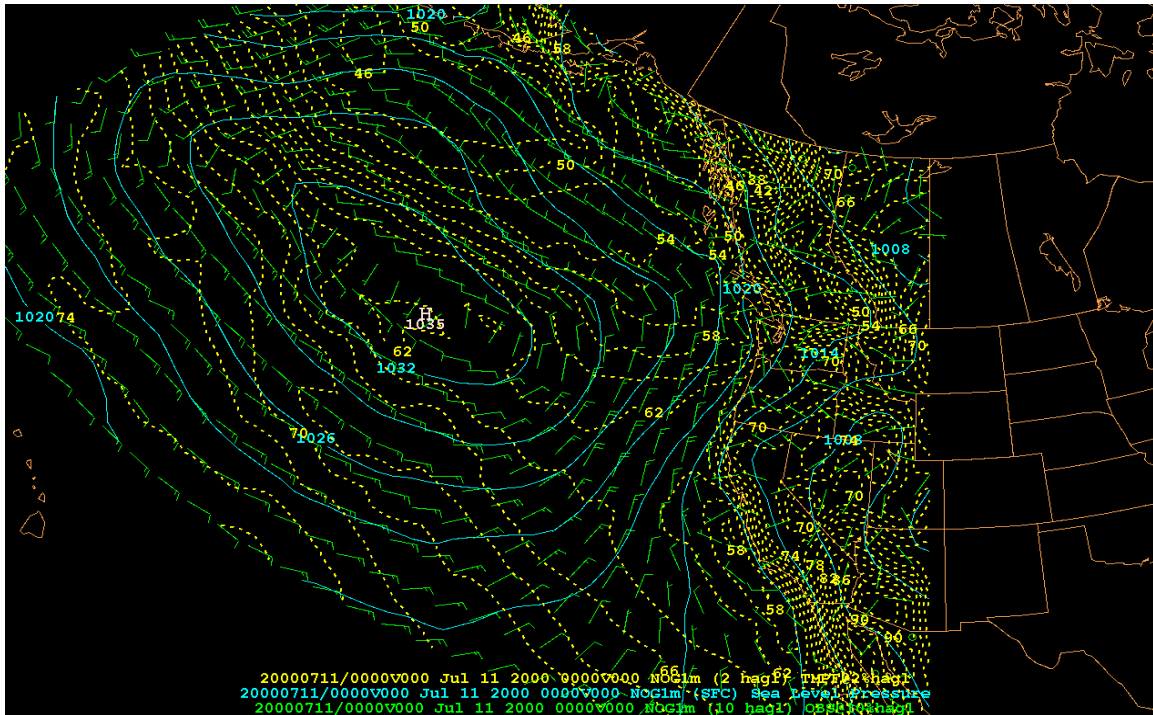
Figure 32. NOGAPS 11/00Z July 00 surface analysis. Note synoptic pattern, in particular, the trough extending through the Eureka region. Compare to Figure 33 below.
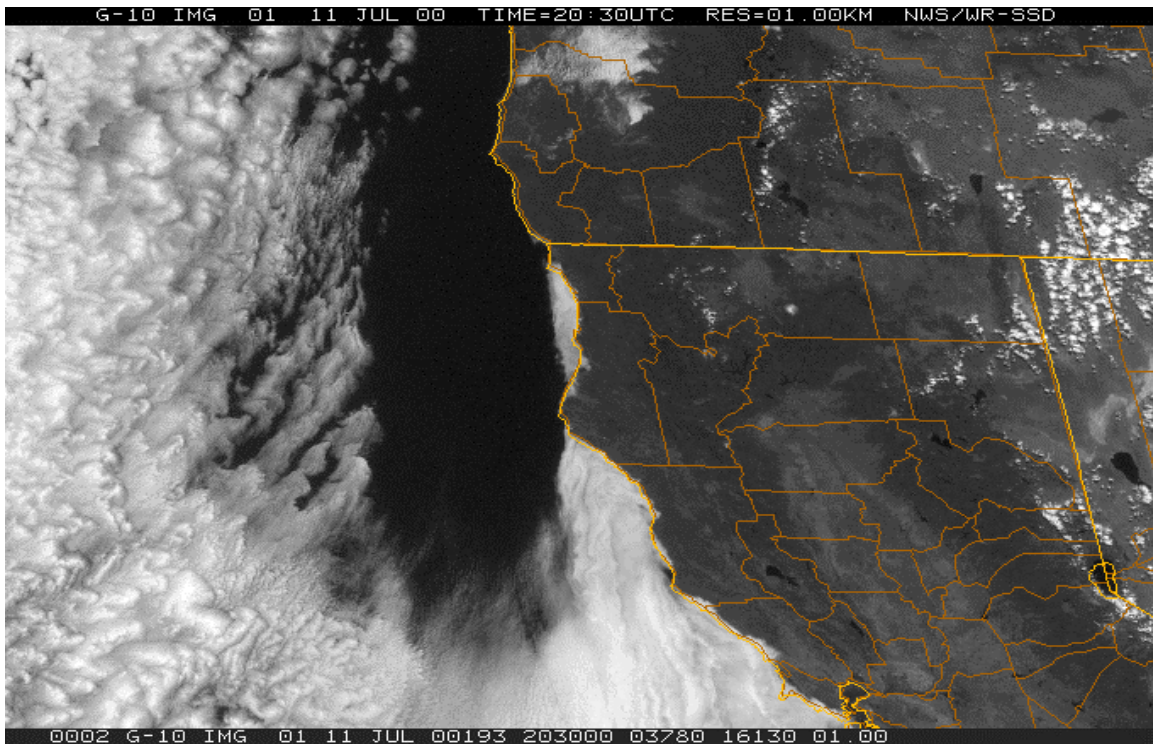
Figure 33. GOES-10 11/2030Z July 00 satellite imagery. Note, MSC event is localized in the region from Eureka to the Oregon border. This is an afternoon local time picture. Compare to Figure 31 above.

Those periods where the MSC category six (little to no change) occurred, two distinct patterns emerged. First, the 6th and 7th of July saw a continuous MSC event. This resulted from a weak circulation that occurred over water and was an extension of the trough over the Eureka region. Figure 34 shows the synoptic pattern responsible. This is presented to point out possible anomalies that may enhance a known synoptic pattern. Second, events that occurred on the 16th, 20th, 24th, and 29th of July all showed an eastward displacement of the trough. This caused a cessation of the cyclonic flow along the coast and allowed for a more parallel flow, one out of the north-northwest.
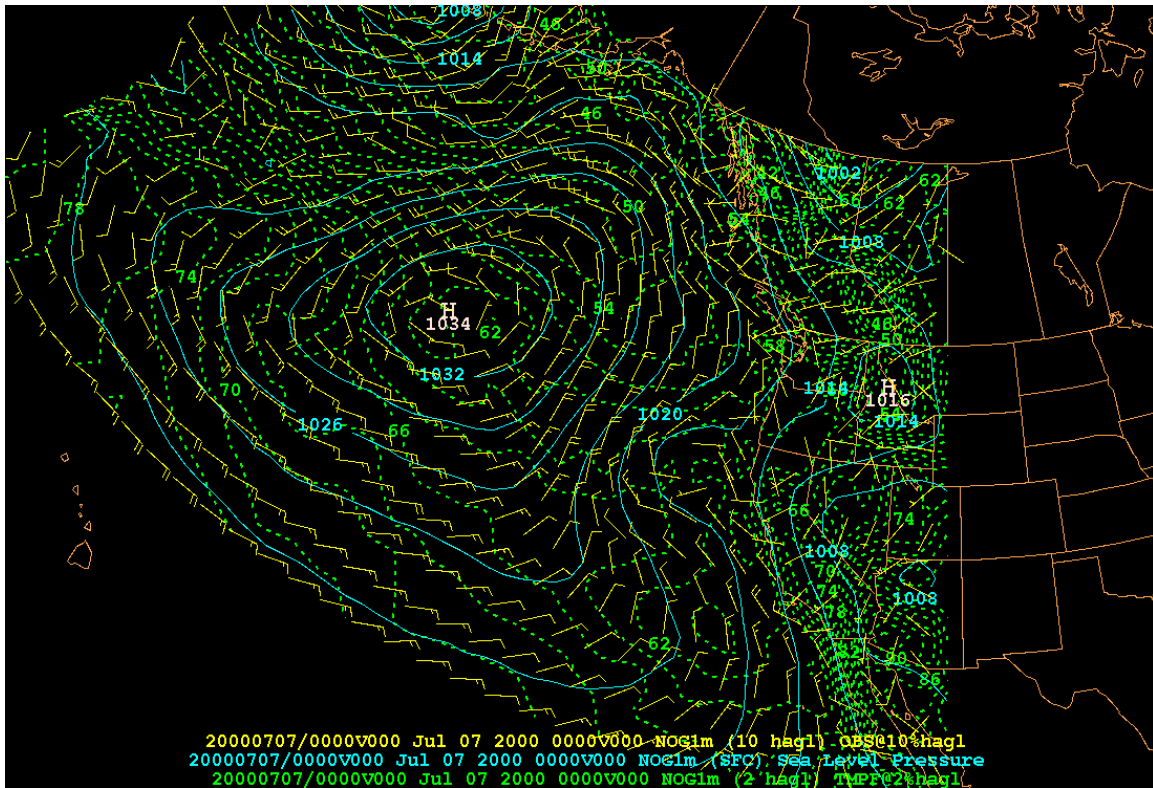
Figure 34. NOGAPS 7/00Z July 00 surface analysis. Note weak circulation off Northern California coast.

Figure 35 shows an example of a more coastal following flow pattern that resulted in persistence of fog and stratus. This particular flow pattern was found more prevalent further south, but the results remain the same. It is hypothesized that this coastal flow pattern intensified the upwelling process whereby deeper, cooler water was brought to the

surface as surface water was pushed further west due to Coriolis, which resulted in the negative heat flux cooling the overlying air to condensation causing fog and stratus. The corresponding satellite series for this day, (not shown) depicted a larger MSC coverage area, especially along the coast.
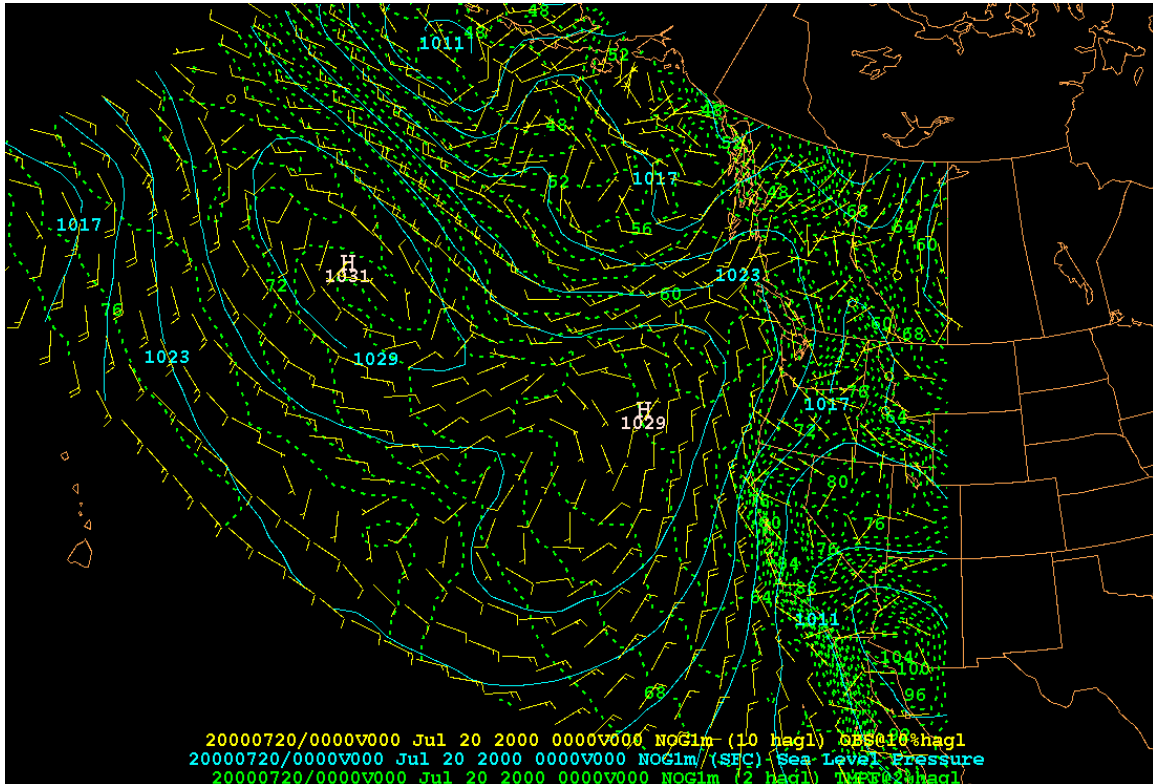
Figure 35. NOGAPS 20/00Z July 00 surface analysis. Note position of inverted surface trough displaced eastward over the high desert.

The theme of little summer variability continued into August. Like previous months, August experienced an MSC event on a daily basis. As shown in Figure 34 previously for the Seattle region, the subtropical high-pressure center moved further north and strengthens. This proved to be of little consequence for the Eureka region in terms of altering the frequency of MSC events or patterns described previously.

The Eureka region balanced nicely with MSC category one events occurring slightly more often than category six events throughout the summer. Only a slight separation appears for August where there were 18 category one events to 8 category six events. Unfortunately, little insight is gained from the prevailing synoptic pattern. While

MSC category one remained unchanged, there did appear a change, albeit slight, in the pattern to indicate a possible key. Figure 36 shows the subtle changes, which once again points to increased cyclonic turning vice an extended along-shore flow. Both are key features in the synoptic pattern as indicators of persistent fog and stratus.

For the August ritual of MSC category six, little summer variability is evident with regards to the larger-scale patterns. Figure 36 shows the subtropical high-pressure system and the weak inland warm-core lows. There are possibly two related differences that the composites reveal. They were a weakening in the pressure gradient resulting in weaker coastal winds (10 knots or less) and a simultaneously lessening of the cyclonic turning as a result of the westward extension of the Nevada trough. This situation consistently prolonged the fog and stratus event.
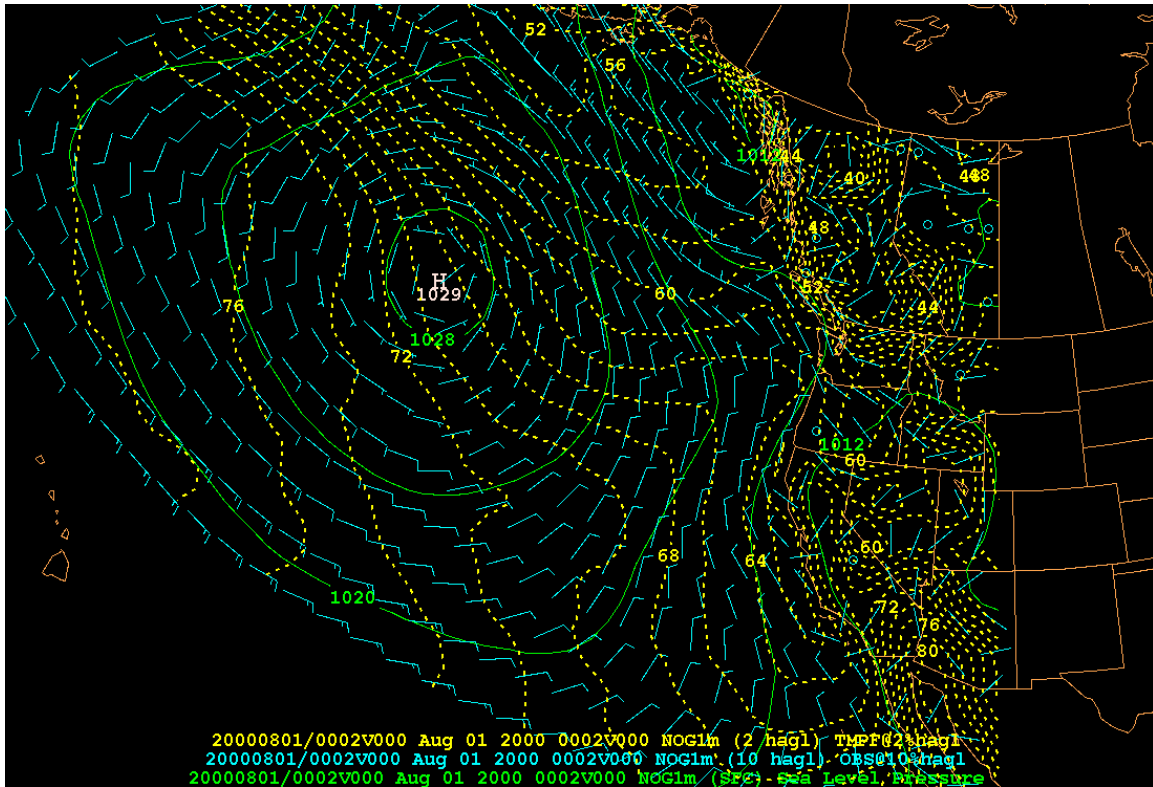
Figure 36. Composite of NOGAPS August 00 surface analysis for MSC category six. Note the weak coastal winds and much weaker cyclonic turning (in northern CA).

Of note, the water temperatures were significantly cooler compared to that of the Seattle region especially at the beginning of the month where coastal water temperatures

were observed at 8 to 9 degrees C at the start, but warmed to 10-13 degrees C by the end. Since MSC events occurred on a daily basis, water temperatures appeared to have not played an important role in and of themselves or in relationship with inland temperatures.

Early summer variability of June was not evident in July as water temperatures did not exhibit such a dramatic change. Temperatures were persistent at 10 to 13 degrees C throughout the month. The only exception was a particularly cool region of 10 degree C water off shore near the Capetown/Eureka area in Northern California where the land has a significant extension into the Pacific Ocean. As mentioned previously, fog and stratus tend to persist from this region northward to the Oregon boarder, but not necessarily at the Capetown/Eureka region where surface waters were cooler. A better observing net in this region might reveal cooler temperature in the entire region, which would account in some ways for the persistence of fog and stratus in the region.

While sea surface temperatures in August experienced a slight decrease of one degree C over July, the slight changes did not have a significant impact on the coastal fog and stratus coverage or consistency.

C.   MONTEREY REGION

This region is arguable the most important region for accurate fog and stratus forecasts due to three coastal international airports (SFO, OAK, and SJC) and a number of regional coastal airports that have tremendous impact on many Pacific Rim flights as well as others. As mentioned in the introduction, delays can be costly and frustrating.

The Monterey region during the month of June was typified by with fog and stratus. There was no overwhelming category. 14 days experienced MSC category one while 11 days experienced MSC category six. The other five days also experienced an MSC event making it a clean sweep in terms of fog and stratus occurring each day of the month.

The composites revealed limited indications in the synoptic pattern that may aid forecasters in forecasting the evolution of the fog and stratus for this region. Figure 37 is a composite of 12Z and Figure 38 is a composite of 00Z, together they present an unmistakable diurnal signal. The 12Z composite shows weak coastal winds as a result of

weak cyclonic turning. This is consistent and a known characteristic that results in category one and six events. However, as Figure 38 illustrates, there is a pronounced baroclinic zone present along the coast, which is consistent with inland warming. But more important, is the development of inland warm-core lows. This alters the coastal flow more inland. While typically a sea breeze develops in this condition, it does not hold the key to forecasting the MSC evolution; the sea breeze has no effect. However, the development of the inland warm-core low, while enhancing the sea breeze, will have an effect and is a key indicator of MSC evolution.
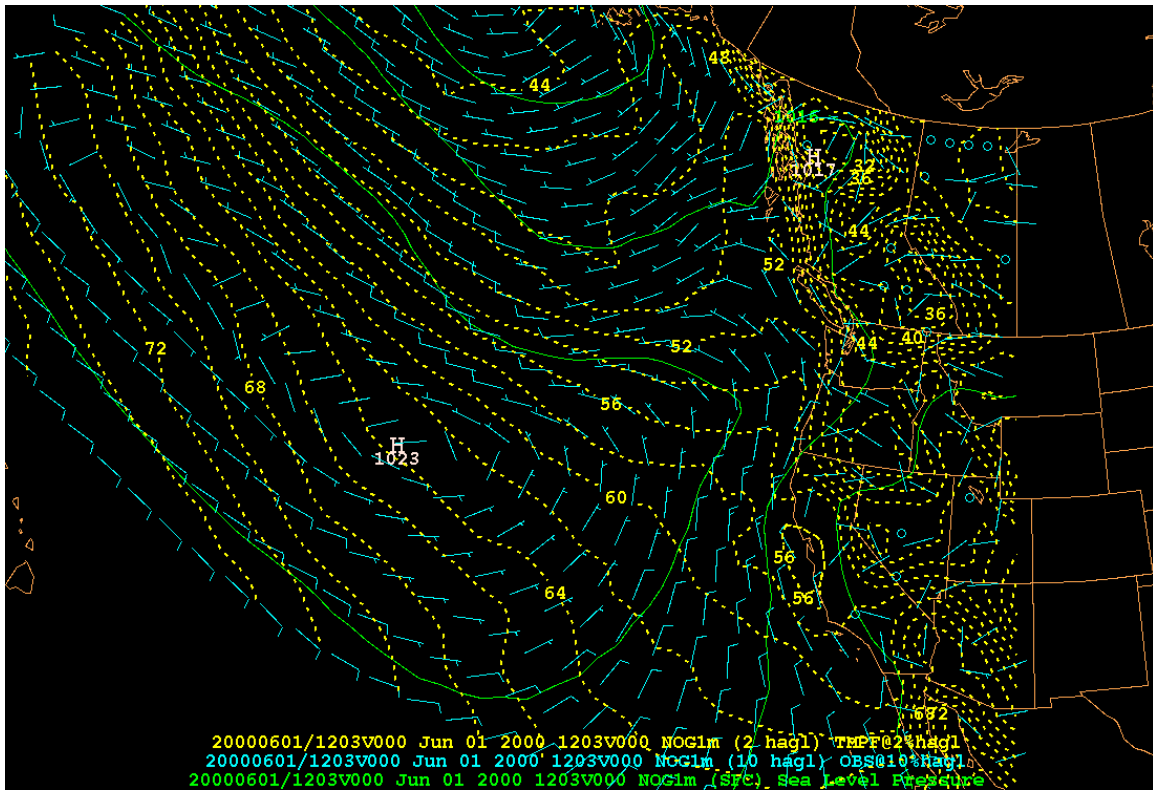
Figure 37. Composite of NOGAPS 12Z June surface analysis for the Monterey region of MSC category one events.

While no or little change is observed in the strength and position of the subtropical high-pressure system, there is a subtle change in the warm-core desert southwest low. As this low develops, it weakens the pressure gradient in the Monterey region and turns the flow inland. There is no doubt while this synoptic flow is weak, it will enhance the sea-breeze effect. Additionally, the land-sea temperature contrast is

significant earlier in the season for this region as compared to the more northern regions' summer variability.

The development of an inland warm-core low has to be of sufficient strength as to alter the large-scale wind field by turning the flow inland. While smaller scale even insignificant flows are occurring such as a sea breeze, it is the overall flow pattern that is
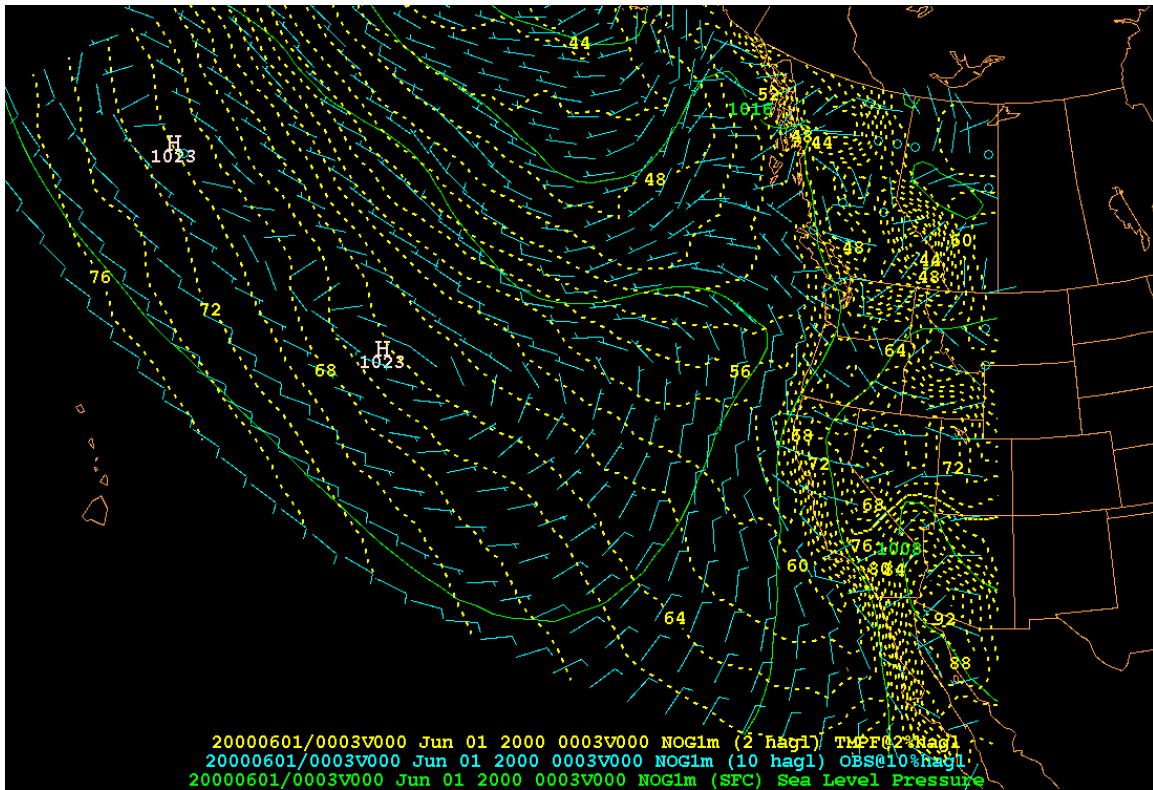
Figure 38. Composite of NOGAPS 00Z surface analysis for the Monterey region for MSC category one events.

important. With the large-scale flow turning inland, it may support flow, surface divergence at the coast, which results is the dissipation of the fog and stratus for the region

MSC category six events are very clear-cut in terms of the synoptic signature. It is very similar to that of the Eureka region. There is an inverted trough extending up the west coast. Where the easterly flow abates, fog and stratus events are the most persistent due to the lack of any significant flow pattern in the region and the slight lifting associated with the inverted trough that normally originates in the desert southwest.

57

The Monterey region for the month of June experienced three different patterns that resulted in the MSC category one, fog and stratus dissipation or decreasing. The first pattern, which was frequent during the first week of June, saw the subtropical high-pressure cell located well south in the North Pacific Ocean and a dynamic/cold-core low pressure system located north of the subtropical high, but south of the Gulf of Alaska. A weak ridge with one or more high-pressure centers located near the west coast provided sufficient subsidence across the region to result in fog and stratus for the Monterey
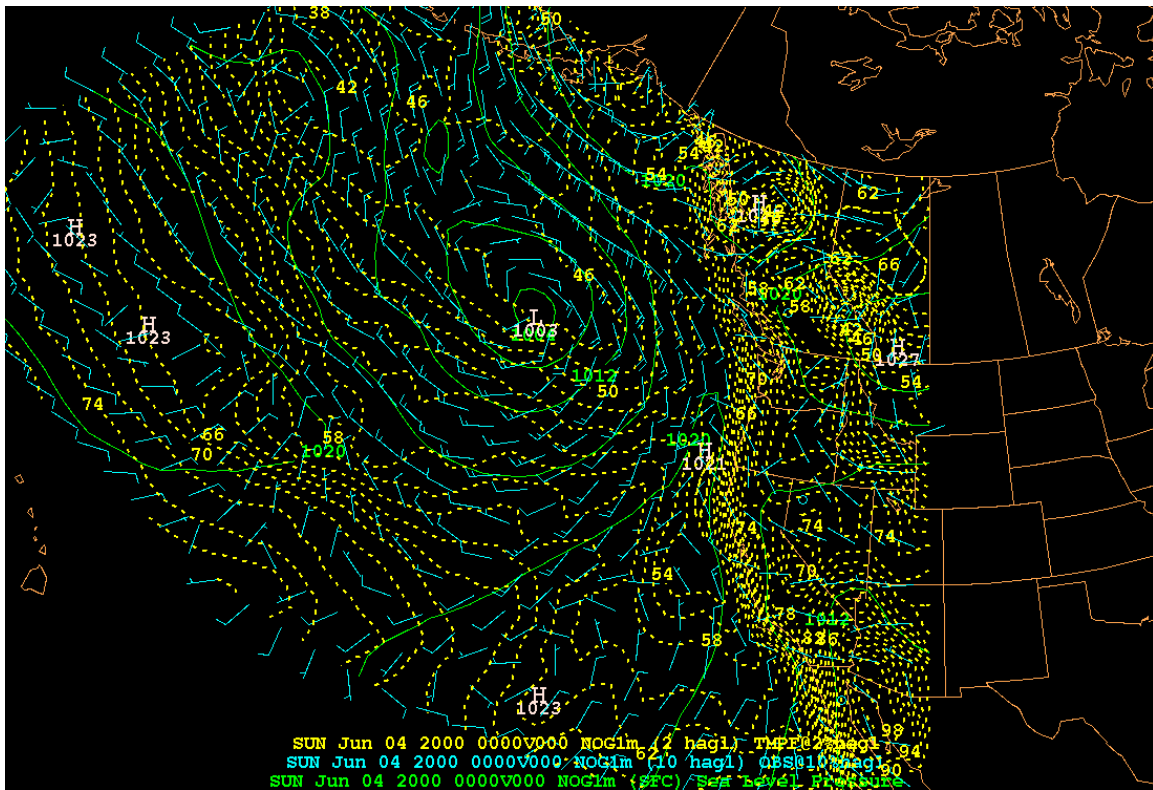
Figure 39. NOGAPS 4/00Z June 00 surface analysis. Note weak ridge along west coast.

region. Figure 39 shows typical synoptic pattern that occurred during the first week of June.

The second pattern while similar to the first depicts ridging from the subtropical ridge that is displayed further south into Southern Oregon and Northern California rather than into the Pacific Northwest. Like the first pattern, both produced relatively lighter coastal winds and subsidence that results in fog and stratus. Figure 40 shows the synoptic

pattern. Additional similarity includes the presence of a dynamic/cold-core low north of the subtropical high-pressure cell once again. It is clear that an occluded frontal system is impacting the Pacific Northwest; it is the displaced ridgeline that is affecting the Monterey region and resulting in fog and stratus.
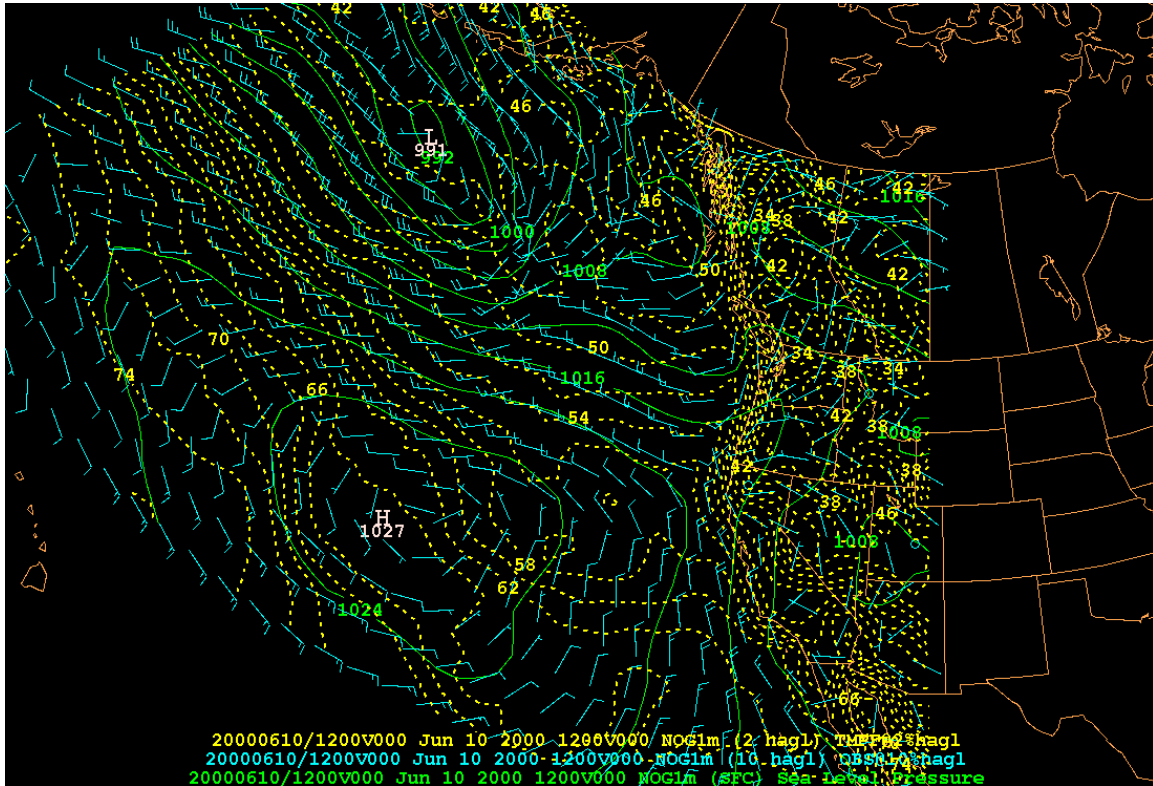
Figure 40. NOGAPS 10/00Z June 00 surface analysis. Note subtropical ridging into Southern Oregon and Northern California.

The third pattern was the most typical synoptic pattern that results in fog and stratus for the Monterey region. The subtropical high-pressure center has moved further north by months end and the inverted trough extend into the Eureka region, which is a common pattern for that region as well. Figure 41 shows the most common synoptic pattern over the Monterey region that resulted in MSC category one events.
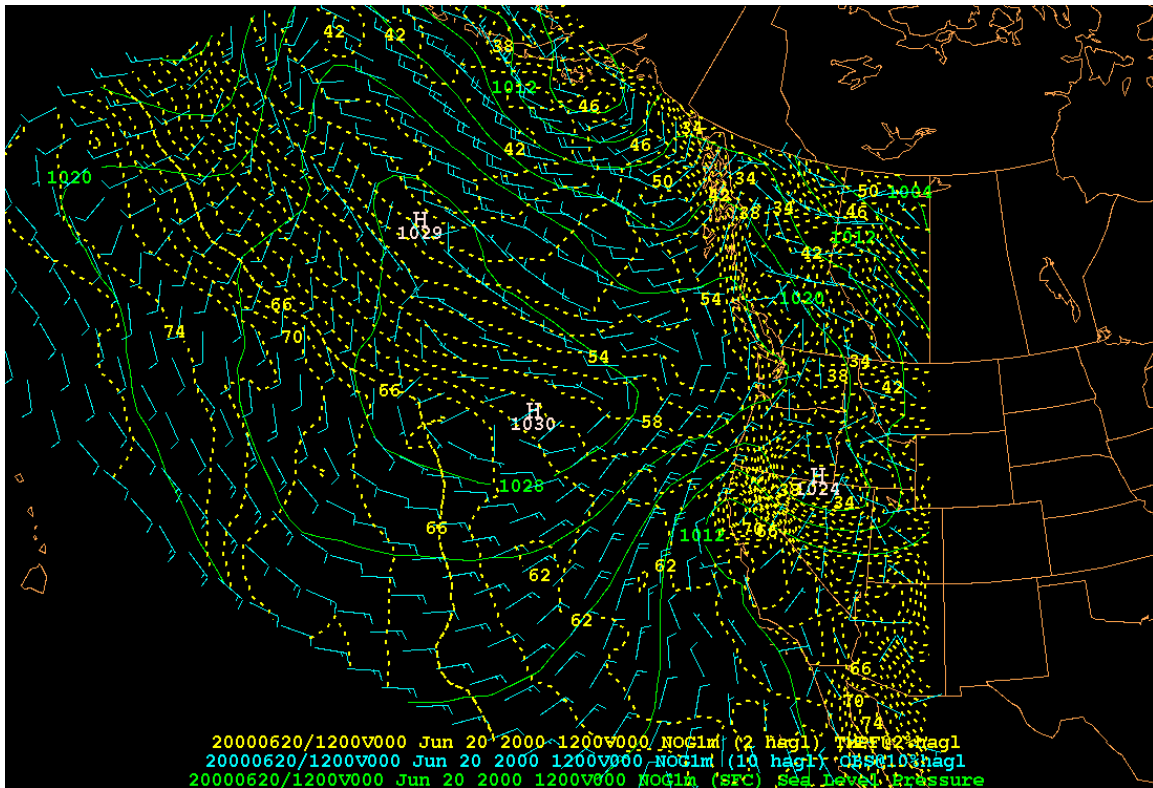
Figure 41. NOGAPS 22/12Z June 00 surface analysis. Note weak flow pattern over Monterey region.

The pattern most responsible for the persistent fog and stratus (category six events) was oddly enough the same pattern that caused clearing for the Seattle and Eureka regions, the inverted trough. However, the difference is that the Monterey region is located far enough south as to not experience the easterly flow that regions located further north experienced. The Monterey region saw very weak flow, and at times a very weak circulation in that flow. Figure 42 shows typical pattern of the inverted trough along the coast, but also shows a notable absence of cross-coast isobars south of Eureka.
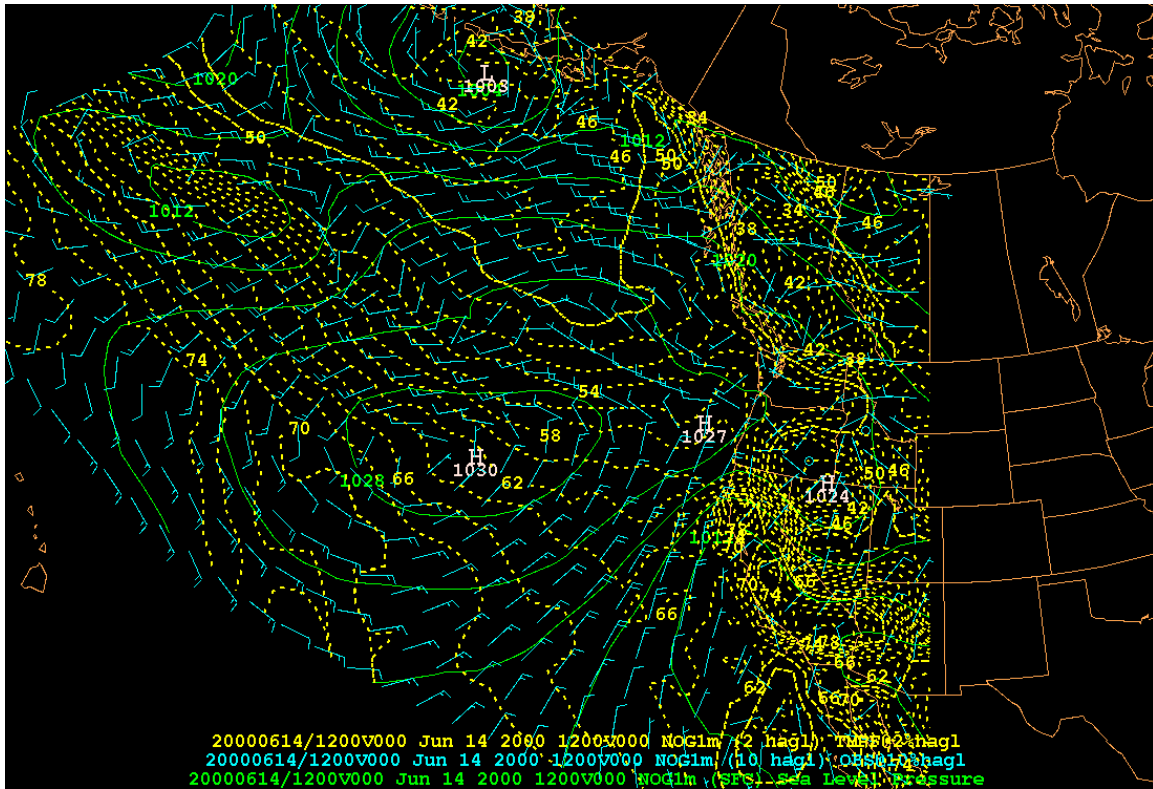
Figure 42. NOGAPS 14/12Z June 00 surface analysis. Note the weak, almost cyclonic flow over the Monterey region.

This would imply a very weak cross-coast pressure gradient and hence a lack of any strong forcing by the wind field in the horizontal. Vertical motion is also weak, but the presence of negative omega (not shown) implies weak upward motion. This weak upward motion in the marine boundary layer (MBL) is the key process to cause persistence in the fog and stratus events. This flow pattern is similar to that which resulted in MSC category one. The very subtle differences in the pattern, of which it appears that flows less than 10 knots with a hint of cyclonic curvature that seems to be the difference.

July for the Monterey region fell into MSC category one, 21 of 31 days. The remainder of days, less three, fell into MSC category six (persistence). The pattern that produced MSC category one was the typical pattern expected and described above. The subtropical high-pressure cell has moved further north as described in previous sections. However, the big change seemed to be the influence now of the warm-core low that develops over the high desert of Nevada to the desert southwest region. With the

61

development of this warm-core low, the resulting flow had a slight onshore component, the effects of which will be seen in the mesoscale chapter (Chapter IV).

MSC category six events while occurring far less in July become more difficult to predict with the synoptic pattern. While the inverted trough is present, is has become less recognizable as the composite shows in Figure 43. However, this appears to be a
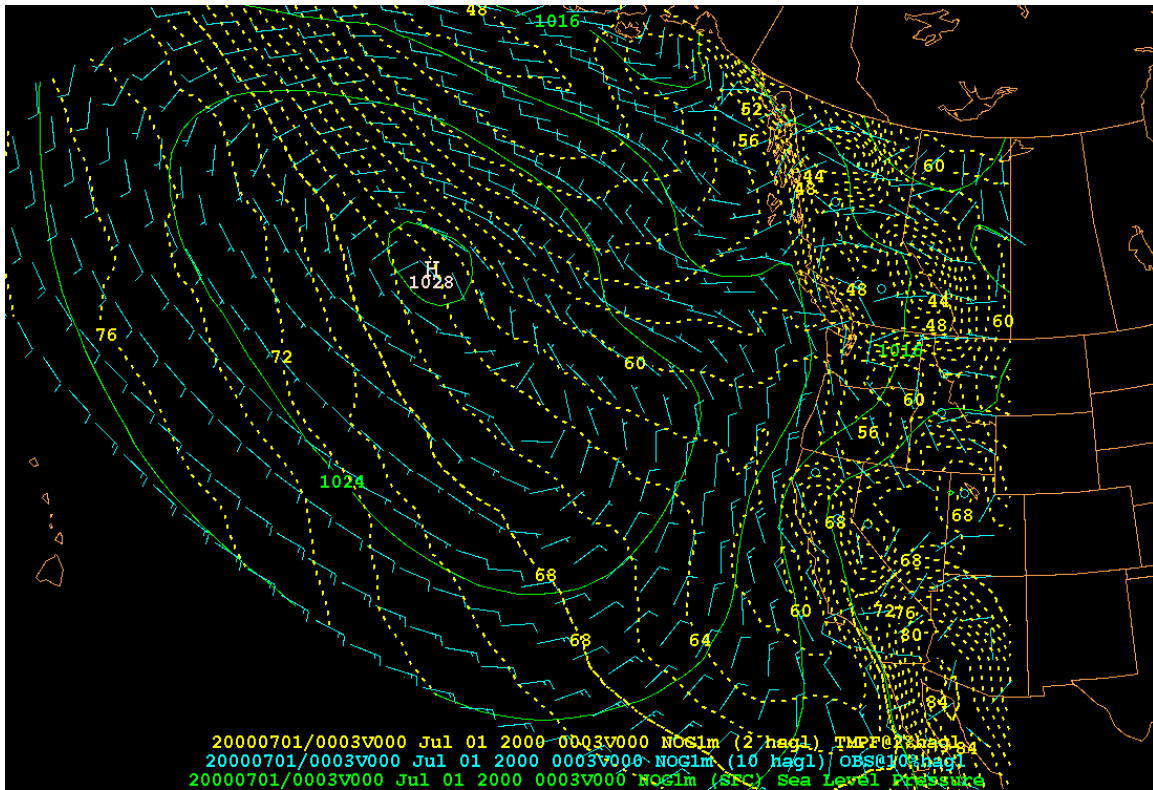
Figure 43. Composite of NOGAPS July surface analysis for Monterey category six events.

function of smoothing out the real synoptic signal as a result of the composite process. Forecasters should continue to key in on the coastal inverted trough as an indicator of persistence noting the lack of cross-coast isobars and resulting weak wind field.

Persistence of the fog and stratus (MSC category six) resulted when the inverted trough that normally influences the Eureka region shifted south to Northern California.
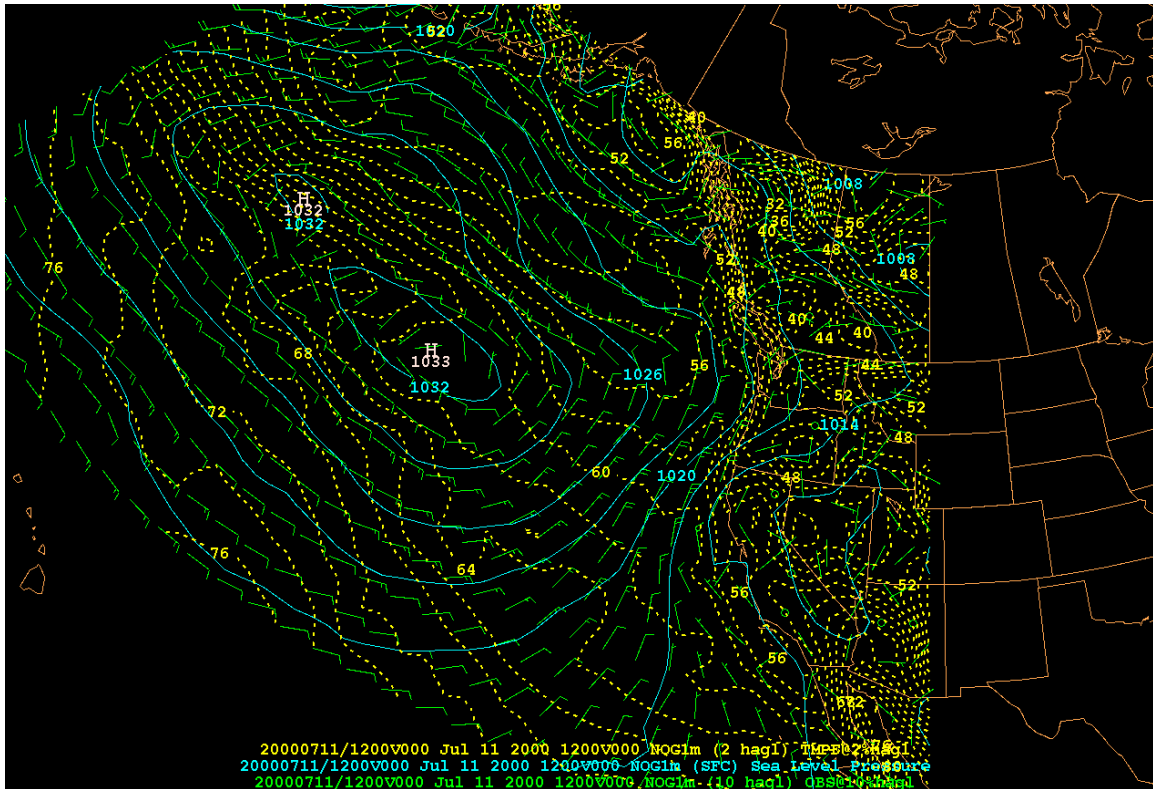
Figure 44. NOGAPS 11/12Z July 00 surface analysis. Note the inverted trough extending from the warm-core low over Nevada to Northern California. (MSC category six)

Figure 44 illustrates an example of the synoptic pattern showing the perturbation that resulted in persistence and is not unlike that which occurred in June for the Monterey region.

Summer variability ceases by mid July. August synoptic patterns were unchanged in terms of the results expected for the Monterey region. While MSC events occurred in each day with categories one and six being the dominant ones, there was a slight increase in the other MSC categories in particular category five, fog and stratus increasing then decreasing.

19 occurrences of category one and only five events of category six were observed for the month of August. Four events of category five were also observed. In the case of category five events, there were no synoptic signatures observed to indicate

persistence prior to dissipation except those previously described, only that the occurrence of which occurred later in the day.

The synoptic pattern for category six continues to be more challenging to interpret through the use of composites.   While the isobar pattern depicted indicate a geostrophic coastal flow, the actual wind field, although weak, hinted at a weak inverted trough, which has already been addressed as a key indication to persistence. As Figure 45 illustrates, weak flow pattern suggests the presence of an inverted trough. Persistence is more likely to been seen as a result of a long trajectory coastal flow that initiates the upwelling process that in turns provides the necessary conditions for extended fog and stratus events.
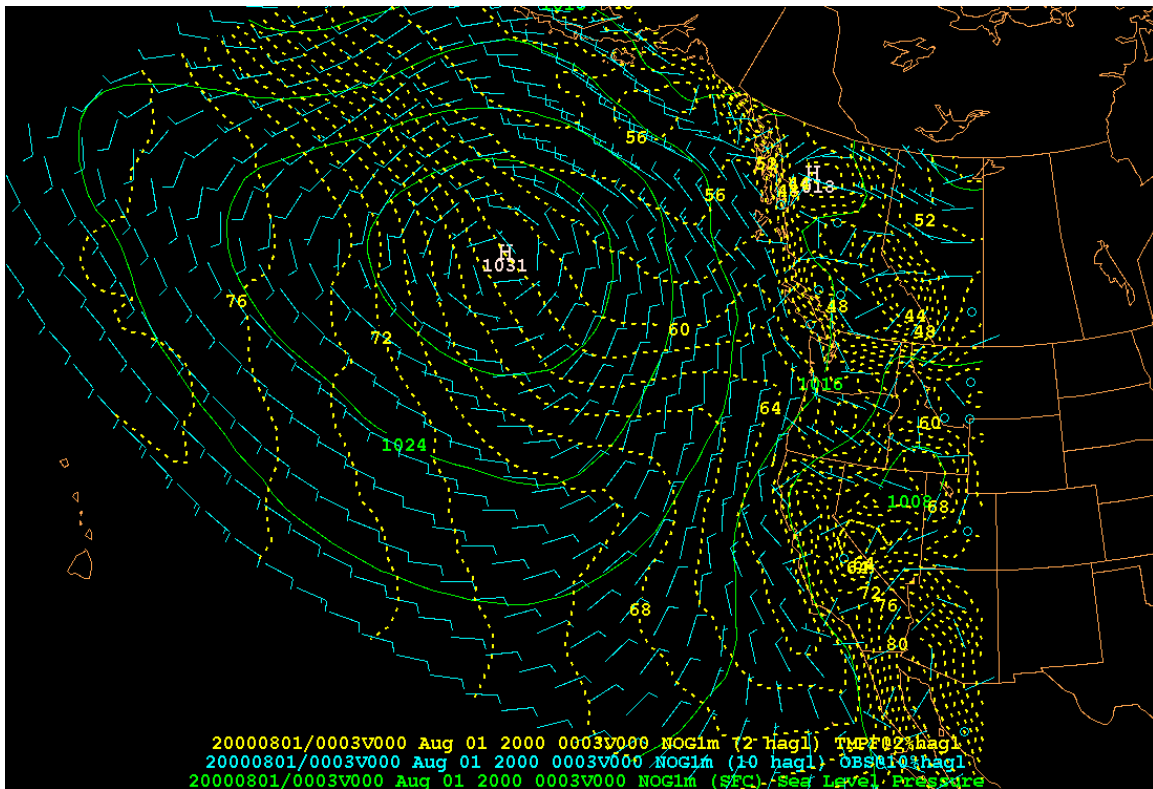
Figure 45. Composite of NOGAPS August surface analysis for the Monterey region for category six events.

There were some very minor flow anomalies within the large-scale pattern throughout the month, but proved inconsequential to the final results.   There did not

appear to be any strengthening of the warm-core low centers in August as one might have expected, at least in the model simulations.

Like the Eureka region, sea surface temperatures experienced a lot of variability early in the summer season with 9 to 10 degree water temperatures at the beginning of June to 13-14 degree water by the end of the June. With a consistent SST field, i.e. without anomalies, little impact was seen in the MSC evolutions.

July and August sea surface temperatures were far more stable with 13 to occasionally 15 degrees during the remainder of the summer. However, one anomaly was noted for the Monterey Bay where the water temperature was 1 to 3 degrees cooler in the latter half of the summer season. This could have played a key role in the micro-climate for the Monterey Bay region, but would not be seen in the model simulations.

D.   LOS ANGELES REGION

The Los Angeles region has the largest fleet concentration area (San Diego) along the west coast, while the Seattle region (Bremerton and Whidbey Island) has the second largest. These two areas are of major concern to U.S. Navy commanders. While fog and stratus events play havoc with the Monterey region in terms of its impact to commercial aviation, it is these two other regions that impact fleet operations nearly daily. The primary fleet workup area is a region off the Southern California coast known as SoCal. This is a region that is frequency inundated with fog and stratus. Carrier operations are known for numerous interruptions due to this weather menace with a significant number of carrier diverts to shore locations. All are costly both in terms of fuel used along with plane and crew accommodations for those unable to return to the ship.

The data collected for the month of June for the Los Angeles region fell primarily into two MSC categories, one and four (no change or decreasing then increasing). MSC category one is the primary event in which 14 occurrences were noted while MSC category four saw 10 events occur. There did not seem to be a strict synoptic pattern responsible for MSC category one. However, there was some variability noted with the subtropical high-pressure cell location during the month of June. This is a significant departure from the other regions and is also significant in that there were a larger number

MSC events that resulted in the afternoon growth of fog and stratus. This too is noteworthy in terms of potential air traffic delays and potential fleet divert fields.

The synoptic pattern that results in category one events are identical to that described for the Monterey region. The formation period as seen in the analyses is characterized by weak coastal winds (5 knots) that exhibit a weak divergent pattern. No cross-coast component is observed. The subtropical high-pressure system is situated well west in the central North Pacific Ocean and no desert southwest warm-core low is evident. As the day progresses, the development of the low is normally observed. The effects are two-fold; an increase in wind speed (10 knots) due to the increase in the pressure gradient force and a cross-coast (onshore) component develops. These two features lessen or even arrest the divergent wind field and are the indicators to fog and stratus dissipation pattern that normally follows. The processes that are responsible are again, not found in the synoptic scale, but in the mesoscale environment that will be addressed later.

There are signatures that are discernible in the synoptic pattern that indicated the increase in afternoon fog and stratus events, category four. Figures 46 and 47 are shown to illustrate the diurnal changes. The key indicator is the weak existence of the warm-
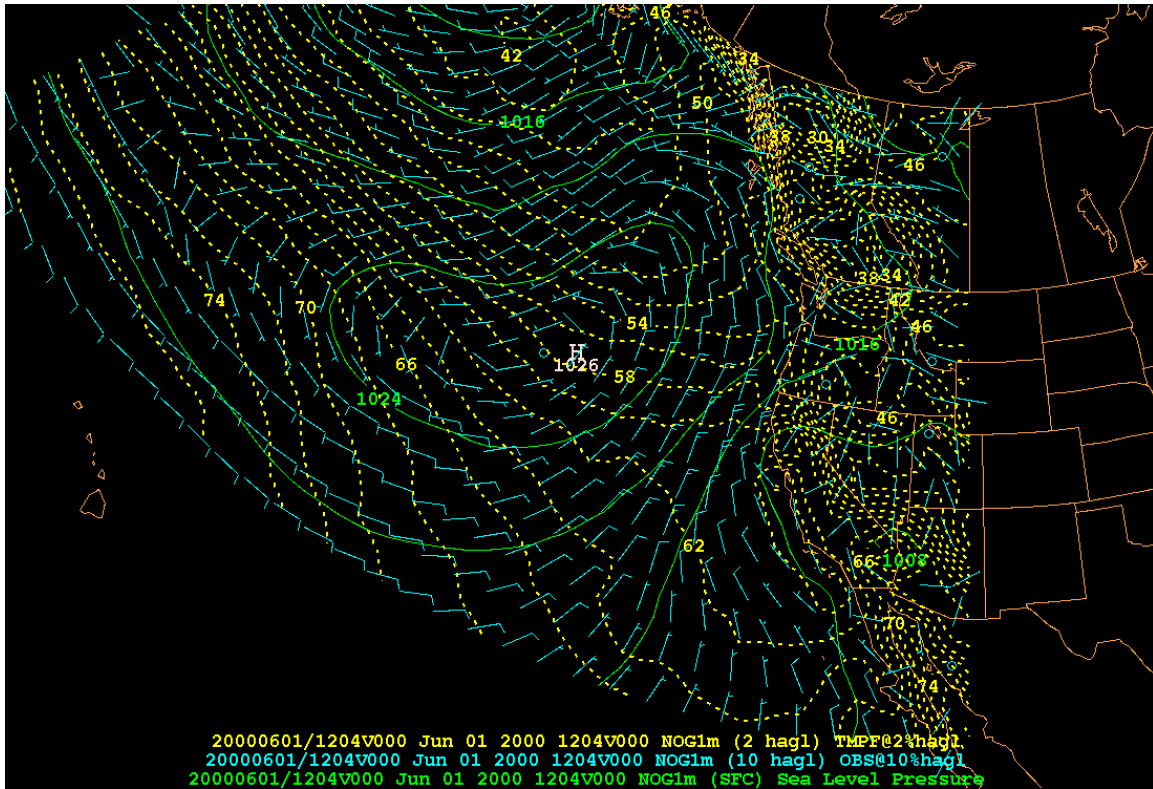
Figure 46. Composites of NOGAPS 12Z June surface analysis for the Los Angeles region for category four events.

core low over the desert southwest on the 12Z composite, illustrated in Figure 46. This feature is not evident in category one events for the same period.
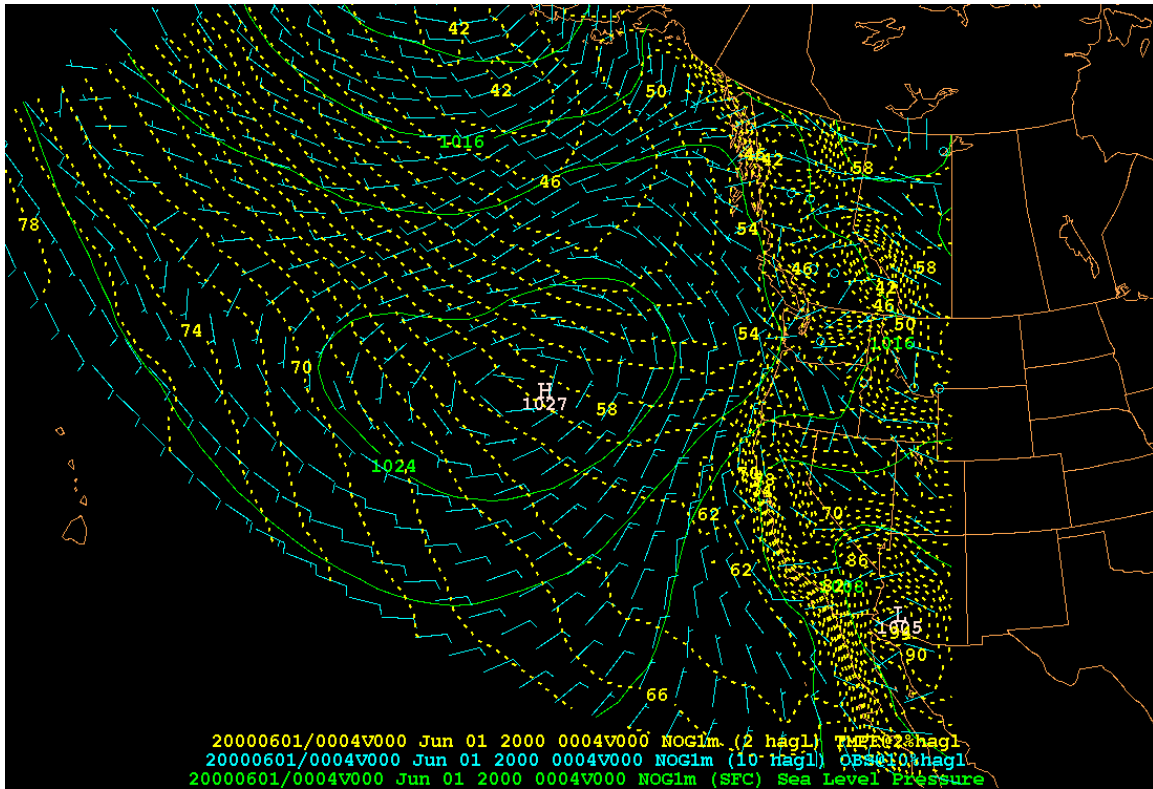
Figure 47. Composite of NOGAPS 00Z June surface analysis for the Los Angeles region for category four events.

Examples of 00Z composites for June revealed the warm-core low over the desert southwest is deeper by 3mb compared to category one events. The deeper low alters the large scale flow inland bringing with it the early return of fog and stratus to the region. While some high clouds were observed in the satellite images, (mainly associated with the subtropical jet stream), they were extremely limited and not the key factor. Of note, the majority of these events were in the latter half of the month of June, a probable indication of seasonal variability.

The high-pressure cell begins the month of June due west of the bight region and slowly migrated north during the month. While there was no distinct ridging like the Pacific Northwest, there were some indications of weak anticyclonic turning across the region as shown in Figure 47. There was a consistent and mostly weak flow that was observed out of the northwest that followed the coastline that is in response to the weak ridging. As a result of being further located south, many times a weak warm-core low

develop during the entire summer period inland that caused a slight turning of the synoptic flow into the coast. While at the same time, a divergent wind pattern in the horizontal can be seen in the region on Figure 48. While not strong indications, these were the synoptic signs to a category one event; weak ridging, weak or absent warm-core low, and a divergent near surface wind pattern.
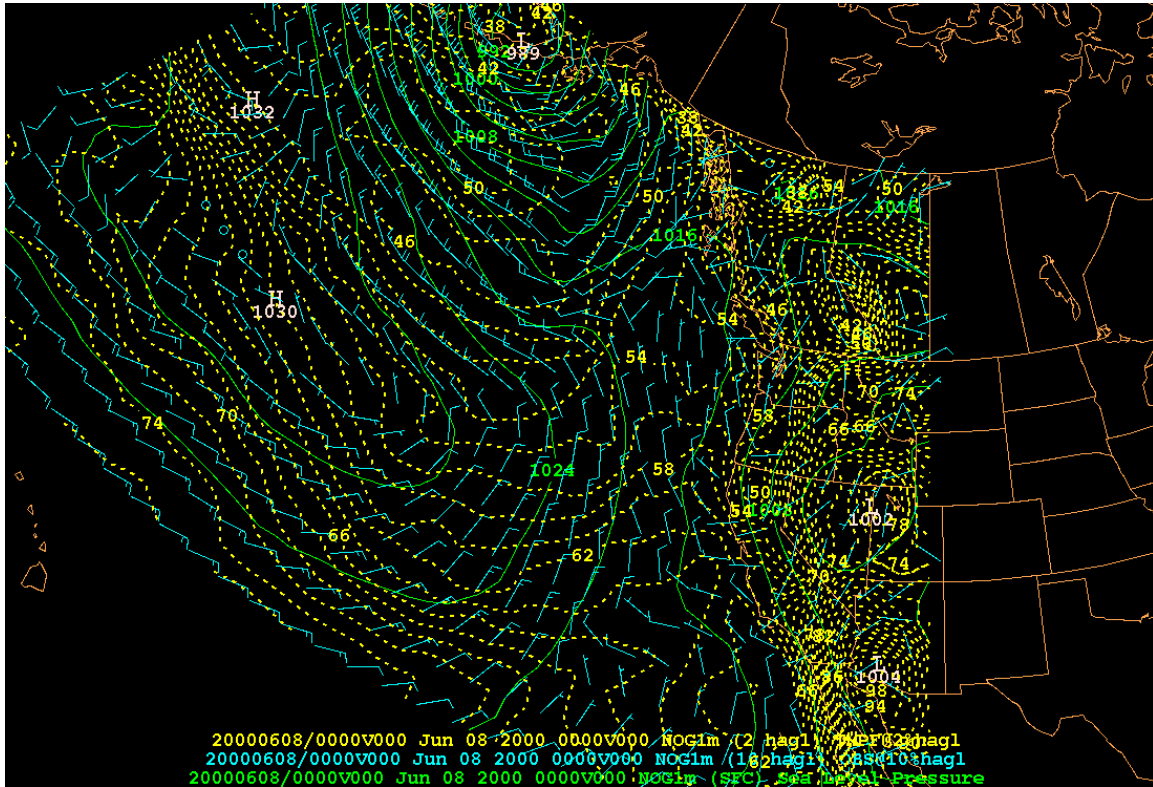
Figure 48. NOGAPS 08/00Z June 00 surface analysis. Note weak warm-core low over northeastern Nevada

Examining satellite imagery during the month, the dissipation pattern of the fog and stratus tended not to dissipate from a north to south manner like the more northern regions, but would dissipate from shore to seaward, much like a large snow plow pushing snow off the road. There was no specific synoptic signal that would indicate this breakup.

In the case of MSC category four, the overriding synoptic pattern remained the same. The subtle difference that resulted in the afternoon intrusion of fog and stratus was the development of a warm-core low over the desert southwest. At first glance, this is a confusing signal as compared to category one patterns. However, the stronger the inland

warm-core low, the stronger the overall flow became. There were two basic cases observed. First, if a warm-core low formed over the high desert of Nevada, the warm-core low over the desert southwest would be the stronger of the two. In the second case, only the formation of the warm-core low over the desert southwest would be observed. In either situation, the stronger warm-core low was over the desert southwest. These cases caused a near direct onshore flow throughout the day, albeit fairly weak, i.e. 10 knots or less as shown in the COAMPS simulations. Figure 49 shows typical pattern for MSC category four where weak ridging can be seen, but more importantly, a much stronger inland warm-core low, i.e. a 999mb low.
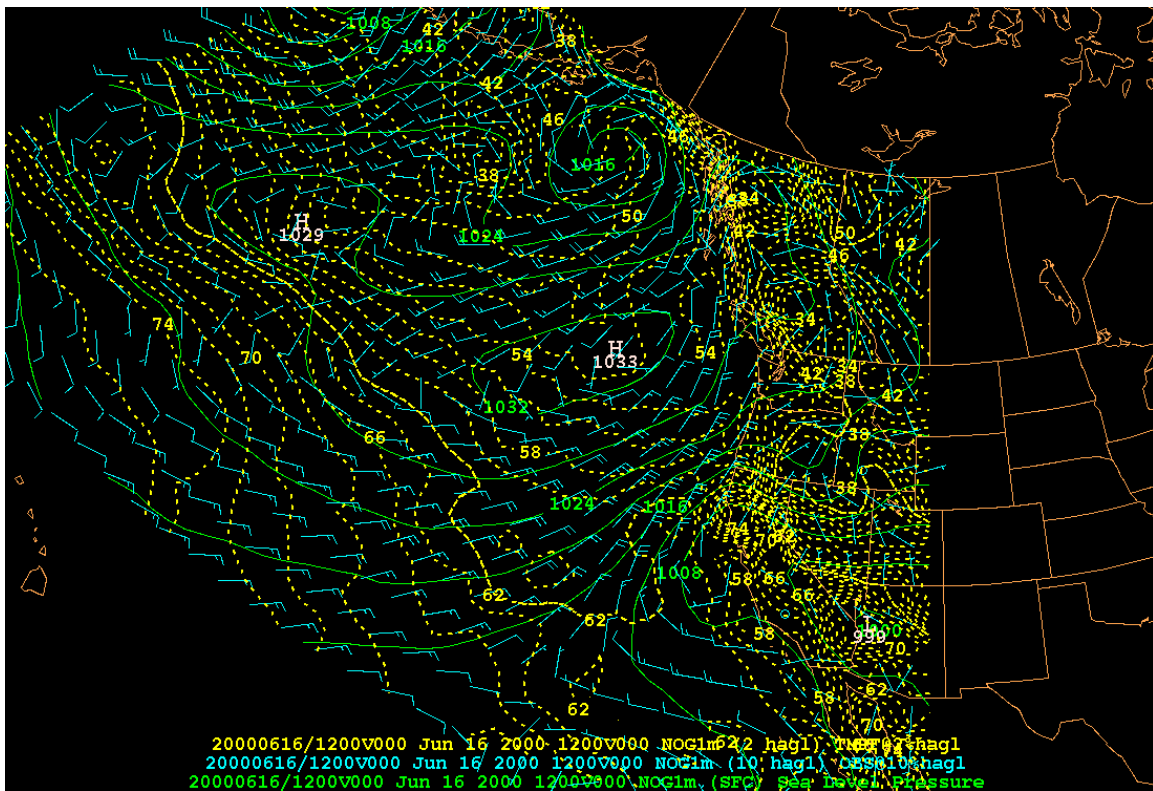
Figure 49. NOGAPS 16/12Z June 00 surface analysis. Note the formation of a 999mb warm-core low over the desert southwest.

Moderate variability is observed during the month of July of which 25 occurrences of MSC category one was observed as compared to 17 cases in June. The synoptic pattern was one of consistency, as one would expect with such a high occurrence of category one events. The Catalina Eddy may have been responsible for some limited number of these events, but not directly addressed due to its infrequent

nature. Some evidence of a dominant warm-core low over the desert southwest was observed however. While this low appeared from time to time, it was either weaker or part of the board high-desert warm-core low-pressure system. The key indicator in the synoptic pattern seemed to be that a horizontal divergent wind flow. While the winds were typically weak, 10 kts or less and many time 5 kts or less, there was a divergent pattern present in the simulation. There was also evidence of weak ridging, but that was not nearly as consistent feature as was the divergent wind flow within the region. It should be noted that the discussion of the divergent wind patterns and other wind patterns refers to the horizontal fields only and does not imply vertical motions. With the absence of a divergent wind pattern, radiative effects may play an important role, i.e., the boundary layer decoupling process.

The month of August resembled that of June by exhibiting greater variability, 14 occurrences of MSC category one, 10 occurrences of MSC category four, and two days with no fog and stratus. Category one synoptic patterns were unchanged from previous months. However, category four events showed some disparity from June. The overnight existence of the warm-core low over the desert southwest was not evident for August in the composites (not shown), as one would have expected. The development of this warm-core low was also not as deep in central pressure as was observed in June composites. They were some 3 to 5 mb's higher. The biggest indicator that resulted in the weaker warm-core low was the presence of light and variable coastal winds, i.e. winds less than five knots.

In the two days where there was no fog and stratus observed in the region, the synoptic pattern showed a minor, but important anomaly. As illustrated in Figure 50, the position of the warm-core low was shifted further south into northern Mexico. This resulted in a weak easterly flow over the region. While not a true Santa Anna wind event, it does have very similar results due to the adiabatic warming experienced from downslope flow over various mountain ranges in the region.
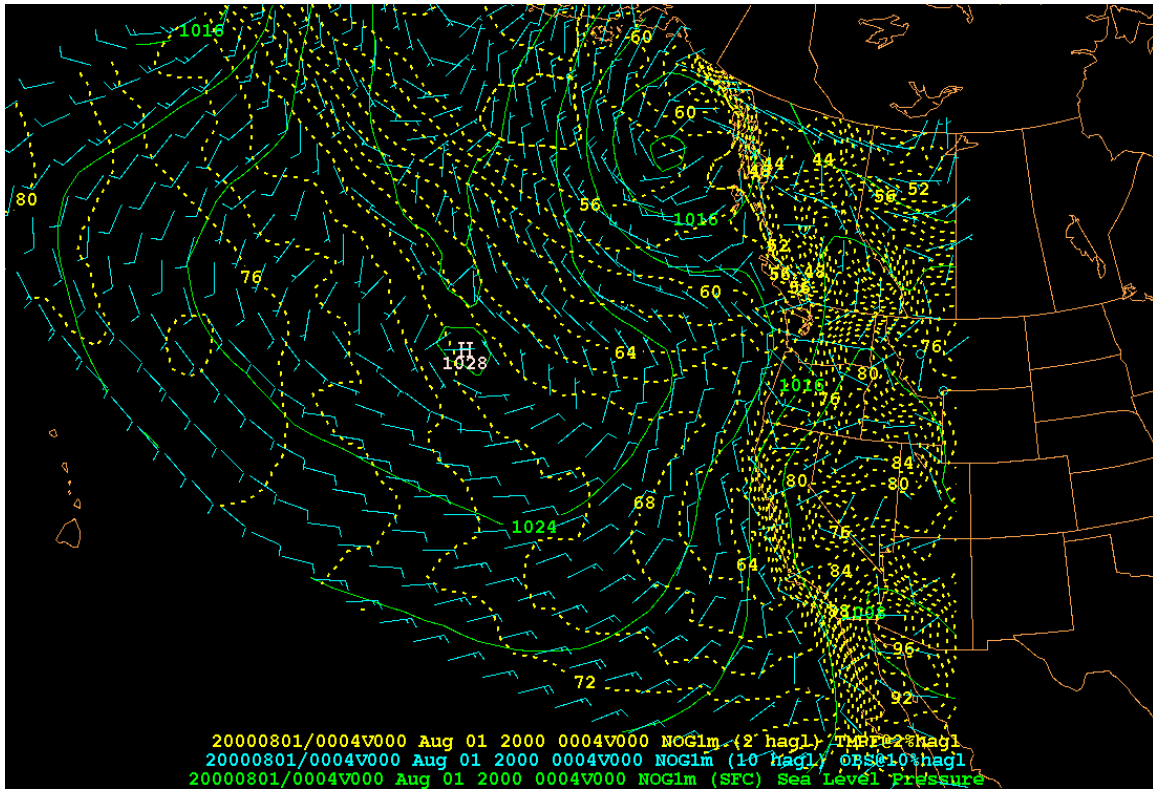
Figure 50. Composite of NOGAPS August surface analysis for the Los Angeles region. This is an example of category seven (no fog and stratus) event.

The Los Angeles region was clearly the most difficult to observe clear synoptic pattern indications of MSC evolution. This was due to two reasons; one of which is the latitudinal location of the region and the other is the geographical relationship to the predominate flow pattern. The strength and locations of both the subtropical high and the inland warm-core low played important roles that appeared to manifest itself in the presence or absence of a divergent, horizontal wind pattern in the bight region. Topography no doubt plays a role as it does in the other regions, but perhaps more so here. The key to this region will lie with mesoscale forcing, which will follow in the next section.

Of the 14 occurrences of MSC category one in August, there were no perturbations out of the typical synoptic pattern. However, MSC category four was somewhat more allusive and a definitive synoptic pattern was not observed, unlike July. Many times the appearance of the warm-core low over the desert southwest that was somewhat absent in July was more prevalent during August, but somewhat inconsistent

throughout the month. There was however, lower pressure across the region, but not the clear presence of a warm-core low as depicted by the analyses. A much smaller scale analysis may have revealed the presence of such a feature. Another, more consistent signal, seemed once again to be the presence of a weak wind field with divergent characteristics in the bight region. There was no correlation between the warm-core low over the desert southwest and light winds with the formation of fog and status. The most promising synoptic scale indication seemed to be the presence of a divergent wind field in the bight region. While weak ridging was often associated with this wind field, it was not always the case. Although diurnal sea breezes were prevalent at the shoreline, it was the broader divergent pattern that occurred in the late afternoon that signaled the return of the fog and stratus prior to sunset.

There were two days in which no fog and stratus were observed in the bight region, the 10th and 17th of August. While the overall synoptic patterns were quite different over the North Pacific Ocean, the resulting flow pattern over the bight region was the same. Figure 51 shows flow pattern over bight region. The single commonality for this event was the presence of an offshore flow. While in the northern bight region the flow was more northerly vice a northwesterly flow, normally a clear signal that initiates the Catalina Eddy, the remaining flow across the region was also offshore. This appeared more as a result of the inland warm-core low being displaced further south than typical. Adiabatic warming and drying from coastal mountains seems is the result of the easterly flow pattern. Additionally, with a strong coastal or slightly inland high-pressure cell, one that would cause abnormally warm temperatures also produces the Santa Anna winds, a warm katabatic wind that dries much of the regions it effects.
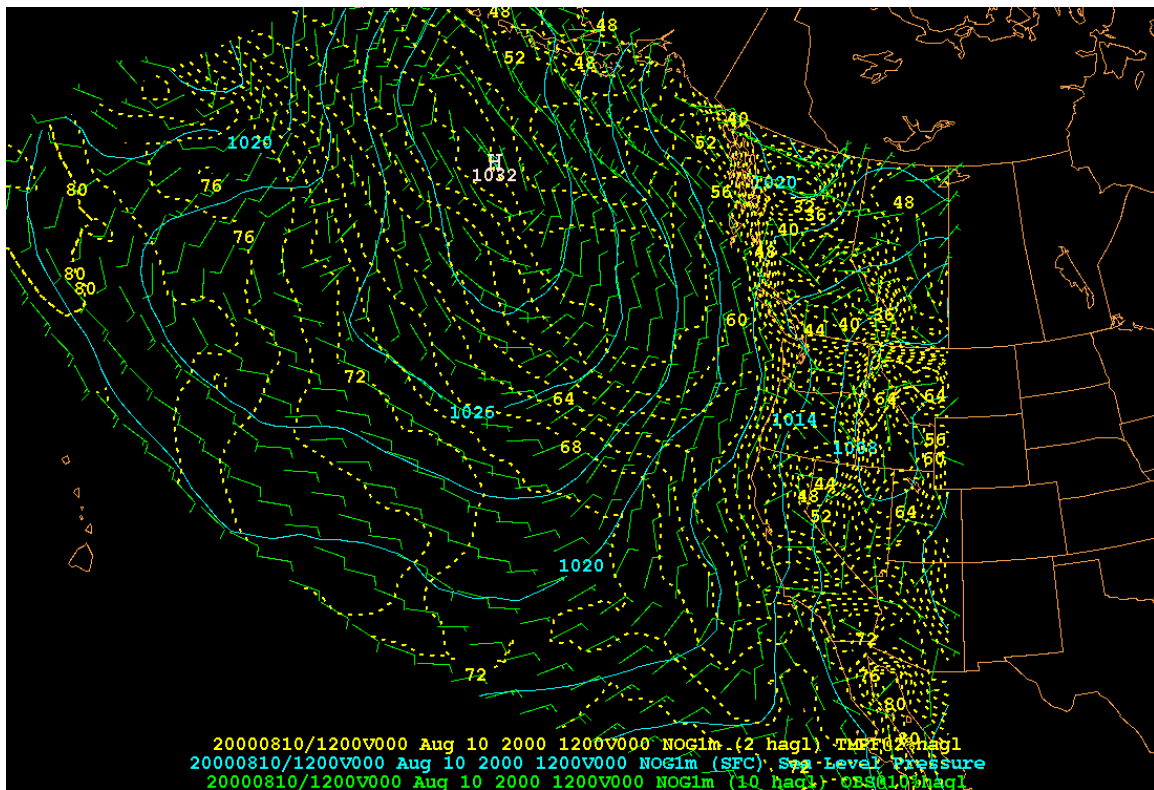
Figure 51. NOGAPS 10/12Z August 00 surface analysis. Note the offshore flow over the bight region.

Significant sea surface temperature variability was observed during the month of June. The lowest water temperatures were consistently near Point Conception at 12 degrees at the start of the month to 15 degrees C by the end of the month. While the remainder of the Bight region was in the range from 18 to 20 degrees C. This was not unlike that which was observed in the Capetown region of Northern California. Nighttime inland marine layer temperatures were slightly cooler. This further allowed the condensation process to occur on a nearly nightly basis.

July water temperatures were cooler. 13 to 15 degrees C at Point Conception and 15 to 20 degrees C throughout the remainder of the region, changing slightly from June, while near shore marine layer temperatures was warmer. This created greater stability in the boundary layer, especially at night.

By August with summer at its peak, so were the sea surface temperatures. The mean temperatures are now at 17 to 22 degrees C with the continued exception of the

Point Conception region where water temperatures remained at 13 to 15 degrees C With the increase of water temperatures, August MSC events once again resembled that of June where in both months the water and near shore temperature relationship was the same.

THIS PAGE INTENTIONALLY LEFT BLANK

IV. MESOSCALE SIGNALS IN THE COASTAL REGIME

The previous chapter demonstrated a relationship between synoptic structure and the evolution of fog and stratus each day. As was noted earlier, 11 cases were chosen to examine the more detailed forcing of MSC by running COAMPS simulations. Although the COAMPS forecasts were not without error, the forecasts by COAMPS were found to be acceptable representations of the weather conditions during the period of study because they had similar large-scale structure to the NOGAPS analyses used in the composites. The emphasis in using the COAMPS forecasts is to relate the observed stratus evolution to synoptic and mesoscale structures in the COAMPS forecasts. Inferences drawn in this examination are of course limited by the forecast error of the COAMPS forecasts, however if a consistent signal is obtained it is suggestive of a probable physical relationship. To more fully establish this relationship, mesoscale verification is required and was not done for this study. Subjective comparisons to NOGAPS analyses and other synoptic scale observations was done is suggests that the forecasts are credible.

In this section, the mesoscale, coastal regime is examined to determine boundary layer mechanics and associated variables and processes that lead to particular stratus evolution. Specifically, trajectory analysis and forecasts using Vis5d, moisture fluxes, low-level Q-vectors to examine forced vertical motions, and the thermal wind relationships are examined for their relationship to stratus evolution. Table 5 below lists the parameters examined.

Synoptic regime	Mesoscale regime
Strength & position of STH	MBL height & tendency
Strength & position of warm-core low	Theta at top of MBL & tendency
Dir & speed of coastal winds	Coastal vertical motions (w)
Dir & speed of ageostropic winds	MBL thermal winds
Dir & speed of geostropic winds	Q-vector analysis's & forecasts
Pressure gradient force indicators	Moisture conv/div & tendencies
SST and tendencies	Clouds present above the MBL

Table 5. Environmental parameters investigated in both the synoptic and mesoscale regimes.

Not all MSC categories were investigated for each region for each month. Instead, the three basic evolutions, decreasing, increasing and no change were the focus for the dates listed in Table 6 as representative case studies. Keep in mind, this study is based on COAMPS with 21km resolution with a model start time 12 hours prior to the events in question to allow the model sufficient time to adjust. Consequently, 12-24h forecasts were examined and compared to the observed evolution of the fog and stratus events as seen in the satellite images.

A.   PRESSURE GRADIENTS

The composite analysis suggested a relationship between the sea level pressure distribution and MSC evolution and forecaster thumb rules often use pressure differences to determine stratus behavior. Consequently, the strength and tendency of the pressure gradient force was examined in each region to evaluate its diurnal effects as well as its seasonal variability on MSC evolution. To construct this measure, a point was chosen for each region and a one-degree spread on either side of a point based on the coast was used to determine the pressure gradient force across the coast.

While the diurnal change was very clear and consistent with the sea breeze evolution, the fog and stratus events did not evolve in any consistent relationship to the magnitude of these pressure differences.   Both the resulting near-surface wind direction and speed were investigated for each of the cases chosen. During the afternoon period when the sea breeze would be at its maximum strength, the MSC event would be retreating, while at other times, the MSC event could be moving onshore with the same flow regardless of speed. The pressure gradient force was simply not a indicator in predicting any facet of a MSC event and should be discarded as such.

B.   BOUNDARY LAYER EVOLUTION

Since the surface pressure showed little consistent signal, the boundary layer structure was presumed to play a role and examined through the use of GARP. In each region, a cross section was chosen at the mid-point of that region in each case studied. The vertical resolution used was from the surface to 700mb at 2 degree K increments. A sufficient cross-coast distance was used to observe the changing boundary layer from seaward to inland.

1.   MSC Events That Lead to Dissipation or Decrease in Coverage

In the case of the MSC events leading to dissipating or decreasing amounts regardless of anomalies (tendency changes in the overall change), the model consistently depicted a lowering of the boundary layer near the coast and steady to mostly decreasing temperatures at the top of the boundary layer.   The degree of dissipation was well correlated with the amount of change the model was predicting.   That is, a change (lowering of the top of the boundary layer) of approximately 1500 feet or more and a temperature change (cooling) of 4 degrees K of potential temperature or more was a strong indicator of a more rapid dissipation of fog and stratus. Weaker changes resulted in steady to slower dissipation rates. It should also be noted that if only one parameter met the criteria and the other did not, then the rate of dissipation would be steady or slowed. Both criteria had to happen for a more rapid dissipation. Keep in mind that this is not to imply cloudy to clear scenarios, but only a decrease or dissipation in coverage, which sometimes leads to clear conditions.

It appeared the COAMPS model handled the boundary layer decoupling quite well. There were no clouds present in the case studies above the boundary layer to influence the decoupling process. It is thought that radiative effects were sufficient enough to weaken the boundary layer inversion. This was suggested in the COAMPS simulation runs where the model showed increasing temperatures (Kelvin) at the top of the boundary layer.

2. MSC Events That Lead to Formation or Increase in Coverage

In these cases, the model changes were more subtle, but recognizable. The top of the boundary layer showed a maximum height change of approximately 1000 feet; often times, much less. This variation was mostly a lowering, but could exhibit a slight rising of the top of the boundary layer. The temperatures at the top of the layer were the real key. Temperatures were primarily steady with only occasional variations of no more than two degrees K in either direction. Steady or rising temperatures indicated a quicker formation period.

Satellite observations for these case studies all showed increasing amounts of fog and stratus throughout the day or most likely near the end of the sun lit hours, which verified the model predictions well in these cases. Boundary layer inversions were quite strong in these cases where radiative effects were not strong enough to break down or even weaken the inversion significantly.

3. MSC Events That Lead to No or Little Change in Coverage

As one would expect, the top of the boundary layer remained virtually unchanged, as did the potential temperature throughout the day. Boundary layer fluctuations were no more than 500 feet while potential temperatures stayed within 2 degrees K. These minor fluctuations could also be errors in the model run or evidence of weak gravity waves in the model and probably fall within the prediction limits of marine boundary layer depth and inversion strength for the model. This highlights the potential for a bad forecast by the model even though it predicts a very consistent signal.

For the 11 cases examined, the marine boundary layer variations failed to follow the aforementioned pattern for the 28 June 2000 run. The model predicted a major lowering of the boundary layer (greater than 1500 feet) and a 4-degree K drop in

potential temperature, which is consistent with dissipation, but observations showed 100 percent coverage of fog and stratus throughout the day (for the Monterey region).

C. TRAJECTORY ANALYSES AND FORECASTS

Given the dependence of the MSC evolutions on the marine boundary layer depth and inversion strength, air parcel trajectory that contributed to their evolution were examined. Trajectory analyses and forecasts were examined through the use of the Vis5d program. The same 36h simulations that were used in GARP are examined in Vis5D. Although, many processes could be examined in detail, the focus was limited to trajectory analyses and forecasts. Moisture analyses and forecasts were also looked at, but the model did not handle cloud development and dissipation well and therefore, it was mostly ignored as a useful predictor of observed behavior. This is an area where the forecast error was large, which apparently did not adversely impact the basic flow patterns as compared to the available observations.

1. MSC Events That Lead to Dissipation or Decrease in Coverage

Flows in and above the boundary layer were investigated over the 36h COAMPS model run with the emphasis on the daylight hours.   These trajectories were compared to the satellite imagery for verification. That is, if the simulations showed a trajectory that was descending, did the corresponding series of satellite images show dissipation? Several model runs were examined and the results were consistent with the air trajectory simulations.   Several examples are presented as evidence.

The summertime synoptic-scale structure varied only somewhat from day-to-day and produced a characteristic type of coastal trajectory. A large majority of the trajectories were typical of flows around the northwestern to western quadrant of the subtropical high-pressure system. These trajectories were mainly along the coast from the north as shown in Figure 52. Two cases had trajectories, due to different synoptic-scale structure that were westerly in nature, i.e. onshore flows that originated well over water as illustrated in Figure 53. Although these were the general character of the trajectories, there were identifiable differences in their association with MSC type.
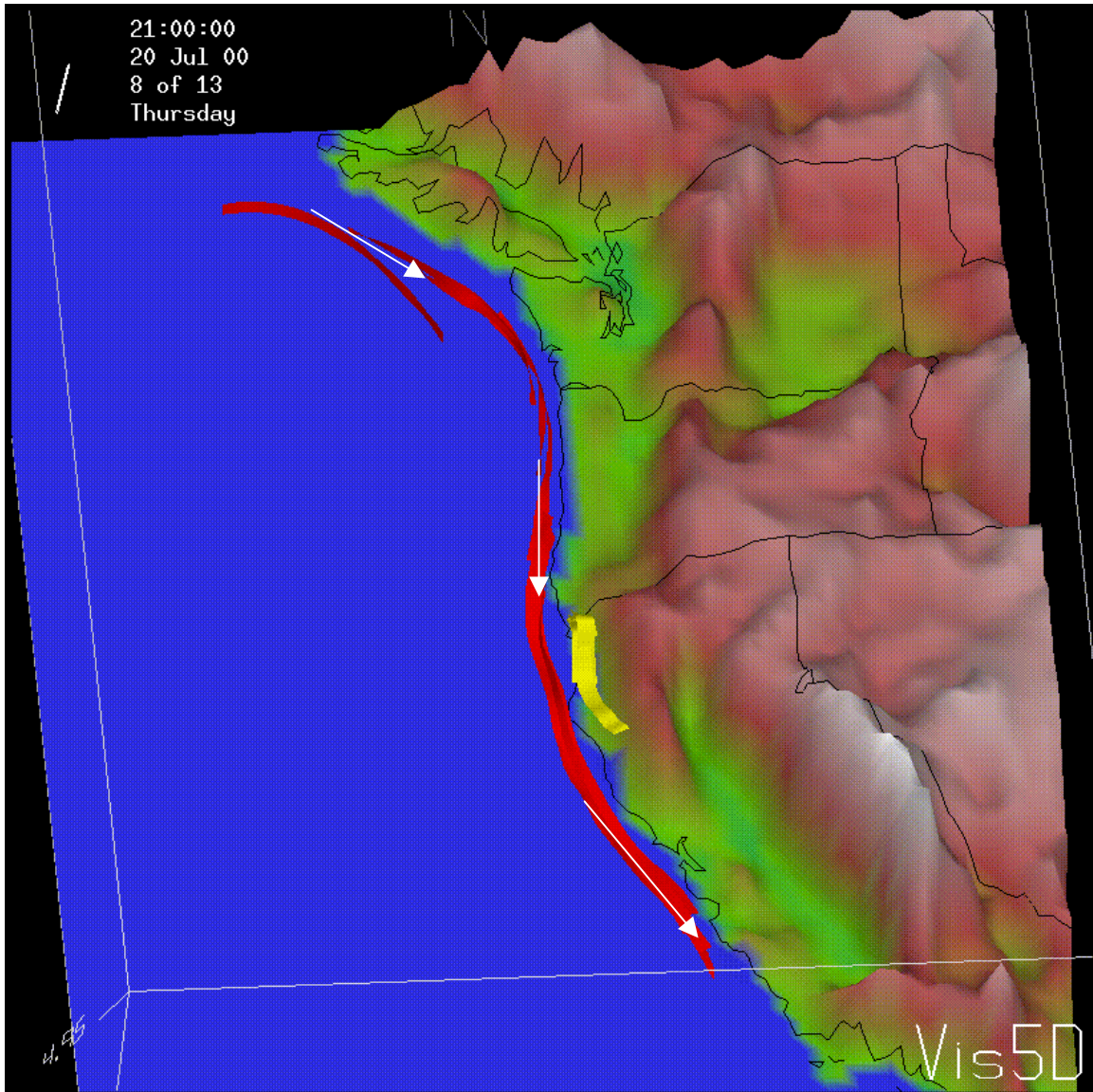
Figure 52. Vis5d illustration of boundary layer flow denoted in red around subtropical high-pressure system. Arrows indicate direction of flow.
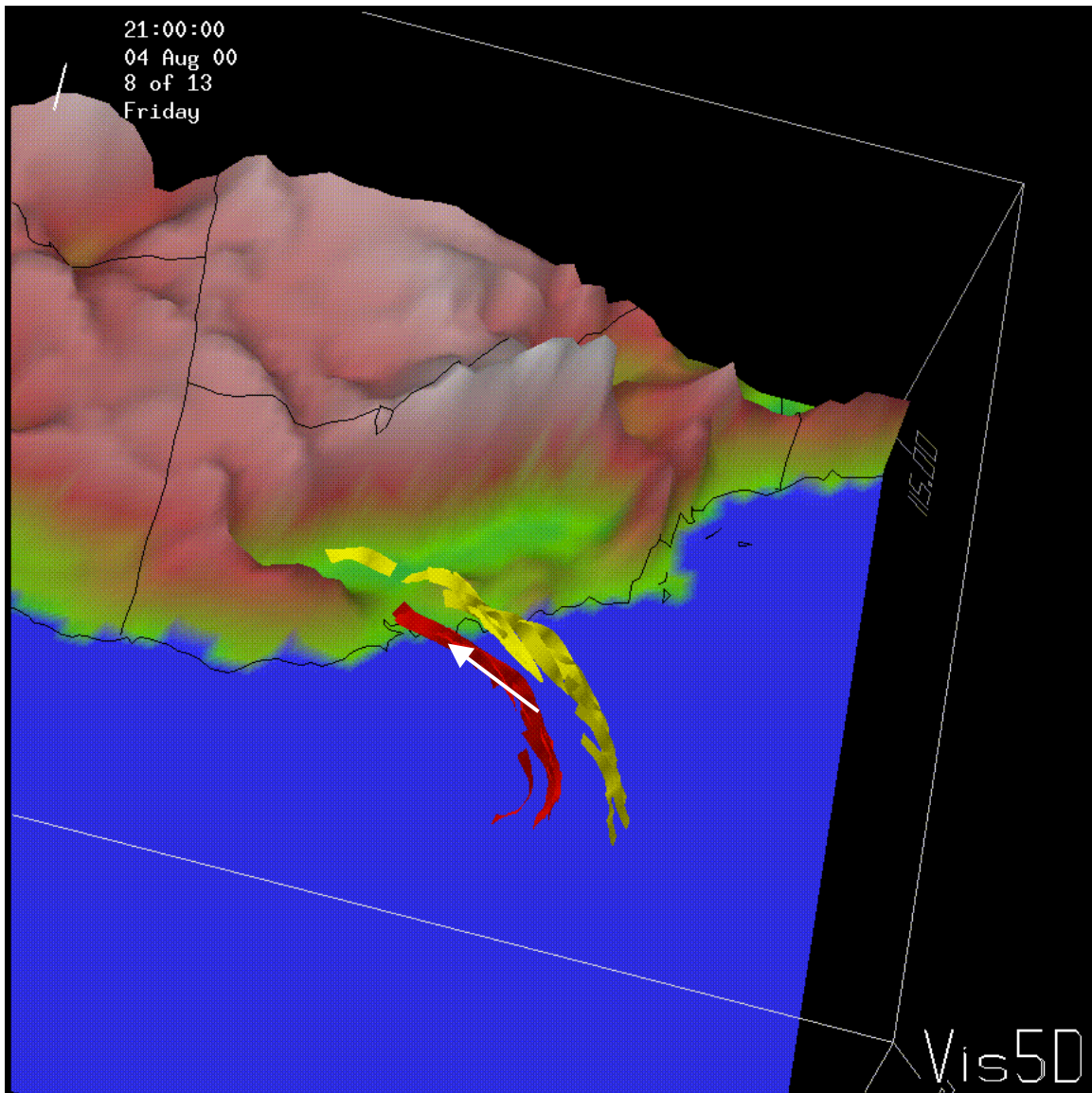
Vis5D

Figure 53. Vis5D illustration of westerly on shore flow. Boundary layer winds denoted in red and flow above the boundary layer denoted in yellow.

The key trajectory profile that indicated dissipation of the MSC event was one where the air was descending in the boundary layer or more likely air just above the boundary layer was descending into the layer. It is hypothesized that entrainment of warmer, drier air located just above the MBL would help account for the dissipation of the fog and stratus.

There were three basic flow patterns that were found in the majority of the cases, first was the flow along the coast from the north, the second was the trajectory shown

above in Figure 48, and the last was a southerly trajectory. Figures 54 and 55 show descending air. In this case both a northerly and southerly flow converged and descended
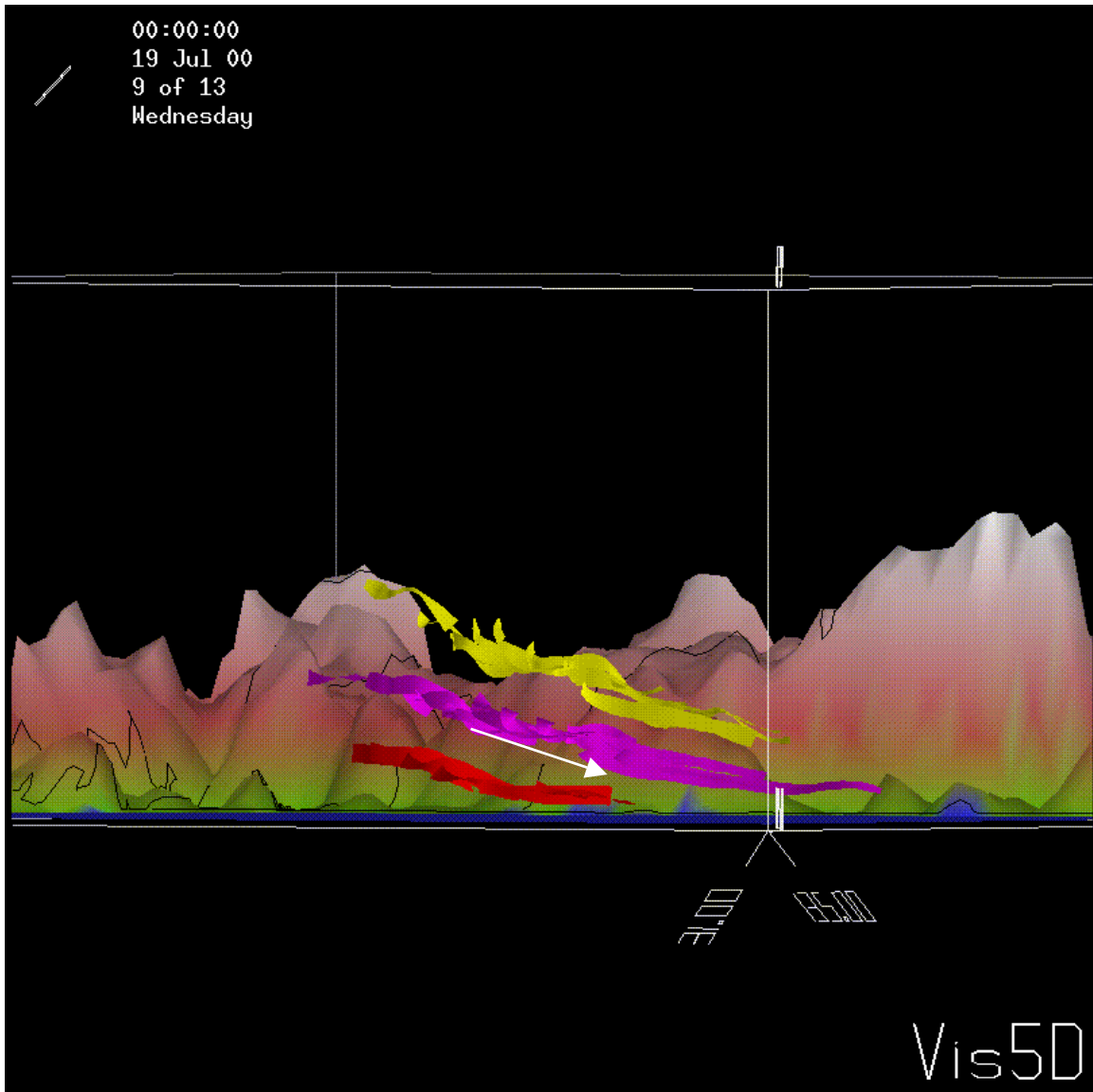
Figure 54. Vis5D trajectories of late afternoon locally on 18 July 00 for the Eureka region. All three flows indicate descending air into or towards the MBL.
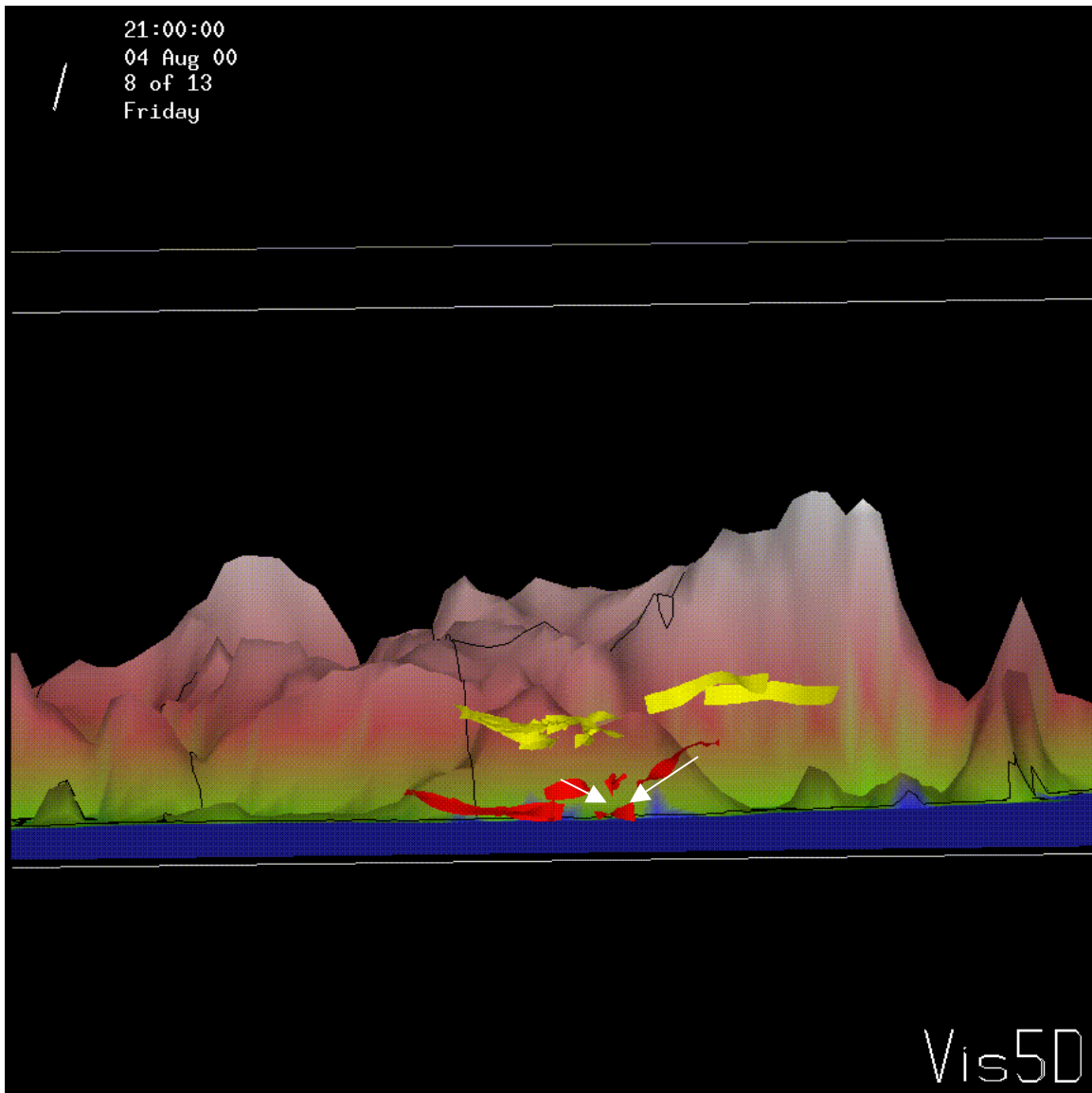
Vis5D

Figure 55. Vis5D illustration at 21Z 4 Aug 00 for the Eureka region.

into the boundary layer. The combination of boundary layer decoupling, possibly through radiative effects, weakening the boundary layer inversion allows for entrainment of warmer and drier air into the boundary layer

2.   MSC Events That Lead to Formation or Increase in Coverage

The case studies in this category also had common characteristics, but there were a few anomalies. Figure 56 illustrates the characteristic trajectory for this MSC category, the flow is nearly horizontal within the boundary layer and along the coast. The
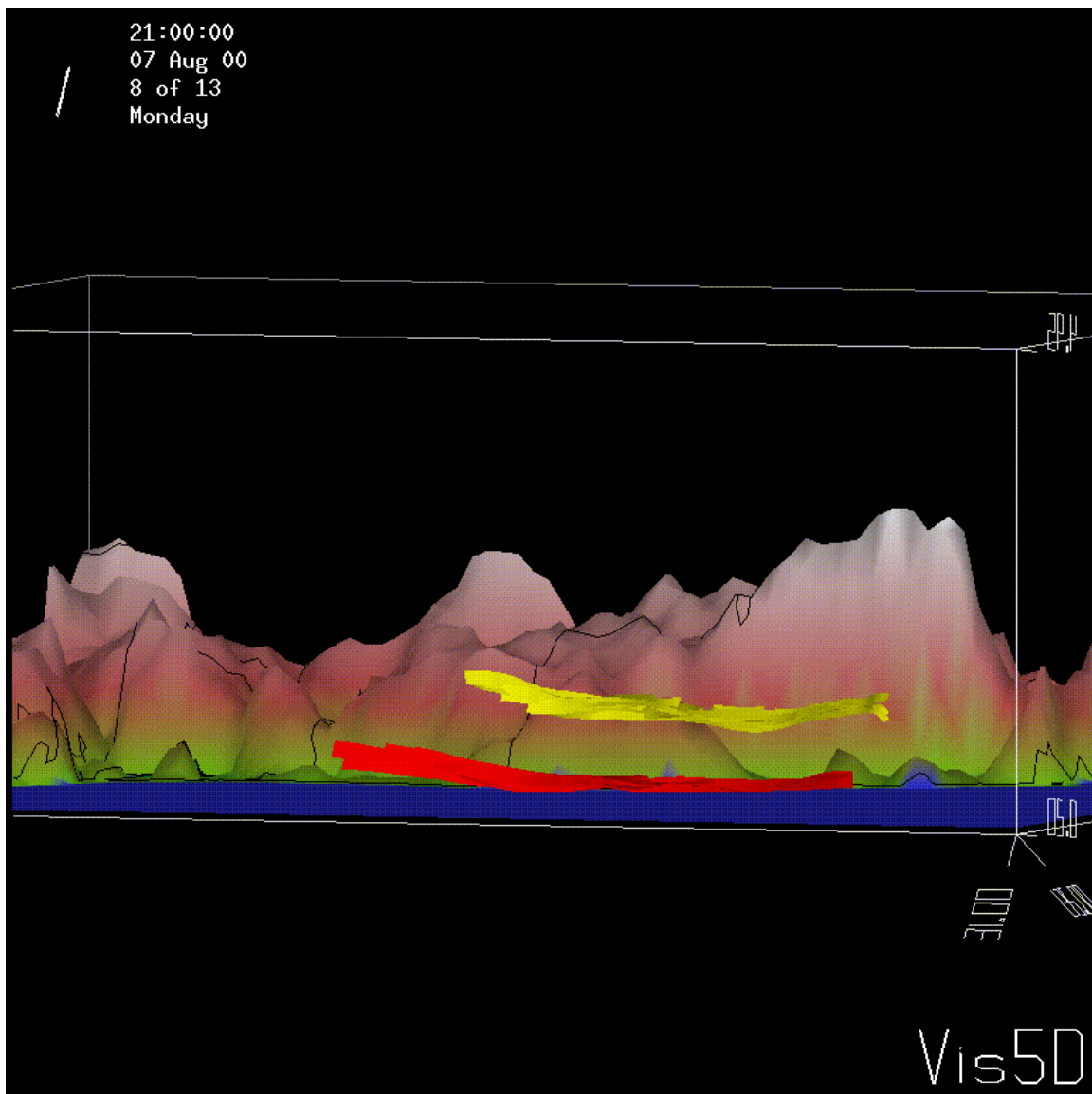
Vis5D

Figure 56. Vis5D illustration at 21Z 7 Aug 00 of the Eureka region. Red denotes flow in the boundary layer.

trajectory many times did not start out as horizontal, but spends several hours afterwards in a nearly horizontal flow. Satellite observations correlated well, often depicting a decreasing coverage in the MSC event during period when there was weak descending air, but the process is arrested shortly after the flow becomes horizontal. One possible explanation in that the boundary layer is a cooler, moisture-laden air in a coastal-following flow in the boundary layer that advances the upwelling process.   The upwelling process results in cooler water being brought to the surface through air-sea

interactions, which further cools the air just above it. Due to the high moisture content of the air just above the water, it condenses and fog and stratus results. While the horizontal flow does not change the marine boundary layer depth, it was associated with MSC increases.

3.   MSC Events That Lead to No or Little Change in Coverage

There are two key factors that stand out in the prediction of this MSC event. Unlike the previous MSC category, this event requires two trajectory components. First as shown in Figure 57, the trajectory is normally several hundred kilometers to a thousand kilometers long over the same 36h period. It is the result of the flow around the subtropical high-pressure system. The trajectory, once it encounters the continent, follows the coast southward with little to no onshore component.

The second key factor as shown in Figure 58, is that the long trajectory flow must stay within the confines of the boundary layer. This extended flow within the MBL differs from category one in that category one flow is characterized by descending air. This coastal air mass is homogenous and laden with moisture. The strength of the subtropical high is large, normally greater than 1030mb. Subsidence in the western quadrant produces a strong capping boundary layer inversion and prevents any entrainment from air above. This is consistent with the lack of change in MBL inversion strength or depth noted in the previous section. The flow as described in the previous section develops and enhances the upwelling process over a very long coastal region and
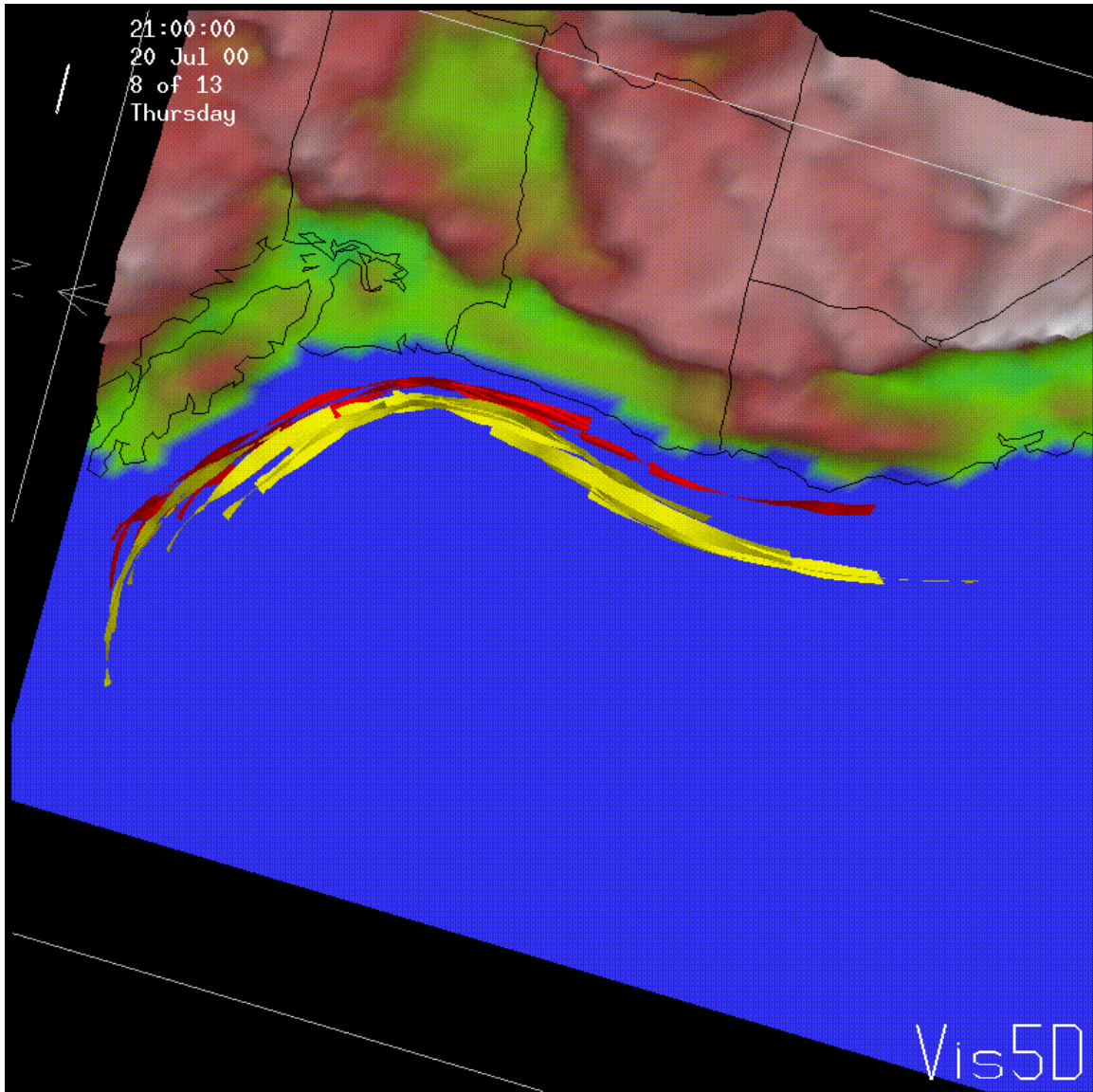
Figure 57. Vis5D illustration at 21Z 20 Jul 00 along the West Coast. Red denotes boundary layer flow and yellow denotes flow above. Note the long trajectory around the subtropical high-pressure system.

normally for a long period of time. Two or more days of continuous periods of fog and stratus with little change is not uncommon for these types of trajectories.
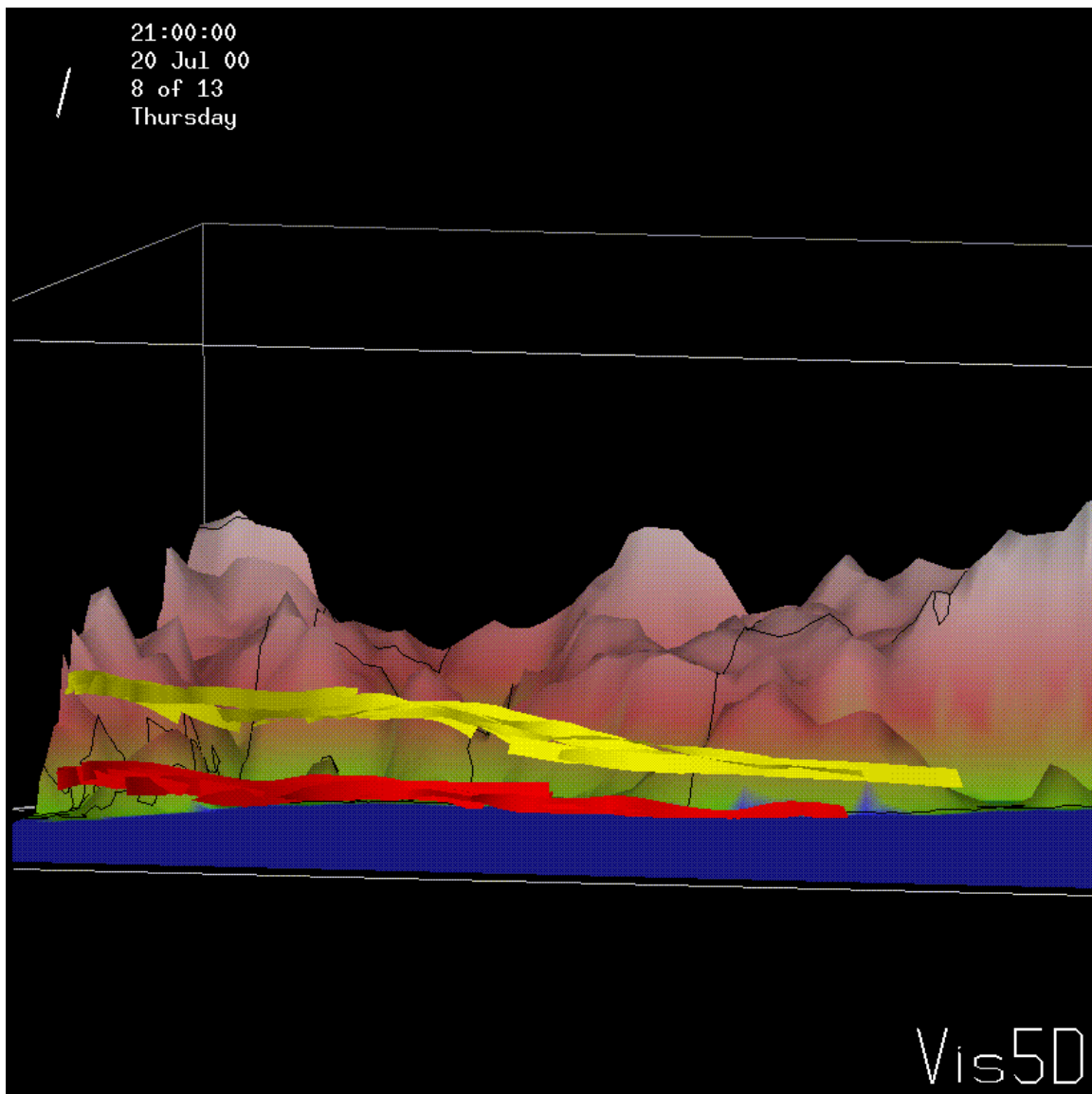
Figure 58. Vis5D illustration from 21Z 20 Jul 00. Red denotes boundary layer flow, which is horizontal with no mixing evident.

D. Q-VECTORS

In view of the fact that both the trajectory analysis and the boundary layer structure analysis indicate a dependence of MSC evolution on the three-dimensional motion, perhaps a simpler method such as Q-vectors can be applied. Q-vectors are useful to calculate synoptic-scale vertical motions and only require one level to be evaluated. A change in synoptic-scale subsidence is likely to be associated with changes in the boundary layer depth and MSC evolution.

This large-scale lifting and sinking are deviations can be determined from the omega equation, $\sigma \blacktriangledown^2 \omega + f^2 \omega_{\rho\rho} = -2h \blacktriangledown \cdot \mathbf{Q}$ where the Q vector is defined as

$\mathbf{Q} = -(u_x\theta_x + \upsilon_x\theta_y)$. σ is static stability. Omega is vertical motion in isobaric coordinates. f is the Coriolis parameter. $\omega_{\rho\rho}$ is the partial derivative of omega with respect to h is height. $\blacktriangledown$ is the gradient operator on an isobaric surface. An important property of Q is that is can be evaluated reliably using $(u_y\theta_x + \upsilon_y\theta_y)$ geostropic approximation for the derivatives of the wind components. Unlike the evaluation of wind divergence, where divergence is very sensitive to small inaccuracies in wind data, Q is not prone to large errors due to small observational inaccuracies. The rules about convergence and divergence are quite simple. In regions where there is a convergence of Q-vectors there is upward vertical motion. Likewise, in regions where there is a divergence of Q-vectors there is downward vertical motion. Q-vectors were evaluated using GARP by calculating them using data from the near surface region (1010mb) and represent the near-surface observed wind field. Here, vertical motion is implied from the horizontal near-surface wind and temperature field. While vertical motion is available from the model itself, it tends to be rather small scale and the omega equation extracts the synoptic scale forcing more directly.

1. MSC Events That Lead to Dissipation or Decrease in Coverage

COAMPS did a reasonable job in depicting Q-vectors along the coastal regions based on comparisons with satellite imagery with the exception of the bight region where COAMPS did not depict Q-vectors immediately along the coast due to the 1010 mb surface being underground, but was able to depict them somewhat offshore where the surface is above ground. Therefore, the model could not easily be compared with the

forecast evolution of MSC events in this region based on satellite images. During periods and areas of fog and stratus dissipation, Q-vector divergence was the primarily indication of fog and stratus dissipation in the COAMPS simulation runs, as shown in Figure 59.
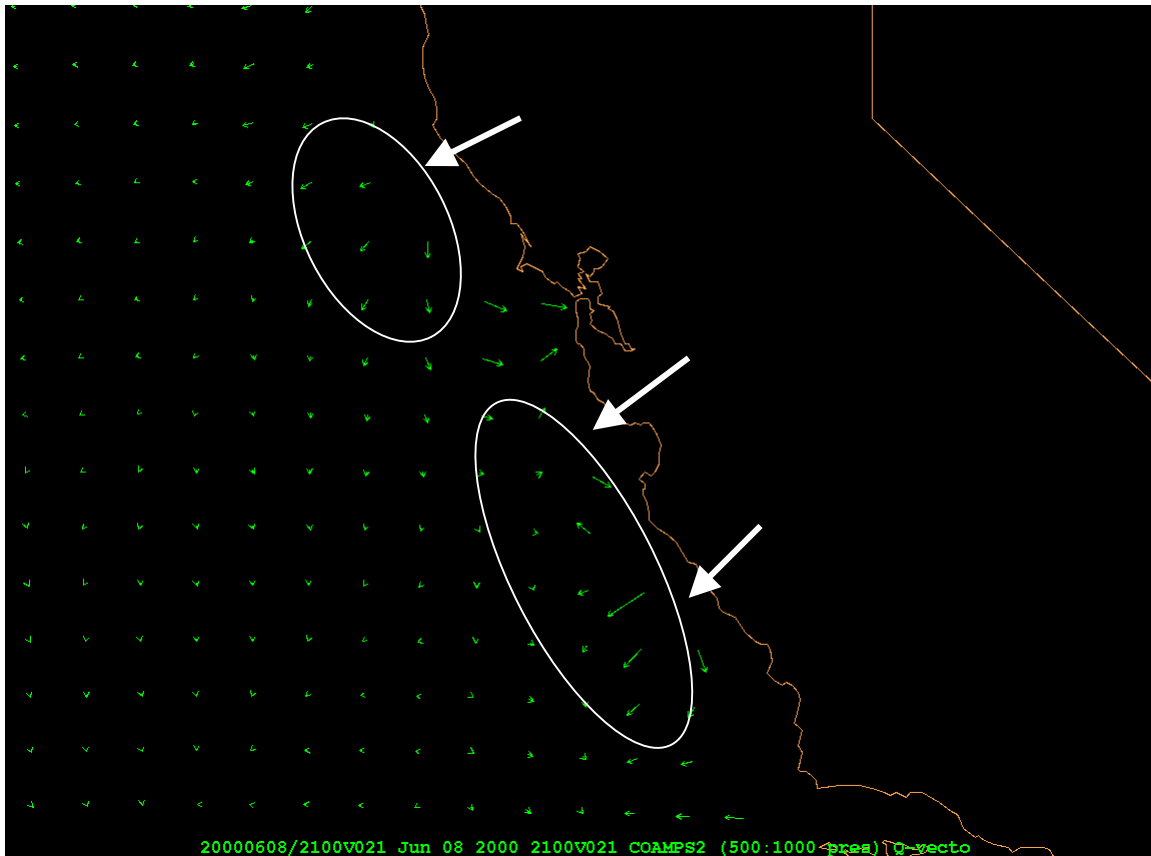
Figure 59. Q-vectors from 8 Jun 00. Divergence in the Q-vectors is the primary indication in the Monterey region where fog and stratus dissipated.

This feature normally verified well with satellite imagery and thus led credence to the concept of using Q-vectors for MSC evolution. In areas where strong divergence of Q-vectors was found, MSC dissipation was also found through comparison with satellite images. Where the magnitude of Q-vectors were small, and no clear indication of a divergent pattern was indicated in the model simulations, the MSC event was slow to dissipate or only small areas cleared, but not necessarily where the model indicated. This is consistent with the marine layer becoming more shallow associated with MSC dissipation.

In the region of Capetown/Eureka to the Columbia River, MSC events occurred more frequently and lasted longer. Many times where a divergent pattern would be

indicated elsewhere, a neutral and/or weak convergent pattern of Q-vectors would be indicated here. Numerous sequences of satellite images confirmed the presence of fog and stratus in the region, as seen in Figure 60. This phenomenon can be attributed to the westward extension of land at Capetown, the pertubating point that deflects the flow in the region. It is hypothesized that this generates a gravity wave, which is created by "anything that perturbs the flow".   The resulting gravity waves will move north and south along the coast from the pertubating point. Those gravity waves that flow north against the prevailing wind field will have a Froude number of less than one. This means the gravity wave phase speed is greater than the ambient wind speed or is said to be subcritical. Flows that have a Froude number of less than one exhibit the characteristic of not having the energetics to not go over a barrier. In the absence of topography that would allow a flow to go around a barrier, the flow becomes trapped, as in this case. Gravity waves that are able to flow south with the prevailing flow will have Froude number's greater than one. This means the wind speed is greater than the gravity wave phase speed and is said to be supercritical. Super- and Subcritical flows were noted in several meteorological parameters in the region. The gravity waves may be evident by the presence of fog and stratus whereas the surrounding areas are clear.
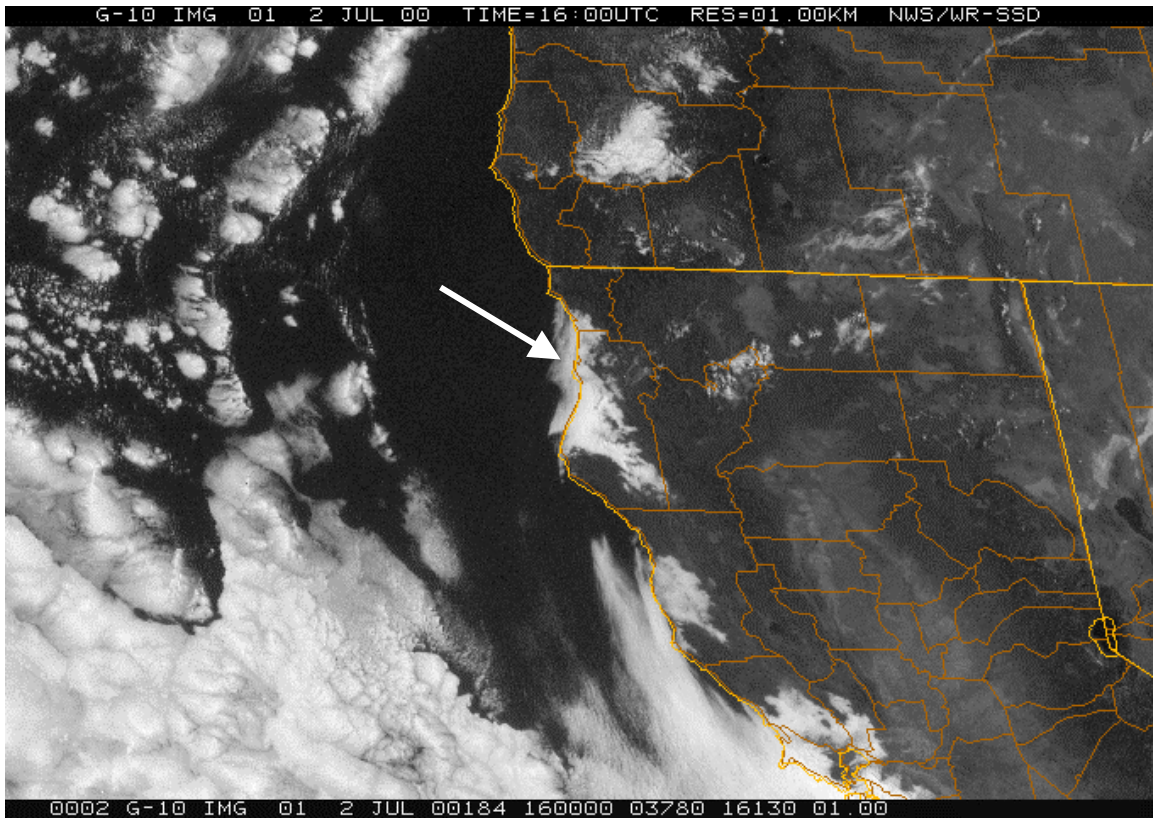
Figure 60. GOES-10 satellite image from 1600, 2 Jul 00. Note the presence of fog and stratus from Capetown/Eureka region to near the Oregon/California border.

To further this concept, the momentum equation, not given, implies that there must be a height change that must accompany any change in acceleration or deceleration of the flow is consistent with the shallow water flow dynamics. The momentum equation can also be integrated along a streamline to determine the energy balance given by Bernoulli's equation, (not given). The results of which implies that total energy (kinetic plus potential) must be conserved following a parcel. This further implies that for high winds, as in the case of supercritical flow, the inversion must be low. A low inversion implies MSC dissipation. Again figure 60 shows a great example of this. The area south of Capetown is clear of fog and stratus. In cases where the flow is subcritical, this implies a higher MBL, which usually implies the presence of fog and status.

2.   **MSC Events That Lead to Formation or Increase in Coverage**

Q-vector derived vertical motion for this category was different and more challenging to interpret from COAMPS simulation runs because the simulations were not as consistent as hoped. The convergence of Q-vectors as shown in Figure 61 is a good

example of cases where the MSC event increased in coverage. However, this was not a consistent signal, perhaps due to model error associated with weak wind fields. In those cases where the wind field was not weak, Q-vectors were consistent in showing convergence. Convergence of Q-vectors implies upward vertical motion that would lead to condensation of the moist marine layer, and hence the development of stratus clouds and fog.

Figure 61 also points out some inconsistencies in the simulation runs for this category. For example, the San Francisco Bay region implies (no inland Q-vectors) divergence in the Q-vector pattern, but this day showed an increase in fog and stratus for the Bay area. While this is considered a minor perturbation to the overall divergent field, it does point out the possible inconsistencies that arise.
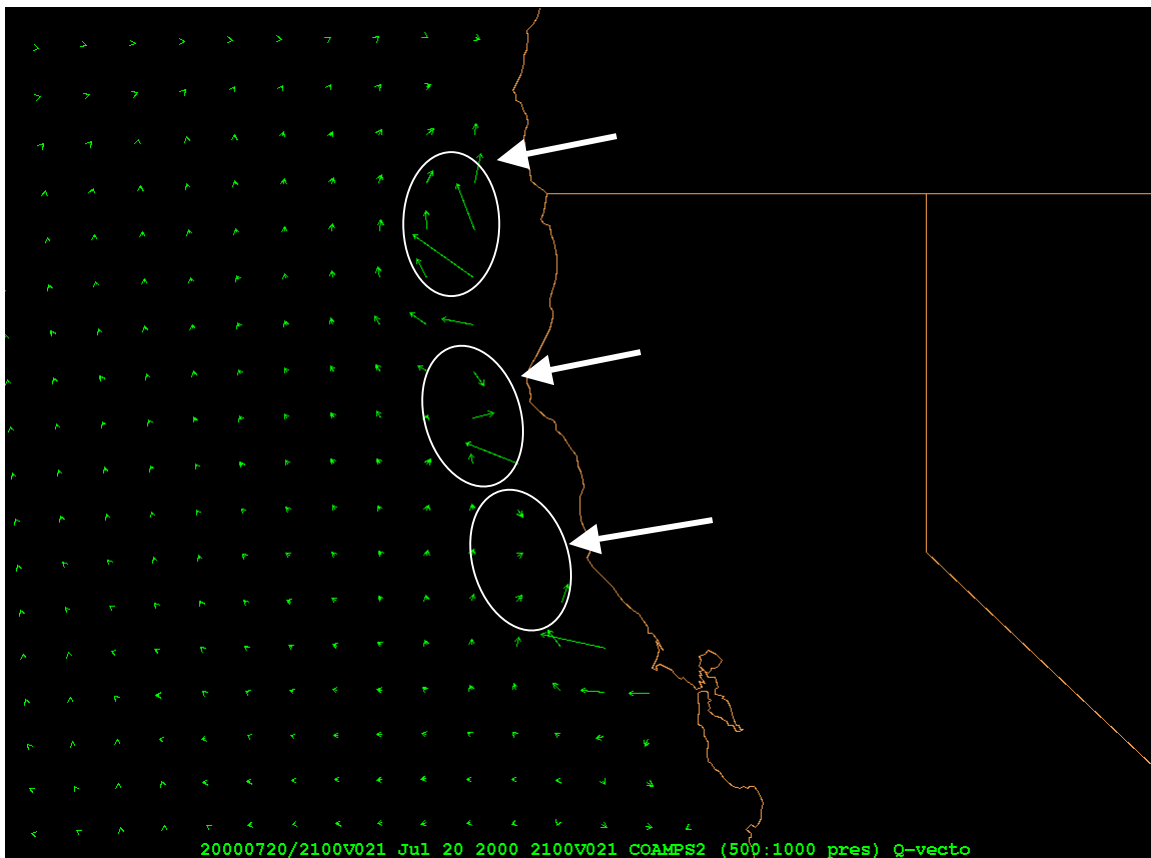
Figure 61. Q-vectors from 20 Jul 00. Note areas of convergence. Areas were consistent with the development of fog and stratus.

3.   MSC Events That Lead to No or Little Change in Coverage

There were two Q-vector patterns that emerged that seemed to indicate the continuation of fog and stratus. The first is a convergent pattern within the Q-vector field as shown in Figure 61. However, the strength of the Q-vectors was weak in most cases. This pattern is consistent with the formation of fog and stratus by the lifting of moist air to the condensation point as described above. A stronger indication or magnitude of Q-vectors would be an indication of less stable air and would probably lead to the formation of stratocumulus clouds.

The second pattern, which is shown in Figure 62, is a Q-vector field that shows neither convergence or divergence, but more of a static situation in the vertical, i.e. less vertical motion. In a large majority of cases, the strength of the Q-vectors is very weak, giving the appearance of a light and variable field, again less vertical motion. This is the pattern in which forecaster can key in on. The lack of any vertical derived motion
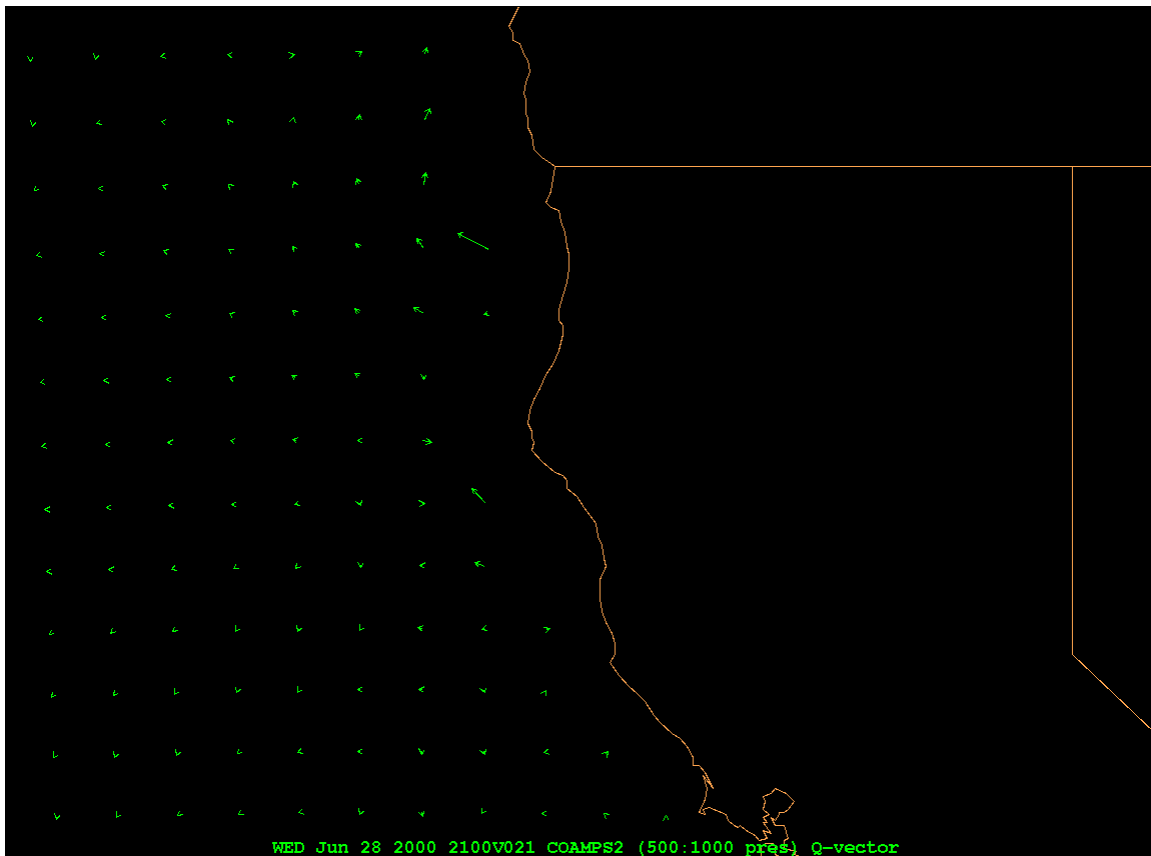
Figure 62. Q-vectors from 28 Jun 01. Note the lack of a defined area along the coast of convergence or divergence. This area experience near continuous coverage of fog and stratus throughout the day.

95

implies a relatively smooth horizontal flow as discussed in air-parcel trajectories without much if any vertical motions. This is consistent with large-scale region of higher MBL's.

Q-vectors appeared to be a good predictor or indicator for the evolution of the MSC events. During periods where the model depicted weak coastal fields, the forecasting problem increased significantly, but if compared to other meteorological parameters such as the expected tendency of the MBL and air-parcel trajectories, it becomes much easier problem to forecast the evolution.

E.   THERMAL WIND RELATIONSHIP WITHIN THE BOUNDARY LAYER

The evolution of MSC events in the boundary layer is related to thermodynamic changes as well as MBL depth changes. Regions of cold advection might tend to favor MSC increases due to MBL cooling . Likewise, warm advection might favor MSC decreases due to warming of the MBL. While thermal changes along the trajectories are what are really required, the Eulerian thermal advection may give some insight into potential MBL temperature changes. One way to assess the character of the thermal advection is to examine the low-level flow. The 11 cases were used characterize the MSC evolution based on the type of advection.

The thermal wind, defined as a difference; $V_T \equiv V2 - V1$ where V1 is the lower-level winds and V2 is the upper-level winds. Assessed in GARP as V1 at the surface and V2 at 850mb, the thermal wind in the boundary layer was compared to the surface flow to get the type of thermal advection. Strong thermal winds imply a strong horizontal temperature gradient in the near-surface layer and lead to the possibility of the existence of a low-level coastal jet. Such studies in the past have included coastal waves during the summer, CALJET, and most recently PACJET, which was conducted during the winter of 2001. The existent of the coastal jet was not examined in this study, but is consistent with strong sloping inversions.

The derivative definition of thermal wind in P-coordinates is $\partial V_g / \partial p = - R/f\rho$ k x $\blacktriangledown T$. An important property of this expression is that the horizontal and vertical derivatives, albeit different variables, can be evaluated from each other. The average

temperature of a layer, the boundary layer in these cases, is proportional to the thickness h: $T = $ const x h. This allows the substitution of temperature for thickness and vice-versa.

Thickness advection is given by $-V \cdot \blacktriangledown h \approx f/g$ k $\cdot$ (V1 x V2) where V is the average wind in the layer. The sign of the advection is determined by $-V \cdot \blacktriangledown h = > 0$ warm advection, < 0 cold advection. Traditional marine expressions for turning ships are often used for wind turning with height. If the thermal wind indicates turning to the left with height then there is backing, which indicates cold air advection. If the thermal wind indicates turning to the right with height then there is veering, which indicates warm air advection. Since the low-level along coast flow was generally from the northwest, a thermal wind vector pointing onshore (offshore) would indicate cold (warm) advection within the layer from level one to level two. More importantly, cold air advection implies lower thickness, while warm air advection implies greater thickness as described above

1.   MSC Events That Lead to Dissipation or Decrease in Coverage

In an examination of the thermal wind within the boundary layer, some interesting results emerged. A thermal wind that was parallel to the coast was an indication that no temperature advection or thickness advection was taking place. For these cases, other factors prevailed in determining the dissipation of fog and stratus. However, when the thermal wind was shown to have an easterly component, i.e. a flow extending from onshore to offshore, there was verification of fog and stratus dissipation though satellite imagery. This was an indication of warm air advection since the winds were veering with height within the boundary layer.

2.   MSC Events That Lead to Formation or Increase in Coverage

As in the above case, when the thermal wind was parallel to the coast, there was no affect or indication towards the evolution of the MSC event. However, when there was a westerly or onshore component of the thermal wind within the boundary layer, there was a clear correlation with the presence of fog and status. This was particularly true in two regions; Capetown/Eureka area to the Columbia River outflow region and the San Francisco Bay area. With backing winds with height, the westerly component of the thermal wind suggests cold air advection into the layer and is consistent with an

increasing buoyancy flux due to cooling temperatures; both of which are consistent features of increasing fog and stratus. These features were often found beginning in the mid to late afternoons, with the exception of the lifting of the MBL. The simulations were slow in lifting the MBL and normally did not occur in the simulations until the evening hours.

3.   MSC Events That Lead to No or Little Change in Coverage

Again, there were clear indications. Like described for the previous two categories, parallel flow of the thermal wind vector to the NW coastal flow provided no indication about the MSC evolutions. There were no temperature or thickness advections taking place. All of the case studies for this category showed a thermal wind vector that was primarily parallel to the coast. This is very consistent with the persistence of MSC events for this category. A static situation in terms of the thermal wind relationship implies no advection of temperature or thickness changes. As seen previously, MBL heights will also remain static in these cases as well as long MBL trajectories.

V. CONCLUSION/SUMMARY

A. CLASSIFICATION OF MSC EVENTS

A classification of the MSC events was completed and can be summarized in a more practicable and efficient manner, complete with realistic definitions and general comments on the potential impact to flight operations. It was found that the original seven categories while good for this study would not be practical or logical to the forecaster in the field. No category was assigned to non-MSC events. To that end, the following four categories can be used in describing a particular MSC event.

MSC category 1. Fog and status dissipating or decreasing in coverage throughout the daylight hours regardless of any initial tendency in coverage throughout the day. Satellite imagery will show a clear change in coverage with a tendency towards less coverage along the coast and inland valleys. This event primarily occurs in the morning hours.

MSC category 2. Fog and stratus forming or increasing in coverage throughout the daylight hours regardless of any initial tendency in coverage throughout the day. Satellite imagery will show a clear change in coverage with a tendency towards more coverage along the coast and inland valleys

MSC category 3. Fog and stratus coverage that exhibits little to no change throughout the day. Changes of the MSC event are limited to one tenth of the area in any of the four satellite regions. Satellite imagery will show no significant changes in coverage along the coast. While the norm of this category has shown coverages of 90 to 100 percent, this category also implies limited overages of a much lesser extent.

MSC category 4. Fog and stratus that is clearly associated with a frontal system, albeit pre or postfrontal. The dynamics associated with the front are the clear cause of the fog and stratus regardless of coverage or tendency. Satellite imagery clearly shows clouds associated with the frontal system. The underling layer(s) of fog and stratus may or may not be evident through satellite imagery.

B.   SUMMARY OF SYNOPTIC-SCALE FORCING ON MESOSCALE FEATURES

Comparison of the composites in each MSC category for each region revealed that the synoptic-scale forcing was effectively the same. There was surface ridging into the Pacific Northwest followed by cyclonic circulation in the Eureka region and a nearly parallel flow down the remainder of the coastline. All resulted in the initiation of MSC category one events. It is the nature of the perturbations in the synoptic-scale forcing that predicts the MSC evolution as modeled by mesoscale simulations. Additionally, the presence and evolution of inland meteorological features played a supporting role in modifying the synoptic forcing mechanisms.

1.   Seattle Region

Perhaps the most predictable region of the four in terms of MSC evolution was the Seattle region. There were unambiguous signals in the synoptic pattern that resulted in MSC events and their evolutions. The greatest indicator was the surface ridgeline into the Pacific Northwest that extended form the subtropical high-pressure system.   The presence of this feature was always associated with fog and stratus along the coast and inland valleys. The key to forecasting this event lies with any mesoscale model's ability to forecast the extent of anticyclonic curvature into the region. As the anticyclonic curvature lessened, so did the coverage of fog and stratus. If the curvature persisted throughout the day, the coverage of fog and stratus also persisted due to implied subsidence.

At least for the summer of 2000, the normal synoptic pattern was for a surface ridgeline to extend into the Pacific Northwest from the subtropical high-pressure system with a distinct daily variability, which included the lessening of the anticyclonic curvature in the region. This does not imply a lowering in surface pressures or a weakening in the pressure gradient. Neither of these proved to be a factor. There was no seasonal variability observed for this region. As the subtropical high strengthened and migrated north, the ridgeline continued to persist. The surface ridgeline could extend from the west to nearly south and the results would be the same. In one case, the surface ridgeline extended from the northwest from a dynamic, cold-core high-pressure system. While fog and stratus were present, the dissipation was rapid and completed by mid-

morning. A rather strong inverted trough along the west coast that occasionally extended into the Pacific Northwest always cleared the region out by changing the normal northerly flow along the coast to an easterly flow that originated overland. The region would also be the first and last to experience a frontal passage during the season. The effects of which are well known and easier to forecast.

2. Eureka Region

The synoptic signal was less unambiguous for this region during the summer months than it was for the Seattle region. It is more difficult to predict, but not totally impossible. The overwhelming synoptic pattern responsible for MSC category 1 events was the presence of an inverted trough extending from the high desert of Nevada through the Eureka region.

As the summer progressed, the forecasting challenge seemed to lie in the evolution of the MSC event. There were times when the MSC event would dissipate while other times the MSC event would persist throughout the day without any appreciable change in the synoptic pattern in either case.   It was clear therefore, that the synoptic pattern did not hold the key in terms of the MSC evolution.

Early indications of persistence were the presence of light winds of less than 10 knots in the base of the inverted trough. While later indications was also the presence of light winds, but with an inverted trough that extended from the desert southwest northward along the coast and only in the regions of coastal light winds.

The key indicator in the synoptic pattern was the presence of light coastal winds in the base of the trough that allowed the persistence of the MSC event.   Again as in the Seattle region, any easterly flow that went cross-coast resulted in clearing in the coastal regions.

3. Monterey Region

The Monterey region as mentioned earlier is arguably the most important region in terms of the presence of three major international airports, all located in the Bay Region.   The importance of accurate MSC forecasts is the most acute here and has the greatest impact on Pacific Rim flights.

While the synoptic patterns were not as clear-cut as hoped in the composites, there are some key indicators that forecasters can focus in on. The biggest of which is the development of the warm-core low over either desert region. This results in an onshore flow that enhances the sea breeze. While this is not the physical process that causes the MSC event to dissipate, it does seem to indicate that dissipation will follow.

The lack of any significant flow along the coast, that is, during periods where an inverted trough extending north up the coast is present, is where forecasters can expect the persistence of the MSC event. Offshore flows as usual, tend to result in clear coastal weather, resulting at times in record high temperatures. Hurray, for an easterly flow!

4.   Los Angeles Region

This region was probably the most difficult region to forecast for in terms of synoptic features. This was due to varying water temperatures, complex coastal orientation, and topography.

The position of the subtropical high-pressure system relative to the bight region normally placed the greatest area of subsidence into this region. Additionally, fog and stratus dissipation pattern was unlike the other three regions in that the dissipation pattern would be inland to seaward, vice north to south.

The biggest synoptic feature that the MSC events seem to hinge on was similar to that of the Monterey region. The presence of light winds 5 to 10 knots during the morning followed by the development of the warm-core low over the desert southwest that increased and turned the flow inland. This indicated, like the Monterey region, that dissipation was sure to follow. A stronger than normal warm-core low, especially early in the season seemed to indicate persistence of the fog and stratus event for the region. While none of these synoptic indicators would give any forecaster great confidence, they were consisting indicators of the MSC events, either dissipating or persisting.

There was one occasion where the development of the warm-core low was further south into Mexico. The flow associated with this feature resulted in weak easterly winds, which will clear and warm the coastal region.

C. RECOMMENDATIONS FOR FORECASTING TECHNIQUES

1. Mesoscale Indicators

This particular section will not be broken down into individual regions because of the close similarities in the mesoscale features. Granted, these features are born from the synoptic-scale, which as been shown to be different for each region. However, the mesoscale features have common threads that are predictable for each region. There are some very limited exceptions of course, and those will be summarized in this section.

There are two unambiguous indicators to the evolution of the fog and stratus events. First and foremost was the ability to compute the air parcel trajectories. A clear indication was seen by the coastal trajectories, especially in the vertical with time. Descending air, i.e. the entrainment of warmer, drier air from just above the layer, was seen to cause dissipation regardless of the region. Long coastal trajectories within the boundary layer were indications to begin the upwelling process that brought cooler water to the surface, and thus cooled the air above causing or continuing the condensation of water droplets, i.e. the development or persistence of the MSC event.

In the cases of the Monterey and Los Angeles regions the development of the warm-core low was seen as an indicator to dissipation by turning the flow more inland via a cross-coast component. Presumably the development of the warm-core low modifies the air-parcel trajectory by a sufficient manner as to aid in the warming and drying of this flow. It is known that the pressure gradient force causes wind to flow from high pressure to low pressure, while other forces such as Coriolis, centripetal, and friction modify the primary flow. The trajectory of this primary flow is one that descends initially. Such is the flow around the eastern quadrant of Northern Hemisphere high-pressure systems. This is where the greatest subsidence is found. Depending on other factors, the flow will begin to lift once again. The lifting region is normally found in and around low-pressure systems. It is during the descent stage of the overall pattern that is being suggested as a possible mechanism that helps in the dissipation of the fog and stratus layer. Other factors such as the strength of the inversion, topography, upper-lever dynamics, radiative processes, and ocean variables all play roles. It is the extent of each of these factors that vary and their relationships that must be considered.

The second indicator was through the use of Q-vectors. While this analysis implies vertical motion, it does not imply three-dimensional trajectories. If vertical motion is shown, the extent and depth of the vertical motion cannot be determined from the near-surface Q-vector analysis, but it is helpful and insightful. As several figures have shown, during the simulation runs where there were indications of convergence of Q-vectors, fog and stratus was shown to increase in coverage. During the convergent pattern, the base of which is considered a hard boundary, i.e. the ocean, the flow is turned upward. The lifted air is cooled and condenses resulting in the formation of clouds. Where Q-vectors were indicating a divergent pattern, fog and stratus would dissipate. The divergent pattern is in response to descending air running into a hard boundary and flowing outward. The descending air warms adiabatically and becomes drier since warmer air has the ability to hold more moisture. Finally, where there was no clear indication of convergence or divergence in the Q-vector field, fog and stratus remained, exhibiting little change. This implies that little to no vertical motion is taking place, but only horizontal flows are occurring.

The thermal wind relationship proved helpful, especially in isolated regions where topography may have played a key role. The two major areas were the regions from Capetown/Eureka to the Columbia River, and the San Francisco Bay area. Monterey Bay region was affected by a much lesser extent. An onshore component of the thermal wind in the boundary layer was a clear indication of fog and stratus in the area. This implied cold-air advection in the boundary layer. However, this type of forecasting is dependent upon the model to accurately forecast this particular parameter. Caution is advised.

Forecasting the evolution of the boundary layer, through the COAMPS simulation runs, was not found to be a terribly insightful. While the daily evolution normally saw the lowering of the boundary layer along the coast that slopes up seaward, which is consistent with subsidence patterns associated with the subtropical high, there were some perturbations in the MBL that could possibly indicate the evolution of the MSC event.

Significant lowering of the marine boundary layer, 1500 feet or greater, indicated dissipation. Subsidence is normally strong in these regions, but the depth of change is critical. Little change in the marine boundary layer indicated MSC persistence. This is

consistent with a relatively static pattern where vertical motions are nearly non-existent. There were no clear indications, at least through the simulations of the MBL that would point to fog and stratus increasing in coverage. One would surmise or expect an increase in the MBL, but the COAMPS model did not depict such occurrences during the day. However, during the final hours of the simulation, there would be indications of the MBL lifting. These final hours of the simulation are during the evening hours. It could be that the simulation runs showed a lag in the diurnal cycle from reality.

As a final remark, the coastal pressure gradient force had limited impact and was not a true indicator of any MSC event. Many times when a strong sea breeze was seen in response to increases in the cross-coast pressure gradient, the fog and stratus would be retreating seaward. Only in the cases on the synoptic–scale where a warm-core low development significantly was the large-scale trajectory modified. This was the key, not the pressure gradient force.

2. Summary of Forecasting Techniques

Tables 6-9 are provided to give a brief summary of forecasting techniques that were consistent during the course of this study. No attempt to add synoptic and mesoscale variability is given in the tables.

Location for Table 6 is for the Seattle region. The following abbreviations are used for Tables 6-9. APT is air-parcel trajectory. D is descending air, A is ascending air, NVM is no or little vertical motion, Conv is convergence, Div is divergence, Neut is neutral, F&S is fog and stratus, Diss is fog and stratus dissipating, and Form is fog and stratus forming.

Synoptic Pattern	APT	Q-Vector	Forecast	MSC Cat
Weakening ridgeline	D	Div	Diss	1
Strengthen ridge line	NVM or A	Conv	Form	2
Persistent Ridging	NVM	Conv or Neut	F&S	3

Table 6. Summary of forecasting techniques for the Seattle Region.

Table 7 below is a summary for the Eureka region.

Synoptic Pattern	APT	Q-Vector	Forecast	MSC Cat
Weak inverted trough (E-W orientation)	D	Div	Diss	1
Parallel flow (Isobars parallel to coast)	NVM or A	Conv or Neut	Form	2
Weak flow pattern (no isobars. Inverted trough oriented NW-SE)	NVM	Conv or Neut	F&S	3

Table 7. Summary of forecasting techniques for the Eureka Region.

Table 8 below is a summary for the Monterey region.

Synoptic Pattern	APT	Q-Vector	Forecast	MSC Cat
Weak parallel flow (Isobars oriented parallel to coast)	D	Div	Diss	1
Large-scale flow turned inland (inland warm-core low present)	NVM or A	Conv or Neut	Form	2
Weak flow pattern (no isobars. Inverted trough oriented NW-SE)	NVM	Conv or Neut	F&S	3

Table 8. Summary of forecasting techniques for the Monterey Region.

Synoptic Pattern	APT	Q-Vector	Forecast	MSC Cat
Weak ridging & divergent wind pattern	D	Div	Diss	1
Parallel to onshore Large-scale flow. (inland warm-core low present)	NVM or A	Conv or Neut	Form	2
Catalina Eddy	NVM or A	Conv or Neut	Form	2
Onshore large-scale flow. (strong inland warm-core low present)	NVM or A	Conv or Neut	Form	3

Table 9. Summary of forecasting techniques for the Los Angles Region.

3.   Final Comments and Recommendations

This final section summarized some forecasting techniques that will help coastal forecasters. They are based in the synoptic patterns, but have smaller mesoscale features or influences, which if detected properly will help the forecasting problem, enormously.

As all good forecasters are acutely aware of, the model is only one tool in a vast array of tools learned over the years.   Dependence on a single tool, and in particular a computer model, will lead the forecaster down the path of embarrassment of a truly busted forecast. It happens to the best of us. If the model does not initialize well, or is not handling the situation well, then other forecasting techniques and experience must be used.

While there are some clear indications in the synoptic pattern in most cases, and further indicators in the mesoscale, the ability to "see" these features are paramount. The development of Vis5D or any other software that allows forecasters to visualize the atmosphere closer to its true state is invaluable. It is highly recommended that Vis5D been downloaded from the University of Wisconsin. There is no charge, simply a hardware requirement to run the software. All of which can be found at the University of Wisconsin web site given previously. The model output will need to be converted to

Vis5D formats and the forecast output periods need to be small, 3hrs, to get reasonable trajectories.

The use of Q-vector, analyses and forecasts, is recommended. While not trajectory forecasts, they give helpful insight into vertical motions occurring in the near-surface environment. This is especially if true mesoscale models (<10km resolution) can be employed.

While the summer of 2000 was only a small snapshot into the synoptic patterns with coastal and mesoscale influences, further studies of several years are recommended to better determine long-term variability, i.e. climatic changes and cycles.

As computing power becomes better, further refinement of sea surface temperature modeling is needed. Greater details could provide better insight in term of air-sea interactions and fluxes, both vertically and horizontally in the MBL.

One factor consistently fell short of expectations within the simulation runs was the poor handling of moisture. Both is the Vis5D depiction of clouds and GARP's depiction of moisture convergence/divergence fields, was inconsistent. The moisture variable is important to the formation, dissipation, and advection of fog and stratus. Better modeling of this important variable in the mesoscale environment is critical.

While much of the information presented is based on COAMPS simulation runs, future studies to include short-period observations and analyses to confirm (or deny) information presented herein is also recommended.

```
program average
      parameter(ix=66,iy=36,iz=9)
      real sum(ix,iy,iz),grid(ix,iy,iz),grid2(ix,iy)
      real sum2(ix,iy,iz),sum3(ix,iy,iz),pgrd(iz),sum6(ix,iy,iz)
      real sum4(ix,iy,iz),sum5(ix,iy,iz),sumh1(ix,iy),sumh2(ix,iy)
      integer n(8,iz)
      character file*8,filename*300,parm(8)*3,outfile*60,outfile2*80
      character dattim*11,gdatim(2)*20,parms(8)*12,hour*4
      logical err
      data parms /'UREL        ','VREL        ','TMPK        ',
     +        'HGHT        ','DPDK        ','OMEG        ',
     +        'PMSL        ','GWTMPK      '/
      data parm /'u  ','v  ','t  ','ght','td ','omg','slp','sst'/

c
      call getarg(1,hour)
      call getarg(2,outfile)
      lo=nblank(outfile)
      izi=iz
       outfile2(1:lo+4)=outfile(1:lo)//'.gem'
c
      do k=1,izi
        do np=1,8
        n(np,k)=0
        enddo
        do i=1,ix
          do j=1,iy
           sum(i,j,k)=0.0
           sum2(i,j,k)=0.0
           sum3(i,j,k)=0.0
           sum4(i,j,k)=0.0
           sum5(i,j,k)=0.0
           sum6(i,j,k)=0.0
           sumh1(i,j)=0.0
           sumh2(i,j)=0.0
          enddo
        enddo
      enddo
c
 10   continue
      read(5,'(a11)',end=40)dattim
```

```fortran
      gdatim(1)=dattim(1:11)//'f000     '
      gdatim(2)=' '
      file(1:8)='20'//dattim(1:4)//'01'
      if(dattim(5:6).gt.'15')file(1:8)='20'//dattim(1:4)//'16'
      filename='/d/rtd4/case/0006-08/gempak/grids/'//file//'_nog1m.gem'
c
      do np=1,8
       call unoggi(grid,grid2,ix,iy,iz,parm(np),filename,gdatim, err,pgrd)
c
      if(np.lt.7)then
       do k=1,izi
         if(grid(1,1,k).eq.-9999.0.or.grid(1,1,k).eq.0.0)go to 20
         n(np,k)=n(np,k)+1
          do i=1,ix
            do j=1,iy
              if(np.eq.1)then
              sum(i,j,k)=sum(i,j,k)+grid(i,j,k)
              elseif(np.eq.2)then
              sum2(i,j,k)=sum2(i,j,k)+grid(i,j,k)
              elseif(np.eq.3)then
              sum3(i,j,k)=sum3(i,j,k)+grid(i,j,k)
              elseif(np.eq.4)then
              sum4(i,j,k)=sum4(i,j,k)+grid(i,j,k)
              elseif(np.eq.5)then
              sum5(i,j,k)=sum5(i,j,k)+grid(i,j,k)
              elseif(np.eq.6)then
              sum6(i,j,k)=sum6(i,j,k)+grid(i,j,k)
              endif
            enddo
          enddo
 20     continue
       enddo
      else
        if(grid(1,1,1).eq.-9999.0.or.grid(1,1,1).eq.0.0)go to 30
        n(np,1)=n(np,1)+1
         do i=1,ix
           do j=1,iy
             if(np.eq.7)then
             sumh1(i,j)=sumh1(i,j)+grid(i,j,1)
             elseif(np.eq.8)then
             sumh2(i,j)=sumh2(i,j)+grid(i,j,1)
             endif
           enddo
         enddo
 30    continue
```

```fortran
      endif
c
      enddo
       go to 10
 40   continue
c
      do k=1,izi
       ng1=n(1,k)
       if(ng1.ne.0)then
       do i=1,ix
         do j=1,iy
          sum(i,j,k)=sum(i,j,k)/float(ng1)
         enddo
        enddo
        else
        do i=1,ix
          do j=1,iy
           sum(i,j,k)=-9999.0
          enddo
         enddo
         endif
c
       ng2=n(2,k)
       if(ng2.ne.0)then
       do i=1,ix
         do j=1,iy
          sum2(i,j,k)=sum2(i,j,k)/float(ng2)
         enddo
        enddo
        else
        do i=1,ix
          do j=1,iy
           sum2(i,j,k)=-9999.0
          enddo
         enddo
         endif
c
       ng3=n(3,k)
       if(ng3.ne.0)then
       do i=1,ix
         do j=1,iy
          sum3(i,j,k)=sum3(i,j,k)/float(ng3)
          enddo
         enddo
         else
```

111

```
      do i=1,ix
        do j=1,iy
         sum3(i,j,k)=-9999.0
        enddo
      enddo
      endif
c
      ng4=n(4,k)
      if(ng4.ne.0)then
      do i=1,ix
        do j=1,iy
         sum4(i,j,k)=sum4(i,j,k)/float(ng4)
        enddo
      enddo
      else
      do i=1,ix
        do j=1,iy
         sum4(i,j,k)=-9999.0
        enddo
      enddo
      endif
c
      ng5=n(5,k)
      if(ng5.ne.0)then
      do i=1,ix
        do j=1,iy
         sum5(i,j,k)=sum5(i,j,k)/float(ng5)
        enddo
      enddo
      else
      do i=1,ix
        do j=1,iy
         sum5(i,j,k)=-9999.0
        enddo
      enddo
      endif
c
      ng6=n(6,k)
      if(ng6.ne.0)then
      do i=1,ix
        do j=1,iy
         sum6(i,j,k)=sum6(i,j,k)/float(ng6)
        enddo
      enddo
      else
```

```
        do i=1,ix
          do j=1,iy
           sum6(i,j,k)=-9999.0
          enddo
         enddo
         endif
        enddo
c
        ng7=n(7,1)
        if(ng7.ne.0)then
        do i=1,ix
          do j=1,iy
           sumh1(i,j)=sumh1(i,j)/float(ng7)
          enddo
         enddo
         else
         do i=1,ix
          do j=1,iy
           sumh1(i,j)=-9999.0
          enddo
         enddo
         endif
c
        ng8=n(8,1)
        if(ng8.ne.0)then
        do i=1,ix
          do j=1,iy
           sumh2(i,j)=sumh2(i,j)/float(ng8)
          enddo
         enddo
         else
         do i=1,ix
          do j=1,iy
           sumh2(i,j)=-9999.0
          enddo
         enddo
         endif
c
c
c  on output assign a time of year month day and hour
        gdatim(1)=dattim(1:4)//'01'//hour(1:4)//'F000'
        gdatim(2)=' '
c
        call gemgrid(ix,iy,izi,outfile2,grid2,sum,sum2,sum3,
     +    sum4,sum5,sum6,sumh1,sumh2,pgrd,
```

```
     +    gdatim,parms,8)
c
c     outfile2=outfile(1:lo)//'00Z'//parm(1:lp)//'.GRD'
c     open(unit=2,file=outfile2,access='sequential',
c    +     form='unformatted',status='new')
c    do k=1,izi
c     do i=1,ix
c       do j=1,iy
c          grid2(i,j)=sum(i,j,k)
c       enddo
c     enddo
c     write(2)grid2
c     print *,sum(1,1,k)
c     enddo
c     close(unit=2)
c
     stop
     end
```

APPENDIX B COAMPS

A. **COUPLED OCEAN/ATMOSPHERE MESOSCALE PREDICTION SYSTEM (COAMPS)**

1. **Background**

COAMPS is the latest product in a series of model developments at the Naval Environmental Prediction and Research Facility (NEPRF), Naval Oceanographic and Atmospheric Research Laboratory (NOARL) and currently, the Naval Research Laboratory (NRL) since 1977. COAMPS is derived from the Navy Operational Global Atmospheric Prediction System (NOGAPS) and the Navy Operational Regional Atmospheric Prediction System (NORAPS) to meet the ever-growing demand from war fighters for highly accurate atmospheric and oceanographic forecasts. As weapons become increasingly smart and technology makes possible for nearly true all-weather operations, it was essential that meteorological and oceanographical models be developed to support the military operations of the future.

2. **Description**

Improved understanding of physical processes, continuous and dramatic improvements in computer technology, increased observational networks (both ashore and afloat), and the fairly recent development and availability of detailed surface parameters such as terrain and ocean height along with soil and vegetation types have lead to the numerical prediction of some meso-β-scale atmospheric phenomena. Meso-β-scale implies that the hydrostatic approximation may be invalid at times, particularly for very-small scale features such as convection and smaller-scale topographic features where the vertical wavelength is a significant fraction of the horizontal wavelength. In these cases the vertical resolution term cannot be ignored.

A three-dimensional mesoscale model represents an analysis-nowcast and short-term (up to 72 hours) forecast tool that is applicable for any given region of the planet. Initialization takes place by either the atmospheric component of NOGAPS or from the most recent COAMPS forecast as the first guess. Several fields describing the surface conditions must be set prior. The surface terrain height is obtained from either the U.S. Navy 20$'$ resolution terrain field or the Navy Imagery and Mapping Agency (NIMA)

Digital Terrain Elevation Data (DTED) level 1 data (100-m resolution). Either database can be bilinearly interpolated to the model grid. In addition to the terrain height, the surface albedo, surface roughness, ground wetness, and ground temperature must be specified initially. The analysis routine is a five-step process and is shown in Figure 63 as a flow chart that provides detailed steps used by COAMPS.

COAMPS includes an atmospheric data assimilation system comprised of data quality control, analysis, initialization, a nonhydrostatic atmospheric model component and an ocean model. The atmospheric system consists of two major components - Analysis and Forecast, and some post-processing software. The COAMPS analysis routine prepares the initial and boundary files used in the forecast model. The forecast routines perform time integration of the model numerics and physics and output prognostics and diagnostic fields in pressure, sigma, or height coordinates.

COAMPS analysis uses the Arakawa-Lamb scheme A grid (no staggering). The forecast model, both horizontal and vertical grids are staggered and utilizes the Arakawa-
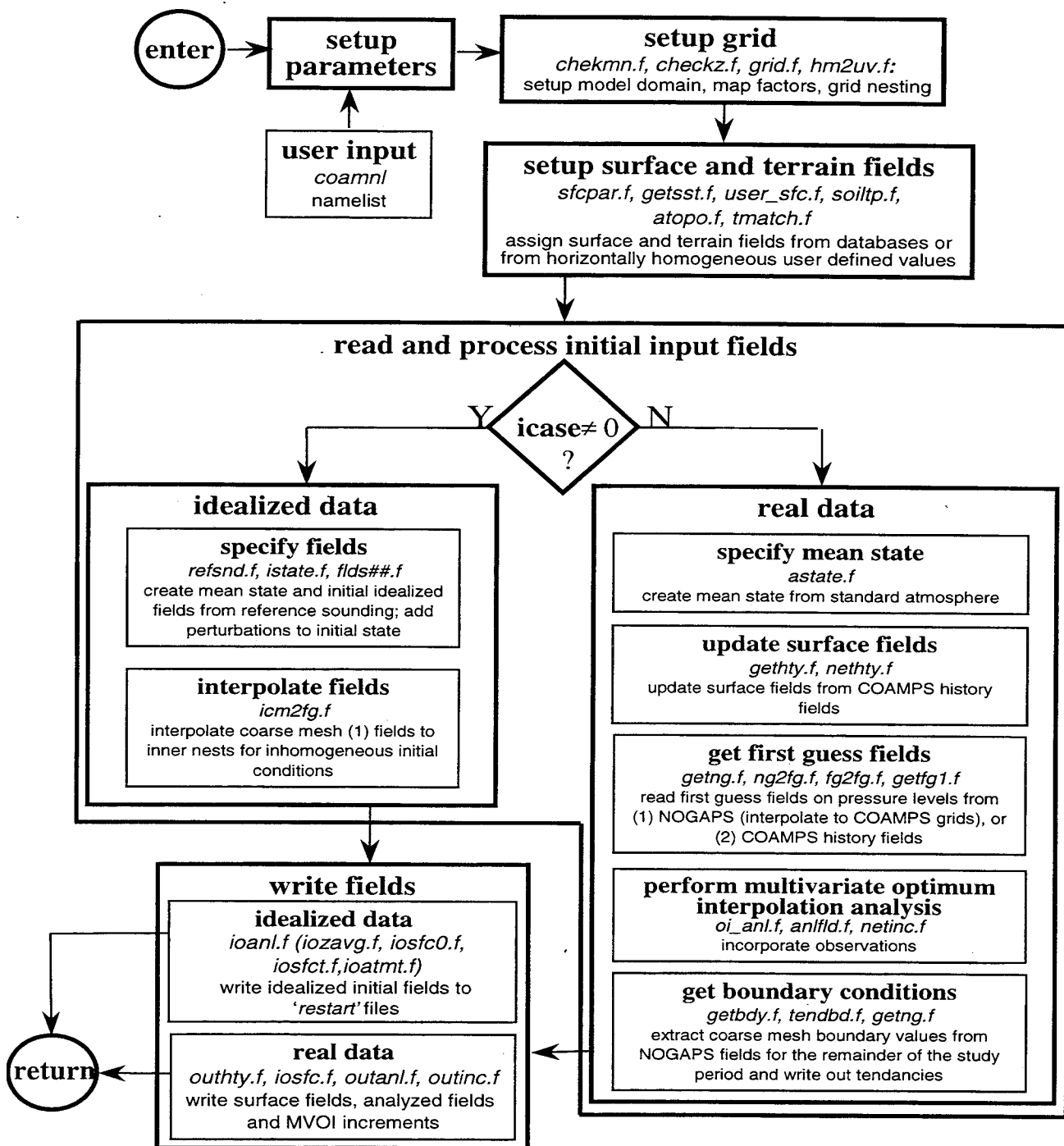
Figure 63. Flow chart of the analysis routine. (COAMPS Training Manual) The analysis routine is described in five parts: setup parameters, setup grid, setup surface and terrain fields, read and process initial input fields and write fields. The subroutines called in each part are shown in italics. The atmospheric fields may be either idealized or real data as indicated by the value of name list parameter **icase**.

117

Lamb scheme C, which is used by both the atmospheric and ocean models. For real data, the Polar stereographic, Lambert conformal, Mercator, or Spherical grid projections are allowed. The model grid projection is specified along with latitude and longitude of any one point in the grid. This makes COAMPS globally relocatable and applicable for forecasting in the polar, midlatitude, and equatorial regions. Currently only the atmospheric model can use nested grids at a reduction ratio of 3:1. The inner grids can be specified arbitrarily within the confines of the next coarser grid.

3. Specific Setup Used

11 events were chosen and then ran in COAMPS using 63km and 21km resolutions. The fields were initialized at 00Z the evening before the MSC event to allow the model to settle out any perturbations, which it did quite well by the six hour forecast run. The COAMPS forecast run was allowed to forecast out to 36 hours with output at three hour increments, a temporal and spatial period that was sufficient enough to capture the following day's MSC event and slightly beyond.

The Specific setup used for this thesis is given in Tables 6 and 7.

COAMPS 2.0 SPECIFICATIONS

Parameter	Information
Basic equations:	Primitive equations including non-hydrostatic effects
Field formats:	Applications grids are latitude-longitude or Cartesian coordinates on horizontal map projection
Variables:	Wind components, potential temperature, mixing ratio, surface pressure, ground temperature, ground wetness, SST
Numerical Techniques:	Arakawa C-grid, vertically and horizontally staggered with split explicit time integration
Integration domain:	Regional, surface to sigma (30) = 31500m (approx 10mb)
Horizontal resolution:	User specified, 63 x 21 km, double nested

Vertical levels:	30 vertical levels on sigma z coordinates
Nested grids:	Two
Forecast time:	36 hours
Initial fields:	An MVOI maps both real and synthetic observations from NOGAPS on the model grid. In the incremental update cycle, analysis increments to the first-guess are interpolated in the vertical to the model vertical levels, and added to the most recent model forecasts
First-guess analysis:	As COAMPS runs in a continuous update cycle, the first-guess fields come from the previous COAMPS forecast
Boundary conditions:	Davies (1976) or Perkey-Kreitzberg (1976) treatment of NOGAPS forecast fields
Orography:	Envelope topography is from the 1 km terrain data, except the from the NIMA DTED level 1 data set
Horizontal diffusion:	Fourth-order diffusion applied to all prognostic variables, except Exner perturbation (pi)
Moisture physics:	Explicit physics (Rutledge and Hobbs, 1983) for horizontal grid resolutions less than specified value (typically 10km). Cumulus convective process (Kain and Fritch, 1990)
Radiation:	Longwave & shortwave radiation (Harshvardhan, 1987)
Planetary boundary layer:	1.5 order turbulence kinetic energy closure (Deardorff, 1980)
Land surface:	Single layer/bucket model
Ocean surface:	COAMPS makes its own SST analysis at the surface every time It runs using optimum interpolation techniques

Table 10. COAMPS 2.0 Specifications (From Dumas, 2001)

COAMPS Model Vertical Spacing

Level #	Spacing (m)	Height (m)	Height (ft)	Pressure (mb)
45	2,000	20,000	65,616.8	55
44	2,000	18,000	59,055.1	75.3
43	2,000	16,000	52,493.4	103.2
42	2,000	14,000	45,931.8	141.5
41	2,000	12,000	39,370.1	193.9
40	2,000	10,000	32,808.4	264.6
39	2,000	8,000	26,246.7	356.2
38	1,000	6,000	19,685.0	472.0
37	1,000	5,000	16,404.2	540.4
36	1,000	4,000	13,123.4	616.6
35	700	3,000	9,842.5	701.2
34	400	2,300	7,545.9	765.9
33	300	1,900	6,233.6	805.0
32	200	1,600	5,249.3	835.3
31	100	1,400	4,593.2	856.1
30	100	1,300	4,265.1	866.6
29	50	1,200	3,937.0	877.2
28	50	1,150	3,773.0	882.6
27	50	1,100	3,608.9	888.0
26	50	1,050	3,444.9	893.4
25	50	1,000	3,280.8	898.8
24	50	950	3,116.8	904.3
23	40	900	2,952.8	909.8
22	40	860	2,821.5	914.2
21	40	820	2,690.3	918.6
20	40	780	2,559.1	923.0
19	40	740	2,427.8	927.5
18	40	700	2,296.6	932.0
17	40	660	2,165.4	936.5
16	40	620	2,034.1	941.0
15	40	580	1,902.9	945.5
14	40	540	1,771.7	950.1
13	40	500	1,640.4	954.6
12	40	460	1,509.2	959.2
11	40	420	1,378.0	963.8
10	40	380	1,246.7	968.4

COAMPS Model Vertical Spacing (con't)				
9	40	340	1,115.5	973.1
8	40	300	984.3	977.7
7	40	260	853.0	982.4
6	40	220	721.8	987.1
5	40	180	590.6	991.8
4	40	140	459.3	996.6
3	40	100	328.1	1001.3
2	40	60	196.9	1006.1
1	20	20	65.6	1010.9
0	0	0	0.0	1013.3

Table 11. The vertical structure of the COAMPS model. (From Dumas 2001) Note: Height (Z) and Pressure (P) values are based on the U.S. Standard Atmosphere

B.   VIS5D

1.   Background

Developed for the Stellar GS-1000 computer system, it was used to give demonstrations at the European Centre for Mid-Range Weather Forecasting (ECMWF) in December 1988 and at the American Meteorological Society (AMS) conference in Anaheim in January 1989. The original version was able to depict time series of multivariate 3-D grids by animated isosurfaces and horizontal contour line slices, world topography map with map boundaries, and wind trajectory tracing with the Vis5d program.

With continued development over the years, the latest version of 5.2 has far-reaching capabilities that allow the scientist to examine the atmosphere in 5-D allowing for better understanding of processes through various isosurfaces to colored slices.

The Visualization Project at the University of Wisconsin-Madison Space Science and Engineering Center (SSEC) developed Vis5D. Written by Bill Hibbard, Johan Kellum, and Brian Paul with the help of:

- Andre Battaiola of CPTEC, Sao Paulo, Brazil
- Dave Santek of SSEC
- Marie-Francoise Voidrot-Martinez of the French Meteorology Office.

- Dave Kamins and Jeff Vroom of Stellar Computer, Inc.

- Simon Baas and Hans de Jong of the Netherlands for the HP/VOGL port

- Pratish Shah of Kubota Computer for the Kubota port

- Mike Stroyan of HP for the PEX support

Additionally, The National Aeronautical and Space Administration (NASA) and the Environmental Protection Agency (EPA) supported the development of Vis5D.

2. Description

Vis5D is a system for interactive visualization of large 5-D gridded data sets such as those produced by numerical weather models. One can make isosurfaces, contour line slices, colored slices, volume renderings, etc of data in a 3-D grid, then rotate and animate the images in real time. There's also a feature for wind trajectory tracing, a way to make text annotations for publications, support for interactive data analysis, etc.

Vis5D is a software system for visualizing data made by numerical weather models and similar sources. Vis5D works on data in the form of a five-dimensional rectangle. That is, the data are real numbers at each point of a "grid" which spans three space dimensions, one time dimension and a dimension for enumerating multiple physical variables. Vis5D works perfectly well on data sets with only one variable, one time step (i.e. no time dynamics) or one vertical level. However, data grids should have at least two rows and columns.

The major new feature of Vis5D version 5.1 is support for comparing multiple data sets. This extra data can be incorporated at run-time as a list of *.v5d files or imported at anytime after Vis5D is running. Data can be overlaid in the same 3-D display and/or viewed side-by-side spreadsheet style. Data sets that are overlaid are aligned in space and time. In the spreadsheet style, multiple displays can be linked. Once linked, the time steps from all data sets are merged and the controls of the linked displays are synchronized.

The Vis5D system includes the vis5d visualization program, several programs for managing and analyzing five-dimensional data grids, and instructions. For more detailed information about this remarkable and capable software program, visit the University of Wisconsin at Madison, Space Science and Engineering Center (SSEC) at http://www.ssec.wisc.edu/~billh/vis5d.html.

3. How Vis5D was Used

Version 5.2 was used to examine the trajectory of air parcels in and above the boundary layer in the coastal regime and to observe the potential influences that the synoptic pattern would have on the coast with these trajectories. Several examples are provided in Chapter IV with results that proved very insightful to the evolution of MSC events.

Vis5D utilized high-resolution topography of the west coast from southern British Columbia to Baja, and was limited in height to 500mb with a one-half kilometer vertical resolution to put the focus in the lower atmosphere. This configuration worked extremely well.

C. THE GENERAL METEOROLOGY PACKAGE (GEMPAK) ANALYSIS AND RENDERING PROGRAM (GARP)

1. Background

GARP was written to support the Cooperative Program for Operational Meteorology, Education and Training (COMET), which were established in 1989. The COMET Residence Program (RP) provides education in mesoscale meteorology for students and instructors from around the world. In support this effort, several software packages for handling data were developed, including a meteorological display package called GEMPAK, which supplies many of the processing and data display functions.

2. Description

GARP (GEMPAK Analysis and Rendering Program) is an X Windows/Motif software application designed by the COMET staff for the display and analysis of meteorological data sets. It provides for a graphics user interface (GUI) around many of the capabilities of GEMPAK. Supported data sets include model data like the Eta, NGM, RUC, and Fleet Numerical Meteorology and Oceanography Center's NOGAPS. A Satellite imagery in NOAA Port GINI format or MCIDAS area file format, NIDS and Nowrad radar data, surface data and upper air data are also supported.

As an application, GARP is layered on top of GEMPAK. GARP uses Motif to create a point and click GUI front end to the display and analysis capabilities of GEMPAK. GARP attempts to make it easy to manage, integrate and visualize multiple meteorological data sets.

Architecturally, GARP is written as a GEMPAK application much like the NAWIPS applications NSAT and NWX. GARP is written almost entirely in ANSI C (with some Fortran 77 interface subroutines). GARP uses GEMPAK software and application libraries to provide a high level framework to manage and control a users interaction with GEMPAK, the data and an X Window display.

The basic design of GARP provides a point-and-click capability for displaying meteorological data in addition to providing access to more sophisticated diagnostic capabilities of GEMPAK. GARP is being implemented as an application layered on top of the existing GEMPAK libraries.

Some caveats to GARP include: GARP has automatic time matching across data types. For example, if one chooses to plot a 5-hour series of satellite images and then choose to overlay surface observations on top of the satellite images, the observation date/times that correspond to the selected satellite images will be pre-selected. However, one is free to change the date/times selected if you turn off time matching; Current version (2.1) of GARP will NOT allow one to combine multiple images. For example, a satellite image and a radar image or an IR and a VIS satellite image.) For more detailed information regarding GARP, go to http://www.comet.ucar.edu/pub_html/garp/.

3.   How GARP was Used

GARP was used extensively to examine a number of meteorological parameters. Beginning with the synoptic patterns, the strength and position of the subtropical ridge was looked at along with the strength and location of any inland warm-core lows. Additionally, any other observable phenomenon was noted such as fronts, eddies, and dynamic high-pressure systems. Notes were taken as to the influences, if any, of the coastal wind broken down into the geostropic and ageostropic components, sea surface temperature observations, and the strength and tendency of the pressure gradient force across the coast.

Afterwards, the coastal environment was studied that included the cross-section examinations of the marine boundary layer using potential temperature and its' tendency in time. Coastal Q-vectors, cross-coast vertical motions, and moisture convergence and divergence tendencies were also considered.

124

LIST OF REFERENCES

Albrecht, Bruce A., David A. Randall, Stephen Nicholls, 1988: **Observations of Marine Stratocumulus Clouds During FIRE.** *Bulletin of the American Meteorological Society*: Vol. 69, No. 6, pp. 618–619.

Betts, Alan K., Reinout Boers, 1990: **A Cloudiness Transition in a Marine Boundary Layer.** *Journal of the Atmospheric Sciences*: Vol. 47, No. 12, pp. 1480–1497.

Bott, A., U. Sievers, W. Zdunkowski, 1990: **A Radiation Fog Model with a Detailed Treatment of the Interaction between Radiative Transfer and Fog Microphysics.** *Journal of the Atmospheric Sciences*: Vol. 47, No. 18, pp. 2153–2166.

Bridger, Alison F.C., William C. Brick, Peter F. Lester, 1993: **The Structure of the Marine inversion Layer off the Central California Coast: Mesoscale Conditions.** *Monthly Weather Review*: Vol. 121, No. 2, pp. 335–351.

Bond, Nicholas A., Clifford F. Mass, James E. Overland, 1996: **Coastally Trapped Wind Reversals Along the United States West Coast During the Warm Season. Part I: Climatology and Temporal Evolution.** *Monthly Weather Review*: Vol. 124, No. 3, pp. 430–445.

Brooks, Ian M., David P. Rogers, 1997: **Aircraft Observations of Boundary Layer Rolls Off the Coast of California.** *Journal of the Atmospheric Sciences*: Vol. 54, No. 14, pp. 1834–1849.

Burk, Stephen D., William T. Thompson, 1996: **The Summertime Low-Level Jet and Marine Boundary Layer Structure Along the California Coast.** *Monthly Weather Review*: Vol. 124, No. 4, pp. 668–686.

Chen, Sue, Cook, John, Cummings, Jim, Hodur, Richard M., Holt, Teddy, Liou, Chi-Sann, Schmidt, Jerome, Thompson, William, Van Tuyl, Andrew, 19xx: **COAMPS Training Manual.**

Davis, Anthony, Alexander Marshak, Warren Wiscombe, Robert Cahalan, 1996: **Scale Invariance of Liquid Water Distributions in Marine Stratocumulus. Part I: Spectral Properties and Stationarity Issues.** *Journal of the Atmospheric Sciences*: Vol. 53, No. 11, pp. 1538–1558.

Davis, Christopher, Simon Low-Nam, Clifford Mass, 2000: **Dynamics of a Catalina Eddy Revealed by Numerical Simulation.** *Monthly Weather Review*: Vol. 128, No. 8, pp. 2885–2904.

Dorman, C. E., C. D. Winant, 2000: **The Structure and Variability of the Marine Atmosphere around the Santa Barbara Channel.** *Monthly Weather Review*: Vol. 128, No. 2, pp. 261–282.

Dorman, C. E., D. P. Rogers, W. Nuss, W. T. Thompson, 1999: **Adjustment of the Summer Marine Boundary Layer around Point Sur, California.** *Monthly Weather Review*: Vol. 127, No. 9, pp. 2143–2159.

Dorman, C. E., T. Holt, D. P. Rogers, K. Edwards, 2000: **Large-Scale Structure of the June–July 1996 Marine Boundary Layer along California and Oregon.** *Monthly Weather Review*: Vol. 128, No. 6, pp. 1632–1652.

Dumas, John L., 2001: **Numerical Predicition of Marine Fog Using the Coupled Ocean/Atmosphere Mesoscale Prediction System (COAMPS).** *Thesis:* 160p.

Doyle, James D., Thomas T. Warner, 1990: **Mesoscale Coastal Processes During GALE IOP 2.** *Monthly Weather Review*: Vol. 118, No. 2, pp. 283–308.

Doyle, James D., Thomas T. Warner, 1990: **Mesoscale Coastal Processes During GALE IOP 2.** *Monthly Weather Review*: Vol. 118, No. 2, pp. 218–233.

Duynkerke, Peter G., Phillip Hignett, 1993: **Simulation of Diurnal Variation in a Stratocumulus-capped Marine Boundary Layer during FIRE.** *Monthly Weather Review*: Vol. 121, No. 12, pp. 3291–3300.

Felsch, Peter, Woodrow Whitlatch, 1993: **Stratus Surge Prediction along the Central California Coast.** *Weather and Forecasting*: Vol. 8, No. 2, pp. 204–213.

Garand, Louis, James A. Weinman, Christopher C. Moeller, 1989: **Automated Recognition of Oceanic Cloud Patterns. Part II: Detection of Air Temperature and Humidity Anomalies above the Ocean Surface from Satellite Imagery.** *Journal of Climate*: Vol. 2, No. 4, pp. 356–366.

Golding, B.W., 1993: **A Study of the Influence of Terrain on Fog Development.** *Monthly Weather Review*: Vol. 121, No. 9, pp. 2529–2541.

Guan, Hong, André Tremblay, George A. Isaac, Kevin B. Strawbridge, Catharine M. Banic, 2000: **Numerical Simulations of Stratus Clouds and Their Sensitivity to Radiation—A RACE Case Study.** *Journal of Applied Meteorology*: Vol. 39, No. 11, pp. 1881–1893.

Haack, Tracy, Stephen D. Burk, Clive Dorman, David Rogers, 2001: **Supercritical Flow Interaction within the Cape Blanco–Cape Mendocino Orographic Complex.** *Monthly Weather Review*: Vol. 129, No. 4, pp. 688–708.

Hodur, Richard M., 1997: **The Naval Research Laboratory's Coupled Ocean/Atmospheric Mesoscale Prediction System (COAMPS)**. *Monthly Weather Review:* Vol 125, No 7, pp. 1414-1430.

Hoerling, Martin P., Arun Kumar, Min Zhong, 1997: **El Niño, La Niña, and the Nonlinearity of Their Teleconnections.** *Journal of Climate*: Vol. 10, No. 8, pp. 1769–1786.

Hudson, James G., Gunilla Svensson, 1995: **Cloud Microphysical Relationships in California Marine Stratus.** *Journal of Applied Meteorology*: Vol. 34, No. 12, pp. 2655–2666.

Jackson, Peter L., Chris J. C. Reason, Shucai Guan, 1999: **Numerical Modeling of a Coastal Trapped Disturbance. Part II: Structure and Dynamics.** *Monthly Weather Review*: Vol. 127, No. 4, pp. 535–550.

Josey, Simon A., Elizabeth C. Kent, Peter K. Taylor, 1999: **New Insights into the Ocean Heat Budget Closure Problem from Analysis of the SOC Air–Sea Flux Climatology.** *Journal of Climate*: Vol. 12, No. 9, pp. 2856–2880.

Klein, Stephen A., Dennis L. Hartmann, 1993: **The Seasonal Cycle of Low Stratiform Clouds.** *Journal of Climate*: Vol. 6, No. 8, pp. 1587–1606.

Kloesel, Kevin A., 1992: **Marine Stratocumulus Cloud Clearing Episodes Observed during FIRE.** *Monthly Weather Review*: Vol. 120, No. 4, pp. 565–578.

Leidner, S. Mark, David R. Stauffer, Nelson L. Seaman, 2001: **Improving Short-Term Numerical Weather Prediction in the California Coastal Zone by Dynamic Initialization of the Marine Boundary Layer.** *Monthly Weather Review*: Vol. 129, No. 2, pp. 275–294.

Leipper, Dale F., 1994: **Fog on the U.S. West Coast: A Review.** *Bulletin of the American Meteorological Society*: Vol. 75, No. 2, pp. 229–348.

Leipper, Dale F., 1995: **Fog Forecasting Objectively in the California Coastal Area Using LIBS.** *Weather and Forecasting*: Vol. 10, No. 4, pp. 741–762.

Mass, Clifford F., Mark D. Albright, 1989: **Origin of the Catalina Eddy.** *Monthly Weather Review*: Vol. 117, No. 11, pp. 2406–2436.

Mass, Clifford F., Nicholas A. Bond, 1996: **Coastally Trapped Wind Reversals along the United States West Coast during the Warm Season. Part II: Synoptic Evolution.** *Monthly Weather Review*: Vol. 124, No. 3, pp. 446–461.

Mass, Clifford F., W. James Steenburgh, 2000: **An Observational and Numerical Study of an Orographically Trapped Wind Reversal along the West Coast of the United States.** *Monthly Weather Review*: Vol. 128, No. 7, pp. 2363–2397.

Minnis, Patrick, Patrick W. Heck, David F. Young, C.W. Fairall, J.B. Snider, 1992: **Stratocumulus Cloud Properties Derived from Simultaneous Satellite and Island-based Instrumentation during FIRE.** *Journal of Applied Meteorology*: Vol. 31, No. 4, pp. 317–339.

Norris, Joel R., 1998: **Low Cloud Type over the Ocean from Surface Observations. Part II: Geographical and Seasonal Variations.** *Journal of Climate*: Vol. 11, No. 3, pp. 383–403.

Norris, Joel R., 1998: **Low Cloud Type over the Ocean from Surface Observations. Part I: Relationship to Surface Meteorology and the Vertical Distribution of Temperature and Moisture.** *Journal of Climate*: Vol. 11, No. 3, pp. 369–382.

Norris, Joel R., Conway B. Leovy, 1994: **interannual Variability in Stratiform Cloudiness and Sea Surface Temperature.** *Journal of Climate*: Vol. 7, No. 12, pp. 1915–1925.

Norris, Joel R., Stephen A. Klein, 2000: **Low Cloud Type over the Ocean from Surface Observations. Part III: Relationship to Vertical Motion and the Regional Surface Synoptic Environment.** *Journal of Climate*: Vol. 13, No. 1, pp. 245–256.

Norris, Joel R., Yuan Zhang, John M. Wallace, 1998: **Role of Low Clouds in Summertime Atmosphere–Ocean Interactions over the North Pacific.** *Journal of Climate*: Vol. 11, No. 10, pp. 2482–2490.

Nuss, Wendell A., John M. Bane, William T. Thompson, Teddy Holt, Clive E. Dorman, F. Martin Ralph, Richard Rotunno, Joseph B. Klemp, William C. Skamarock, Roger M. Samelson, Audrey M. Rogerson, Chris Reason, Peter Jackson, 2000: **Coastally Trapped Wind Reversals: Progress toward Understanding.** *Bulletin of the American Meteorological Society*: Vol. 81, No. 4, pp. 719–744.

Paluch, I. R., D. H. Lenschow, S. Siems, S. McKeen, G. L. Kok, R. D. Schillawski, 1994: **Evolution of the Subtropical Marine Boundary Layer: Comparison of Soundings over the Eastern Pacific from FIRE and HaRP.** *Journal of the Atmospheric Sciences*: Vol. 51, No. 11, pp. 1465–1479.

Ralph, F. M., P. J. Neiman, P. O. G. Persson, J. M. Bane, M. L. Cancillo, J. M. Wilczak, W. Nuss, 2000: **Kelvin Waves and Internal Bores in the Marine Boundary Layer Inversion and Their Relationship to Coastally Trapped Wind Reversals.** *Monthly Weather Review*: Vol. 128, No. 2, pp. 283–300.

Rogerson, A. M., 1999: **Transcritical Flows in the Coastal Marine Atmospheric Boundary Layer.** *Journal of the Atmospheric Sciences*: Vol. 56, No. 16, pp. 2761–2779.

Samelson, R.M., A.M. Rogerson, 1996: **Life Cycle of a Linear Coastal-Trapped Disturbance.** *Monthly Weather Review*: Vol. 124, No. 8, pp. 1853–1864.

Skamarock, William C., Richard Rotunno, Joseph B. Klemp, 1999: **Models of Coastally Trapped Disturbances.** *Journal of the Atmospheric Sciences*: Vol. 56, No. 19, pp. 3349–3365.

Tag, Paul M., James E. Peak, 1996: **Machine Learning of Maritime Fog Forecast Rules.** *Journal of Applied Meteorology*: Vol. 35, No. 5, pp. 714–724.

Thompson, William T., Stephen D. Burk, J. Rosenthal, 1997: **An Investigation of the Catalina Eddy.** *Monthly Weather Review*: Vol. 125, No. 6, pp. 1135–1146.

Thompson, William T., Tracy Haack, James D. Doyle, Stephen D. Burk, 1997: **A Nonhydrostatic Mesoscale Simulation of the 10–11 June 1994 Coastally Trapped Wind Reversal.** *Monthly Weather Review*: Vol. 125, No. 12, pp. 3211–3230.

Ueyoshi, Kyozo, John O. Roads, 1993: **Simulation and Prediction of the Catalina Eddy.** *Monthly Weather Review*: Vol. 121, No. 11, pp. 2975–3000.

Ulrickson, Brian L., J. Steven Hoffmaster, Jeremy Robinson, Daniel Vimont, 1995: **A Numerical Modeling Study of the Catalina Eddy.** *Monthly Weather Review*: Vol. 123, No. 5, pp. 1364–1373.

Wilkin, John L., David C. Chapman, 1990: **Scattering of Coastal-Trapped Waves by Irregularities in Coastline and Topography.** *Journal of Physical Oceanography*: Vol. 20, No. 3, pp. 396–422.

Winant, C.D., C.E. Dorman, C.A. Friehe, R.C. Beardsley, 1988: **The Marine Layer off Northern California: An Example of Supercritical Channel Flow.** *Journal of the Atmospheric Sciences*: Vol. 45, No. 23, pp. 3588–3605.

Welch, R.M., K.S. Kuo, B.A. Wielicki, S.K. Sengupta, L. Parker, 1988: **Marine Stratocumulus Cloud Fields off the Coast of Southern California Observed Using LANDSAT Imagery. Part I: Structural Characteristics.** *Journal of Applied Meteorology*: Vol. 27, No. 4, pp. 341–362.

Wylie, Donald, Barry B. Hinton, Kevin Kloesel, 1989: **The Relationship of Marine Stratus Clouds to Wind and Temperature Advection.** *Monthly Weather Review*: Vol. 117, No. 11, pp. 2620–2625.

Zuidema, Paquita, Dennis L. Hartmann, 1995: **Satellite Determination of Stratus Cloud Microphysical Properties.** *Journal of Climate*: Vol. 8, No. 6, pp. 1638–1657.

THIS PAGE INTENTIONALLY LEFT BLANK

INITIAL DISTRIBUTION LIST

1.   Defense Technical Information Center
        Ft. Belvoir, Virginia

2.   Dudley Knox Library
        Naval Postgraduate School
        Monterey, California